POLDER-3 / PARASOL BRDF Databases

User Manual

Issue 1.20

Prepared by Roselyne Lacaze (POSTEL Service Centre / MEDIAS-France)
in collaboration with Emilie Fédèle and François-Marie Bréon (LSCE)

Change Record

Issue/Rev	Date	Pages	Description of Change	Release
I1.00	12.12.2007	All		
I1.10	16.06.2008	All	Update after the inclusion of polarized reflectance in the files	
I1.20	31.07.2009	22-85	Update after the regeneration of the databases in February 2009	

Table of Content

1. INTRODUCTION 5
2. THE INPUT DATA 7
  2.1. THE POLDER-3/PARASOL DATA 7
  2.2. THE IGBP LAND COVER MAP 7
  2.3. THE GLC2000 LAND COVER 8
3. METHODOLOGY FOR BUILDING THE DATABASES 10
  3.1. SELECTION OF THEMATICALLY-HOMOGENEOUS PIXELS 10
  3.2. THE PRE-SELECTION OF A FIXED NUMBER OF PIXELS 14
  3.3. THE FINAL SELECTION OF THE BEST BRDFS 14
  3.4. COMPARISON WITH THE POLDER- 2 METHODOLOGY 15
4. THE BIDIRECTIONAL POLARIZED REFLECTANCE DISTRIBUTION FUNCTION (BPDF) 17
5. FILES DESCRIPTION 18
6. ANALYSIS OF THE DATABASES 21
  6.1. NUMBER OF SELECTED BRDFS 21
  6.2. SPATIAL DISTRIBUTION OF SELECTED PIXELS 23
  6.3. TEMPORAL DISTRIBUTION OF SELECTED PIXELS 31
  6.4. THEMATIC CONTENT OF THE SELECTED PIXELS 33
  6.5. ANALYSIS OF THE BPDF 34
  6.6. SOME POTENTIAL USES OF THE DATABASES 34
7. CONCLUSION 39
8. REFERENCES 40
9. ACKNOWLEDGMENT AND CONTACT 44
ANNEX1 : POLDER FULL RESOLUTION REFERENCE GRID 45
ANNEX2 : MULTI-TEMPORAL BRDFS OF THE YEARLY DATABASES 48
ANNEX3 : BRDFS OF MISCLASSIFIED OR MIXED PIXELS 58
ANNEX4 : EXAMPLES OF BPDF MEASURED AT 865NM 63
ANNEX5 : EXAMPLES OF MEASURED AND SIMULATED BRDF 71

List of Figures

Figure 1 : Majority GLC2000 vegetation class for POLDER pixels 11
Figure 2 : Percentage of homogeneity of POLDER land pixels in terms of GLC2000 classes. 11
Figure 3 : Majority IGBP classes for POLDER pixels 12
Figure 4 : Percentage of homogeneity of POLDER land pixels in terms of IGBP classes. 12
Figure 5 : Extract of a BRDF ASCII file 19
Figure 6 : Location of the 22 012 pixels of the GLC2000-based MONTHLY database. 27
Figure 7 : Location of the 2 016 different pixels of the GLC2000-based YEARLY database 28
Figure 8 : Location of the 14 649 pixels of the IGBP-based MONTHLY database. 29
Figure 9 : Location of the 1 299 different pixels of the IGBP-based YEARLY database. 30
Figure 10 : Directional signatures measured by POLDER-3 in the principal plane over an Evergreen Broadleaf forest (up-left), an Evergreen Needleleaf forest (up-right), a mixed forest (bottom-left), and a Deciduous Broadleaf forest (bottom-right). These pixels are selected in both MONTHLY databases. 37
Figure 11 : Directional signatures measured by POLDER-3 in the principal plane over shrubland (top-left), herbaceous area (top-right), a Cultivated and Managed region (bottom-left), and Snow and Ice (bottom-right). These pixels are selected in both MONTHLY databases. 38

List of Tables

Table 1 : The vegetation classes of the IGBP land cover map. 8
Table 2 : The vegetation classes of the global GLC2000 land cover map. 9
Table 3 : Percentage of land cover classes (GLC2000 at left, IGBP at right) among the thematically-homogeneous pixels of the POLDER grid. 13
Table 4 : Comparison of methodologies for BRDFs selection. 16
Table 5 : Number of BRDFs of the YEARLY database which are also present in the MONTHLY database (GLC2000-based). 22
Table 6 : Number of BRDFs of the YEARLY database which are also present in the MONTHLY database (IGBP-based). 22
Table 7 : Common BRDFs to both MONTHLY databases for some vegetation types. The last column gives the percentage of BRDFs of the GLC2000 class which belong to the corresponding IGBP class. 23
Table 8 : Distribution of BRDFs of the MONTHLY database per GLC2000 class and per month 24
Table 9 : Distribution of BRDFs of the YEARLY database per GCL2000 class and per month 24
Table 10 : Distribution of BRDFs of the MONTHLY database per IGBP class and per month 25
Table 11 : Distribution of BRDFs of the YEARLY database per IGBP class and per month 26
Table 12 : Distribution over the year of BRDFs in the GLC2000-based YEARLY database. 32
Table 13 : Distribution over the year of BRDFs in the IGBP-based YEARLY database. 33
Table 14 : Summary of comparison for similar GLC and IGBP vegetation classes 33

1. Introduction

The Bi-directional Reflectance Distribution Function (BRDF) describes how the terrestrial surfaces reflect the sun radiation. Its potential has been demonstrated for several applications in land surface studies. These includes the correction of bi-directional effects in time series of vegetation indices and reflectances (Leroy and Roujean, 1994; Wu et al., 1995), the direct use of angular measurements for estimation of leaf area index and other biophysical parameters by inversion of radiative transfer models (Knyazikhin et al., 1998; Bicheron and Leroy, 1999), albedo retrieval (Wanner et al., 1997; Cabot and Dedieu, 1997; Capderou, 1998), land cover classifications (Abuelgassim et al., 1996; Bicheron et al., 1997; Hyman and Barnsley, 1997), and radiance to flux conversion factors for Earth radiation budget studies (Manalo-Smith et al., 1998). Then, many users need spatial and temporal variations of the BRDF, for different types of biomes and at different seasons.

The BRDF has been measured in the field (e.g. Kimes, 1983; Deering et al., 1992) or from airborne instruments (Irons et al., 1991; Leroy and Bréon, 1996), with most often an adequate sampling of directional space but with a poor spatial coverage. Directional effects on land surfaces have been seen from space with AVHRR (e.g. Gutman, 1987) or with ATSR (Godsalve, 1995). Then, the spatial coverage is potentially adequate, but the sampling of the BRDF is limited in the angular plane of acquisition. The space-borne POLDER instrument has provided the first opportunity to sample the BRDF of every point on Earth for viewing angles up to 60°-70°, and for the full azimuth range, at a spatial resolution of about 6km, when the atmospheric conditions are favourable (Hautecoeur et Leroy, 1998).

POLDER1 and POLDER-2 have delivered 8 months (November 1996 – June 1997) and 7 months (April – October 2003) of global data onboard the Japanese ADEOS-1 and ADEOS-2 platforms, respectively. Since the beginning of 2005, the POLDER-3 sensor onboard the PARASOL micro-satellite has been flying in the A-Train.

The Service Centre of the POSTEL Thematic Centre on the Land Surface built two global databases of 24,857 BRDFs from POLDER-1 data, and 24,090 BRDFs from POLDER-2 data collected at 443, 565, 670, 765 and 865nm on the basis of the 22 land cover classes of the GLC2000 land cover classification (GLC, 2003). These databases are available for downloading on the POSTEL web site (www1). User manuals presenting the methodology of pixels selection and analysis of the databases are also available.

The Laboratoire des Sciences du Climat et de l'Environnement (LSCE), one of the Expertise Centres of POSTEL, defined a new method to select the BRDFs from the POLDER-3/PARASOL data acquired between November 2005 and October 2006 in order to build 4 new databases:

1. 2 MONTHLY databases gathering the best quality BRDFs for each month, independently: one based upon the IGBP land cover map, the second based upon the GLC2000 land cover map.

2. 2 YEARLY databases designed to follow the annual cycle of surface reflectance and its directional signature. The selection of high quality pixel is based on the full year. The first one is based upon the IGBP land cover map, the second one is based upon the GLC2000 land cover map.

The objective is to collect directional information on homogeneous pixels representing the main continental ecosystems to serve for the development and prototyping of science applications of the BRDF measurements.

This document presents the methodology applied to build the POLDER-3 BRDF data sets, describes the file content, and analyses the databases.

2. The input data

2.1. The POLDER-3/PARASOL data

The POLDER-3 instrument is a radiometer designed to measure the directionality and polarization of the sunlight scattered by the ground atmosphere system. The instrument is made of a bi-dimensional CCD matrix, a rotating wheel that carries filters and polarizers, and a wide field of view lens (114°). The field of view seen by the CCD matrix is ± 51° along track and ± 43° across track. The view zenith angle s seen at surface level are larger due to Earth curvature, ± 61 ° along track and ± 50 ° acro ss track (± 70° in the matrix diagonal). This orientation of the telecentric optics array favours multidirectional viewing over daily global coverage, compared to POLDER-1 & 2. The pixel size on the ground is about 6 km for a PARASOL altitude of 705 km. The rotating wheel carries filters that allow spectral measurements at 9 wavelengths (443, 490, 565, 670, 763, 765, 865, 910, and 1020nm). The 1020nm waveband has been added, compared to POLDER1&2, to conduct observations for comparison with data acquired by the lidar on CALIPSO, one of the PARASOL companion satellites in the A-Train. Three of the channels (490, 670 and 865nm) measure the polarization of the incident light. Images of the same band are acquired every 19.6 s, which permits a large overlap between successive images. During the PARASOL overpass, a surface target is viewed up to 16 times with a different viewing angle. The directional configuration changes each day due to orbital shift between successive days. Therefore, after a few days, assuming favourable atmospheric conditions, the slices of measurements provide a sampling of the BRDF in the limits of the instrument field of view.

The POLDER-3 data are processed to obtain the geocoded, calibrated, cloud screened and atmospherically-corrected land surface reflectances for each orbit. These algorithms consist of a cloud detection, a correction from the effects of absorbing gazes, stratospheric and tropospheric aerosols. Then, a semi-empirical BRDF model (Maignan et al., 2004) is inverted on the directional land surface reflectances acquired during 30-days to assess the spectral and broadband directional-hemispherical reflectances (DHR), and bi-hemispheric reflectances (BHR), and the anisotropy-corrected NDVI derived from the DHR at 670 and 865 nm. The final biogeophysical products are available on 5th, 15th and 25th of each month. Details on the Level 2 and Level 3 “Land Surface” algorithms can be found in Lacaze and Maignan (2007). The POLDER-3/PARASOL Land Surface products can be downloaded on the POSTEL web site (www1).

2.2. The IGBP land cover map

The International Geosphere Biosphere Programme (IGBP) 1-km AVHRR 10-day composites for April 1992 through March 1993 map (Eidenshink and Faundeen, 1994) are the base data used to elaborate the land cover. Multi-temporal AVHRR NDVI data are used to divide the landscape into land cover regions, based on seasonality. While the primary AVHRR data used in the classification is NDVI, the individual channel data sets are used for post classification characterization of certain landscape properties. A data quality evaluation was conducted and is reported by Zhu and Yang (1996).

The IGBP land cover map contains 17 classes (Table 1) and can be downloaded at www2 . Class n°17, labelled "Water Bodies", is not considered for the BRDF selection.

N°	IGBP Land Cover Class
1	Evergreen Needleleaf Forest
2	Evergreen Broadleaf Forest
3	Deciduous Needleleaf Forest
4	Deciduous Broadleaf Forest
5	Mixed Forest
6	Closed Shrublands
7	Open Shrublands
8	Woody savannas
9	Savannas
10	Grasslands
11	Permanent Wetlands
12	Croplands
13	Urban and Built-up
14	Cropland/Natural Vegetation Mosaic
15	Snow and Ice
16	Barren or Sparsely Vegetated
17	Water Bodies

Table 1 : The vegetation classes of the IGBP land cover map.

2.3. The GLC2000 land cover

The co-ordination of the Global Land Cover 2000 project has been carried out under the 5th Framework Program 1999-2002 for Research of the European Commission. It is part of the project of the European Commission called Global Environment Information System (GEIS).

In contrast to former global mapping initiatives the GLC2000 project is a bottom up approach to global mapping. In this project more than 30 research teams have been involved, contributing to 19 regional windows. There were two conditions to be fulfilled by the regional experts to guarantee a certain degree of consistency. The data had to be based on SPOT-4 VEGETATION VEGA2000 dataset, which was made freely available by Cnes. Secondly, the partners agreed to use the Land Cover Classification System (LCCS) provided by FAO (Di Gregorio and Jansen, 2000). The regional legends are compatible with the LCCS, which describes land cover according to a hierarchical series of classifiers and attributes. These separate vegetated or non-vegetated surfaces; terrestrial or aquatic/flooded; cultivated and managed; natural and semi-natural; life-form; cover; height; spatial distribution; leaf type and phenology. Coding each class with LCCS allows a map legend to be progressively more detailed for regional, and in some cases, national level users. Due to its hierarchical structure it is possible to translate the regional classification into a more general one – the global legend (Table 2). More information on the GLC2000 products is available on the project web site (www3).

The GLC2000 land cover map is truncated at 56°S. The missing data between 56°S and 90°S have been filled using a land/sea mask. The land pixels were labelled as “Snow & Ice” (Class n°21) and the water pixels were labelled as “Water Bodies” (Class n°20).

N°	GLC2000 Land Cover Class
1	Tree Cover, broadleaved, evergreen
2	Tree Cover, broadleaved, deciduous, closed
3	Tree Cover, broadleaved, deciduous, open
4	Tree Cover, needle-leaved, evergreen
5	Tree Cover, needle-leaved, deciduous
6	Tree Cover, mixed leaf type
7	Tree Cover, regularly flooded, fresh
8	Tree Cover, regularly flooded, saline, (daily variation)
9	Mosaic: Tree cover / Other natural vegetation
10	Tree Cover, burnt
11	Shrub Cover, closed-open, evergreen (with or without sparse tree layer)
12	Shrub Cover, closed-open, deciduous (with or without sparse tree layer)
13	Herbaceous Cover, closed-open
14	Sparse Herbaceous or sparse shrub cover
15	Regularly flooded shrub and/or herbaceous cover
16	Cultivated and managed areas
17	Mosaic: Cropland / Tree Cover / Other Natural Vegetation
18	Mosaic: Cropland / Shrub and/or Herbaceous cover
19	Bare Areas
20	Water Bodies (natural & artificial)
21	Snow and Ice (natural & artificial)
22	Artificial surfaces and associated areas

Table 2 : The vegetation classes of the global GLC2000 land cover map.

3. Methodology for building the databases

We elaborated the BRDF databases using the measurements acquired from November 2005 to October 2006. This year was chosen as it is well suited to follow a full vegetation cycle in the Northern hemisphere, and also because the instrument suffered few interruptions during this period.

For both databases, the methodology relies on 3 main steps:

1. the selection of thematically-homogeneous pixels, according to the land cover map (IGBP or GLC2000).
2. a pre-selection of a fixed number of pixels according to the quality of the inversion of the reflectance model against one month of data. This criterium allows removing the noisiest BRDFs and those with few observations.
3. the final selection of the best BRDFs. In this last step, the selection accounts for the quality of the reflectance model inversion over one single orbit, which allows removing the noisy orbits that could disturb the overall quality of the BRDF.

After several tests, we choose to apply the steps 2 and 3 on the reflectances measured at 670nm, because it allows selecting BRDFs which are generally clean at all wavebands.

3.1. Selection of thematically-homogeneous pixels

On the one hand, the GLC2000 land cover map is available in a regular latitude/longitude grid at 1/112° space resolution, and the IGBP is available in a regular latitude/longitude grid at 1/120° space resolution. On the other hand, the POLDER-3/PARASOL surface reflectances are located in a reference grid based on the sinusoidal equal area projection with a constant step along a meridian with a resolution of 1/18° (Annex1).

Because the space resolution of a POLDER pixel is larger than the space resolution of a GLC2000 pixel or an IGBP pixel, a POLDER pixel can contain different vegetation classes. For each POLDER pixel, the vegetation classes located on its area are identified, and the majority class is allocated to the pixel. Figure 1 and Figure 3 show the resulting maps for GLC2000 and IGBP, respectively. A pixel is considered as “homogeneous” if the majority class represents at least 80% of the number of 1-km pixels contained in its area. According to this definition, 57% of the land pixels of the POLDER grid are homogeneous in terms of GLC2000 class (Figure 2), whereas 52,7% of the land pixels of the POLDER grid are homogeneous in terms of IGBP class (Figure 4). This result indicates that the spatial variability of the GLC2000 land cover map is smoother, even with more classes than the IGBP land cover, and that the ecosystems are more homogeneous and better delimited.

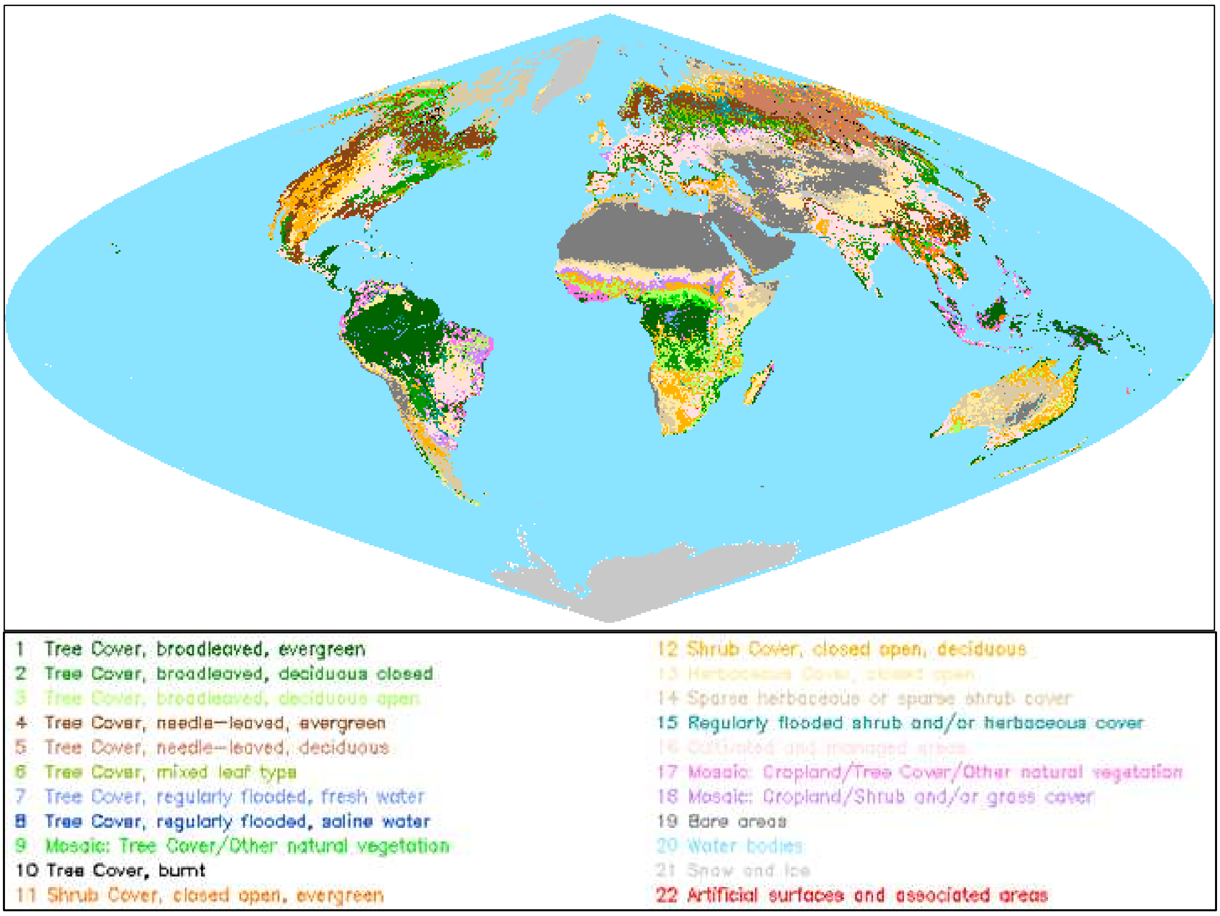
1 Tree Cover, broadleaved, evergreen
2 Tree Cover, broadleaved, deciduous closed
3 Tree Cover, broadleaved, deciduous open
4 Tree Cover, needle-leaved, evergreen
5 Tree Cover, needle-leaved, deciduous
6 Tree Cover, mixed leaf type
7 Tree Cover, regularly flooded, fresh water
8 Tree Cover, regularly flooded, saline water
9 Mosaic: Tree Cover/Other natural vegetation
10 Tree Cover, burnt
11 Shrub Cover, closed open, evergreen
12 Shrub Cover, closed open, deciduous
13 Herbaceous Cover, closed open
14 Sparse herbaceous or sparse shrub cover
15 Regularly flooded shrub and/or herbaceous cover
16 Cultivated and managed areas
17 Mosaic: Cropland/Tree Cover/Other natural vegetation
18 Mosaic: Cropland/Shrub and/or grass cover
19 Bare areas
20 Water bodies
21 Snow and Ice
22 Artificial surfaces and associated areas

Figure 1 : Majority GLC2000 vegetation class for POLDER pixels

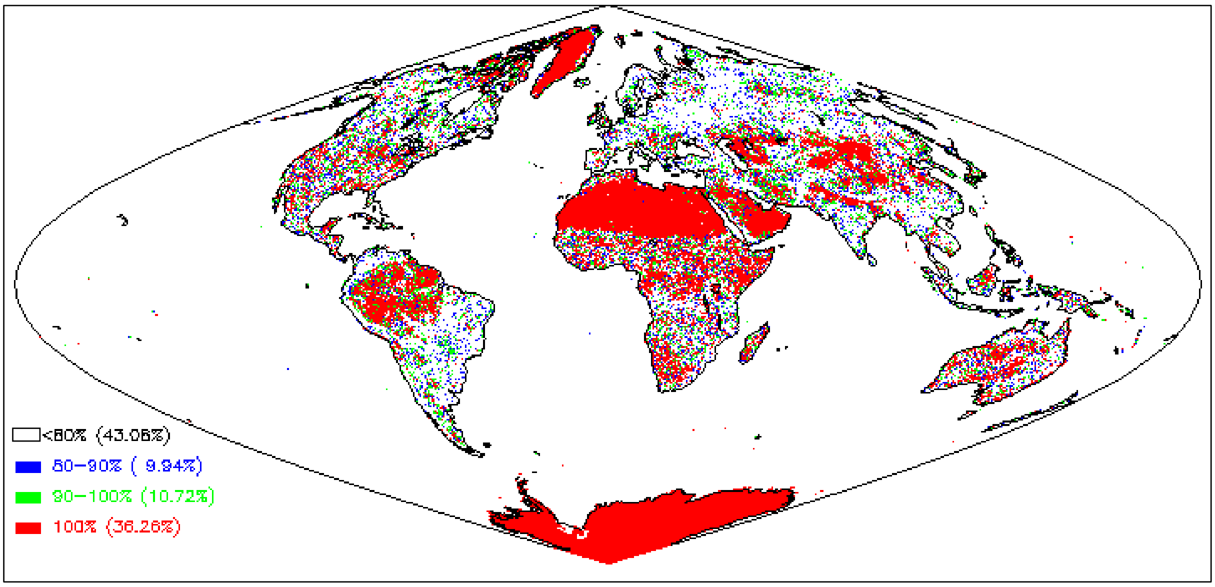
<80% (43.06%)
80–90% (9.94%)
90–100% (10.72%)
100% (36.26%)

Figure 2 : Percentage of homogeneity of POLDER land pixels in terms of GLC2000 classes.

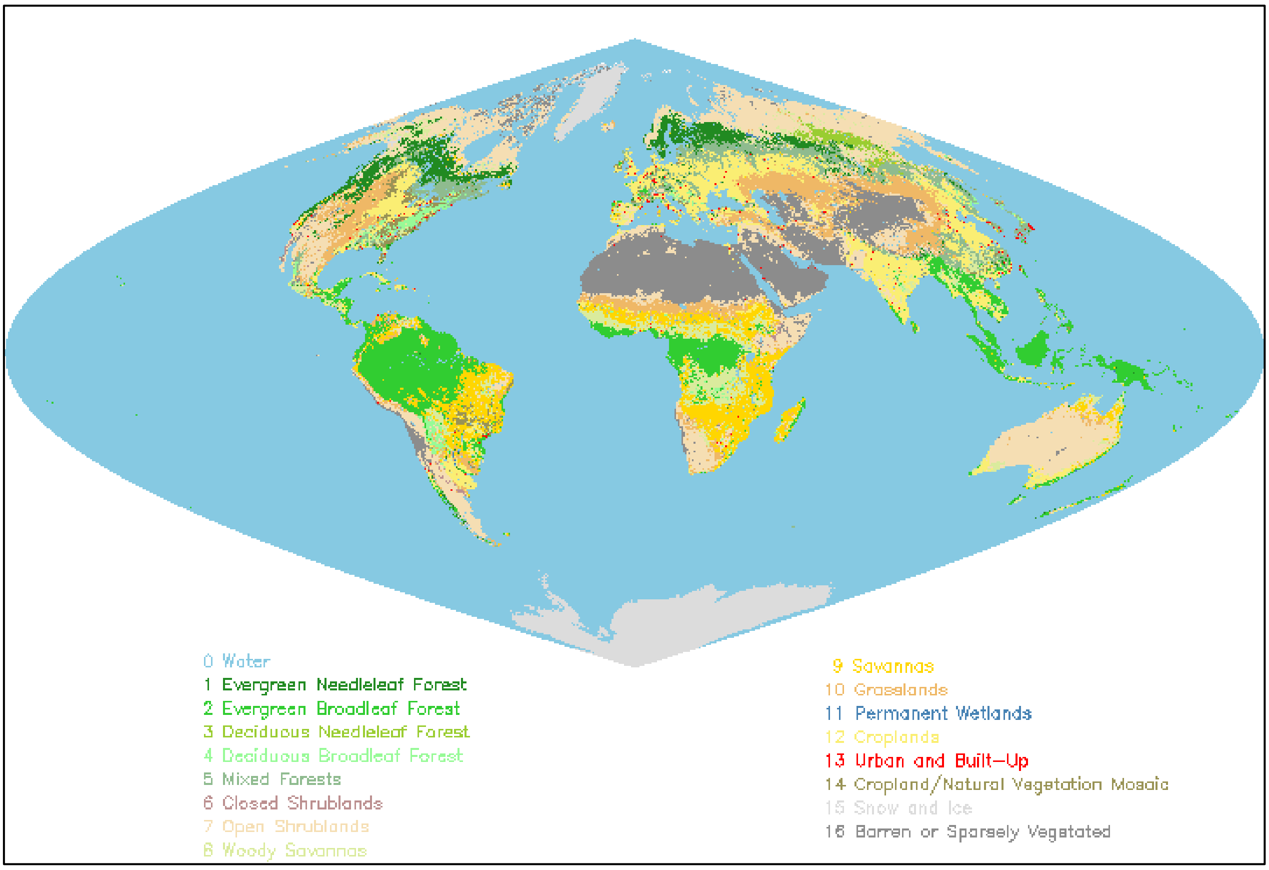
0 Water
1 Evergreen Needleleaf Forest
2 Evergreen Broadleaf Forest
3 Deciduous Needleleaf Forest
4 Deciduous Broadleaf Forest
5 Mixed Forests
6 Closed Shrublands
7 Open Shrublands
8 Woody Savannas
9 Savannas
10 Grasslands
11 Permanent Wetlands
12 Croplands
13 Urban and Built–Up
14 Cropland/Natural Vegetation Mosaic
15 Snow and Ice
16 Barren or Sparsely Vegetated

Figure 3 : Majority IGBP classes for POLDER pixels

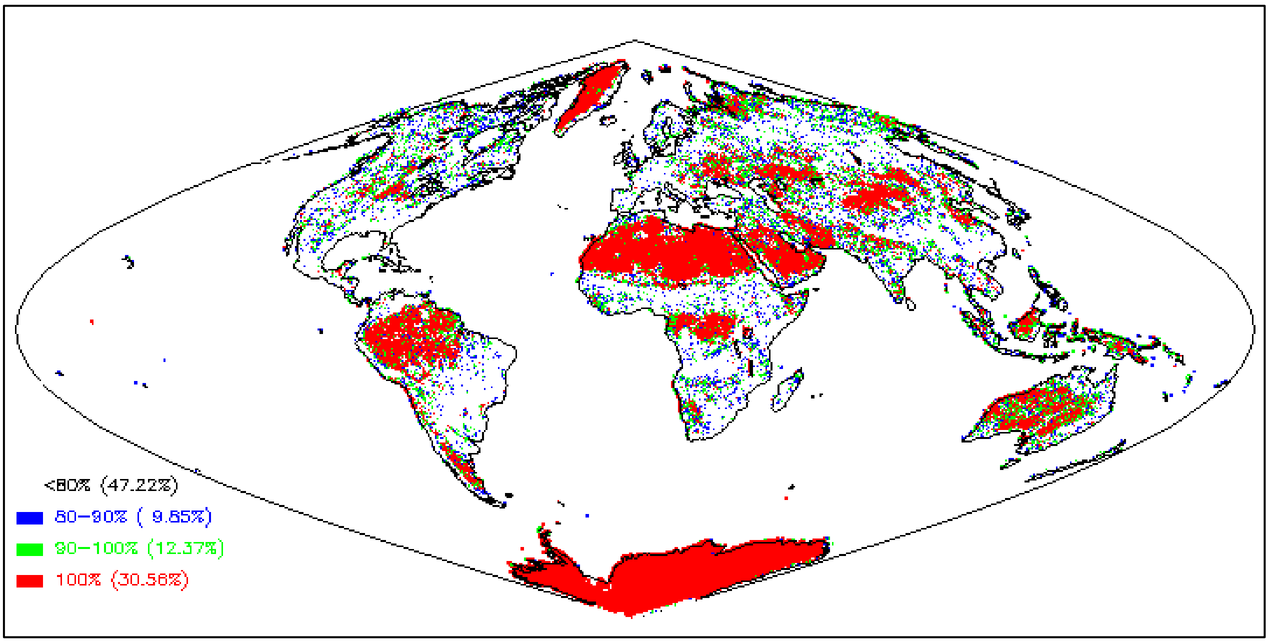
<80% (47.22%)
80–90% (9.85%)
90–100% (12.37%)
100% (30.56%)

Figure 4 : Percentage of homogeneity of POLDER land pixels in terms of IGBP classes.

In both cases, the most populated classes of thematically-homogeneous pixels are "Bare Areas" (~21% for GLC2000 and IGBP) or “Snow and Ice” (~18% for GLC2000, ~19% for IGBP) (Table 3). For the GLC2000 land cover map, the “Cultivated and Managed areas” and the “Evergreen Broadleaf Forest” gather more than 10% of these homogeneous pixels. At the opposite, the regularly flooded forests and the burnt areas concern some ten thousand of pixels, only. For the IGBP land cover map, the "Open Shrubland", and the "Evergreen Broadleaf Forest" represent more than 18% and 14% of the homogeneous pixels, respectively. At the opposite, the "Permanent Wetlands" and the "Closed Shrubland" gather some ten thousand of pixels, only.

GLC2000 Class	%
GLC_01	10.95
GLC_02	3.02
GLC_03	2.20
GLC_04	4.89
GLC_05	2.15
GLC_06	0.77
GLC_07	0.26
GLC_08	0.03
GLC_09	0.65
GLC_10	0.06
GLC_11	0.25
GLC_12	5.35
GLC_13	7.25
GLC_14	8.68
GLC_15	0.28
GLC_16	11.05
GLC_17	1.02
GLC_18	0.96
GLC_19	21.07
GLC_20	1.09
GLC_21	17.92
GLC_22	0.09

IGBP Class	%
IGBP_01	2.45
IGBP_02	14.52
IGBP_03	0.31
IGBP_04	0.35
IGBP_05	2.09
IGBP_06	0.05
IGBP_07	18.97
IGBP_08	1.62
IGBP_09	2.65
IGBP_10	6.77
IGBP_11	<0.01
IGBP_12	9.67
IGBP_13	0.24
IGBP_14	0.18
IGBP_15	18.94
IGBP_16	21.17

Table 3 : Percentage of land cover classes (GLC2000 at left, IGBP at right) among the thematically-homogeneous pixels of the POLDER grid.

Table 3 shows that the 2 maps give quite similar percentages of surface covered by grass (GLC_13 and IGBP_10) and crops (GLC_16 and IGBP_12), even if the figures of GLC2000 are slightly higher. The differences appear on the forest classes: IGBP displays more evergreen broadleaf forests (IGBP_02 and GLC_01) and mixed forests (IGBP_05 and GLC_06) than GLC2000, but it is the opposite for the other forest types. If we consider all the main forest classes (GLC_01 to GLC_06, and IGBP_01 to IGBP_05), the number of homogeneous pixels reach almost 24% for GLC2000, and 20% only for IGBP. The largest difference concerns the areas covered by shrubs: the shrubland classes of IGBP (IGBP_6 and IGBP_7) represent 19% of homogenous pixels, whereas the shrubland classes of GLC2000 (GLC_11 and GLC_12) gather less than 6% of homogenous pixels.

In the next steps, we consider only the 2 159 417 homogeneous pixels of the POLDER grid for GLC2000, and the 1 988 845 homogeneous pixels of the POLDER grid for IGBP.

3.2. The pre-selection of a fixed number of pixels

Only the homogeneous pixels viewed by at least 5 orbits during the month, after the cloud detection and the atmospheric correction, are concerned by the pre-selection. A notation, equal to 1/RMS_{670} or equal to 0 is less than 5 orbits, is allocated to each pixel. RMS_{670} is the Root Mean Square error between the measurements at 670nm and the reflectance model (Maignan et al., 2004) inverted against all data acquired during a period of 30 days centred on the 15th of each month. This RMS_{670} is given in the quality index of the Level3 products. The RMS at 670nm has been chosen because it allows selecting BRDFs which are clean at all wavebands (490, 565, 670 and 865nm) comparing to the RMS at 865nm which extracts BRDFs which are clean only in the near –infrared.

In the case of the MONTHLY database, the 500 pixels with the best notations (the highest) are selected for each of the 4 bands of latitude (0°-20°, 20°-40°, 40°-60°, 60°-90°: North and South are gathered), and for each class of the land cover map (22 classes for GLC2000, 16 classes for IGBP). If a class contains less than 500 pixels, they are all kept. This is done for each month. After this step, 291 556 pixels are pre-selected for GLC2000, and 191 685 pixels are pre-selected for IGBP.

In the case of the YEARLY database, a yearly notation is calculated as the mean of the monthly notations (including notations equal to 0). Only pixels with at least 5 valid monthly notations are considered. The 1000 pixels with the best notations are selected for each band of latitude and each vegetation class. If the class contains less than 1000 pixels, they are all kept. After this step, 49 395 pixels are pre-selected for GLC2000, and 31 529 pixels are pre-selected for IGBP.

3.3. The final selection of the best BRDFs

First, the procedure consists in calculating the RMS, between the observations and the reflectance model, in two ways:

1. the model is inverted per orbit: RMS_{orbit}
2. the model is inverted against all observations acquired during the month: RMS_{month}

In both cases, the observations acquired in the angular range of 5° around the hot spot or around the glitter directions are not accounted for the model inversion.

If $RMS_{orbit} \geq 2 * RMS_{month}$, the orbit is considered not valid.

Then, the reflectance model is inverted over all remaining valid orbits of the month, and RMS_{month} is calculated again. A notation, equal to $1/RMS_{month}$, is allocated to each pixel with at least 5 remaining valid orbits during the month. The notation of other pixels is 0. If RMS_{month} is lower than 0.5, then the notation is equal to 2. If a pixel is viewed under one, or more, hot spot configuration during the month, then its notation is raised of 20%. For each additional orbit, comparing to 5, the notation is raised of 4%. A yearly notation is calculated as the mean of the monthly notations (including notations equal to 0).

The notations, monthly and yearly, are sorted out in decreasing order, excluding the pixels located at a distance less than 35km from a pixel with a better notation. The 30 pixels with the best notations are selected for each band of latitude, and each vegetation class. If a class contains less than 30 pixels, they are all kept. For the MONTHLY database, this is done for each month.

At final, the GLC2000-based MONTHLY database gathers 22 012 pixels, and the IGBP-based MONTHLY database gathers 14 649 pixels.

For the YEARLY database, 2 016 pixels are identified for GLC2000, and 1 299 pixels are identified for IGBP. For each of them, a BRDF file is built for each month with a valid monthly notation. Then, at final, the GLC2000-based YEARLY database contains 21 262 BRDFs, and the IGBP-based YEARLY database contains 13 887 BRDFs.

The NDVI of the selected pixels is calculated following the approach described in Lacaze and Maignan (2007).

3.4. *Comparison with the POLDER- 2 methodology*

The differences between the methodology described above and the approach used to elaborate the POLDER-2 BRDFs database (Lacaze, 2006b) are summarized in Table 4.

Previously, the selection was based upon angular criteria exclusively. In the present approach, the angular criterium is considered with the number of orbit per BRDF only. Now, the selection considers the radiometric quality of measurements mainly, through the quality of the inversion of the reflectance model against the observations. This leads to select the smoothest BRDFs. These changes were done with the aim to improve the usefulness of the selected BRDFs for modelling activities.

The new criterium of the thematic homogeneity, which reduces a lot the number of relevant pixels, has been introduced to consider the "purest" pixels only. The objective was to get typical BRDFs of the main vegetation types.

The criterium of vicinity has been added to avoid the retrieval of clumps of 3, 4 or more neighbouring pixels. Indeed, when one pixel matches the criteria of selection, it is highly likely that its neighbours do also. This clustering of BRDFs was strong in the POLDER-1 and POLDER-2 BRDF databases (Lacaze, 2006a; Lacaze, 2006b), for all vegetation types. This new criterium aims at improving the sampling of ecosystems.

	POLDER-2	POLDER-3
Criteria of selection:		
Number of sequence/orbit	10 ≤	NA
Number of orbit/BRDF	8 ≤	5 ≤
Number of angular regions sampled	5 ≤	NA
Thematic homogeneity of the pixel	NA	80% ≤
RMS of model/observations	NA	1 / RMS
Neighbourhood	NA	Out of about 35km
Selection per:		
GLC_2000 class	22	22
Month	7	12
Bands of latitude	5	4
Class of NDVI	12	NA
Number of best pixels	10	30

Table 4 : Comparison of methodologies for BRDFs selection.

4. The Bidirectional Polarized reflectance Distribution Function (BPDF)

POLDER was the first satellite sensor to measure continuously the linearly polarized Earth-reflected radiance. For 3 spectral bands (490, 670, and 865nm), a polarizer is added to the filters in order to assess the degree of linear polarization and the polarization direction. These parameters are derived by combining measurements in 3 channels with the same spectral filters but with the polarizer axes turned by steps of 60°. The three polarization measurements in a spectral band are successive and have a total time lag of 0.6s between the first and the third (last) measurement. In order to compensate for spacecraft motion during the lag and to register the three measurements, a small-angle, wedge prism is used in each polarizing assembly. As a consequence, the matrix image is translated in the focal plane to offset the satellite motion, and the three polarization measurements are quasi collocated.

Natural light from the sun is not polarized, or rather it is randomly polarized. However, certain physical processes in the atmosphere (molecular scattering, scattering by stratospheric and tropospheric aerosols, scattering by clouds), and some natural surfaces (vegetation, bare soil, snow, ice, water) orient electric vibrations, thus generating polarized light.

Measurements indicate that the surface polarized reflectance is almost constant in the visible and near-IR spectrum, while the polarization degree varies inversely with the reflectance. Therefore, a single channel contains the information on the polarized reflectance. However, as original data are TOA measurements, the contribution of the atmosphere has to be removed to derive the polarized component of the surface. Then, it is more efficient to use the measurements acquired at 865nm since the atmospheric contribution of the atmosphere is smaller at this wavelength than in the visible channels.

The polarized reflectance measured at 865nm is provided for each pixel contained in the 4 databases.

5. Files description

The directories tree is the following:

- The folders are GLC_XX (IGBP_XX) where XX is the class number in the GLC2000 (IGBP) land cover map
- The sub-folders are YYYYMM corresponding to the year (YYYY=2005 or 2006) and the month (MM = 01 to 12) of acquisition.

They contain BRDF files named as brdf_ndviNN.LLLL_CCCC.dat where :

- NN indicates the NDVI range: NN=00 corresponds to NDVI < -0.2 and NN=12 to 0.9 < NDVI < 1.
- LLLL and CCC are the line and the column of the POLDER reference grid where the pixel is located (see Annex1).

The BRDF files are ASCII files starting with three header lines (example on Figure 5). The header provides the pixel location in latitude and longitude, the GLC2000 (or the IGBP) class number, the NDVI, the number of valid orbits, and the number of valid observations (each pass provides up to 16 different directional measurements), and the fraction of the dominant surface type within the POLDER pixel.

The header is followed by the measurements. Each line is one directional observation. The "no data" value is -9.990. The different fields displayed in a columnar format (I6, 3F8.2, 6F7.3, F8.2, 2F8.3, 6X, I6, F8.4) are:

yymmdd	: date of the observation
thetaS	: sun zenith angle (°)
thetaV	: view zenith angle (°)
RelAzi	: relative azimuth angle (°)
R490	: surface reflectance measured at 490nm
R565	: surface reflectance measured at 565nm
R670	: surface reflectance measured at 670nm
R765	: surface reflectance measured at 765nm
R865	: surface reflectance measured at 865nm
R1020	: surface reflectance measured at 1020nm
phiS	: sun azimuth angle (°)
DVzC	: thetaS * COS (RelAzi)
DVzS	: thetaS * SIN (RelAzi)
Orbit_numb	: cccooo where ccc is the PARASOL cycle number (1<ccc<999) and ooo is the orbit number (1<ooo<233)
RP865	: polarized reflectance at 865nm

DVzC and DVzS can be used for slight corrections of the viewing geometry. Indeed, POLDER-3 spectral measurements are not simultaneous so that each channel is acquired with a slightly different viewing geometry. We give here the view angles for the 670nm band. The viewing geometry for the other channels can vary by a few tenths of degrees. For applications that require a higher accuracy, these parameters allow the correction. Further details on these corrections are given in Bréon (2005).

Warning: One month corresponds to a period of synthesis of 30 days, and not to a calendar month. Then, some side effects can appear for months where the number of days is low (e.g. February).

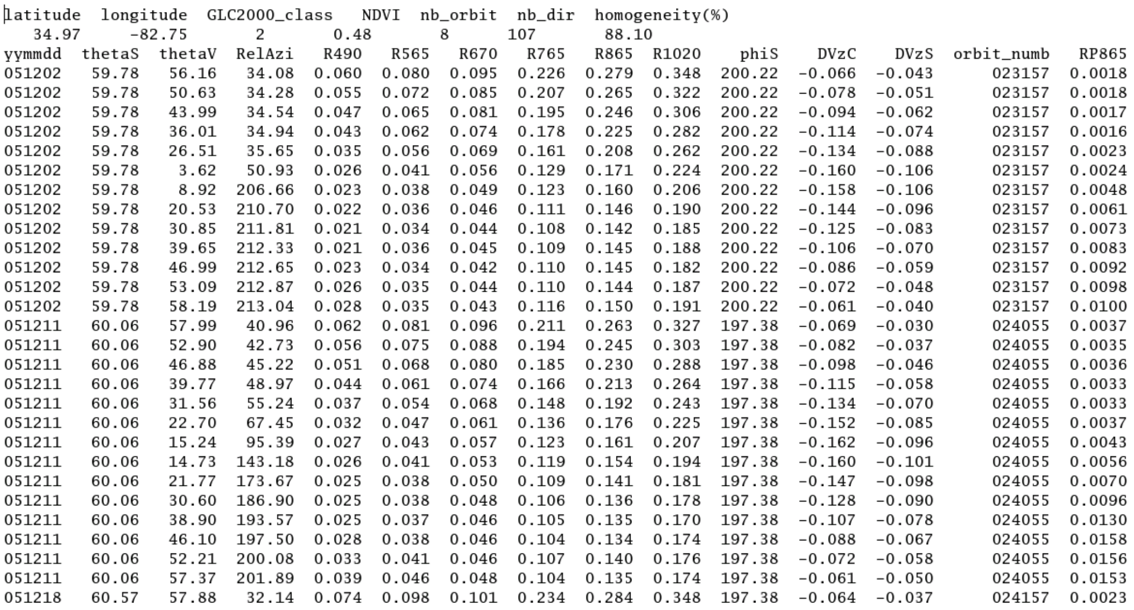

```
latitude  longitude  GLC2000_class   NDVI  nb_orbit  nb_dir  homogeneity(%)
   34.97     -82.75          2        0.48        8      107       88.10
yymmdd  thetaS  thetaV  RelAzi   R490   R565   R670   R765   R865  R1020    phiS    DVzC    DVzS  orbit_numb   RP865
051202   59.78   56.16   34.08  0.060  0.080  0.095  0.226  0.279  0.348  200.22  -0.066  -0.043      023157  0.0018
051202   59.78   50.63   34.28  0.055  0.072  0.085  0.207  0.265  0.322  200.22  -0.078  -0.051      023157  0.0018
051202   59.78   43.99   34.54  0.047  0.065  0.081  0.195  0.246  0.306  200.22  -0.094  -0.062      023157  0.0017
051202   59.78   36.01   34.94  0.043  0.062  0.074  0.178  0.225  0.282  200.22  -0.114  -0.074      023157  0.0016
051202   59.78   26.51   35.65  0.035  0.056  0.069  0.161  0.208  0.262  200.22  -0.134  -0.088      023157  0.0023
051202   59.78    3.62   50.93  0.026  0.041  0.056  0.129  0.171  0.224  200.22  -0.160  -0.106      023157  0.0024
051202   59.78    8.92  206.66  0.023  0.038  0.049  0.123  0.160  0.206  200.22  -0.158  -0.106      023157  0.0048
051202   59.78   20.53  210.70  0.022  0.036  0.046  0.111  0.146  0.190  200.22  -0.144  -0.096      023157  0.0061
051202   59.78   30.85  211.81  0.021  0.034  0.044  0.108  0.142  0.185  200.22  -0.125  -0.083      023157  0.0073
051202   59.78   39.65  212.33  0.021  0.036  0.045  0.109  0.145  0.188  200.22  -0.106  -0.070      023157  0.0083
051202   59.78   46.99  212.65  0.023  0.034  0.042  0.110  0.145  0.182  200.22  -0.086  -0.059      023157  0.0092
051202   59.78   53.09  212.87  0.026  0.035  0.044  0.110  0.144  0.187  200.22  -0.072  -0.048      023157  0.0098
051202   59.78   58.19  213.04  0.028  0.035  0.043  0.116  0.150  0.191  200.22  -0.061  -0.040      023157  0.0100
051211   60.06   57.99   40.96  0.062  0.081  0.096  0.211  0.263  0.327  197.38  -0.069  -0.030      024055  0.0037
051211   60.06   52.90   42.73  0.056  0.075  0.088  0.194  0.245  0.303  197.38  -0.082  -0.037      024055  0.0035
051211   60.06   46.88   45.22  0.051  0.068  0.080  0.185  0.230  0.288  197.38  -0.098  -0.046      024055  0.0036
051211   60.06   39.77   48.97  0.044  0.061  0.074  0.166  0.213  0.264  197.38  -0.115  -0.058      024055  0.0033
051211   60.06   31.56   55.24  0.037  0.054  0.068  0.148  0.192  0.243  197.38  -0.134  -0.070      024055  0.0033
051211   60.06   22.70   67.45  0.032  0.047  0.061  0.136  0.176  0.225  197.38  -0.152  -0.085      024055  0.0037
051211   60.06   15.24   95.39  0.027  0.043  0.057  0.123  0.161  0.207  197.38  -0.162  -0.096      024055  0.0043
051211   60.06   14.73  143.18  0.026  0.041  0.053  0.119  0.154  0.194  197.38  -0.160  -0.101      024055  0.0056
051211   60.06   21.77  173.67  0.025  0.038  0.050  0.109  0.141  0.181  197.38  -0.147  -0.098      024055  0.0070
051211   60.06   30.60  186.90  0.025  0.038  0.048  0.106  0.136  0.178  197.38  -0.128  -0.090      024055  0.0096
051211   60.06   38.90  193.57  0.025  0.037  0.046  0.105  0.135  0.170  197.38  -0.107  -0.078      024055  0.0130
051211   60.06   46.10  197.50  0.028  0.038  0.046  0.104  0.134  0.174  197.38  -0.088  -0.067      024055  0.0158
051211   60.06   52.21  200.08  0.033  0.041  0.046  0.107  0.140  0.176  197.38  -0.072  -0.058      024055  0.0156
051211   60.06   57.37  201.89  0.039  0.046  0.048  0.104  0.135  0.174  197.38  -0.061  -0.050      024055  0.0153
051218   60.57   57.88   32.14  0.074  0.098  0.101  0.234  0.284  0.348  197.38  -0.064  -0.037      024157  0.0023
```

Figure 5 : Extract of a BRDF ASCII file

Two additional files are provided with databases:

1. *GLC_PARASOL.bin* (*IGBP_PARASOL.bin)* gives the majority class of GLC2000 (IGBP) for each POLDER pixel (Figure 1)
2. *Percentage_Max_GLC2000Class.bin* (*Percentage_Max_IGBPClass.bin)* gives the level of homogeneity of the POLDER land pixels according to the land cover map. The pixels with a percentage higher or equal to 80% are displayed in Figure 2 for GLC2000 and Figure 4 for IGBP.

These maps are presented in the POLDER reference grid (Annex1). Values of *GLC_PARASOL.bin* are coded on one byte. The range is between 1 and 22 according to the numbers of GLC2000 classes; 23 is allocated to pixels out of projection. Values of *IGBP_PARASOL.bin* are coded on one byte. The range is between 0 and 17 according to the numbers of IGBP classes. The values of *Percentage_Max_GLC2000Class.bin* and of

Percentage_Max_IGBPClass.bin are coded in floating points on 4 bytes with a maximum equal to 100.

6. Analysis of the databases

6.1. Number of selected BRDFs

The GLC2000-based MONTHLY and YEARLY POLDER-3 databases contain 22 012, and 21 262 BRDFs, respectively, selected among one year of observations.

The methodology of selection of the MONTHLY database consists in keeping the 30 best BRDFs among the 1 056 (22 GLC_CLASS * 12 months * 4 bands of latitude) classes, what corresponds to 31 680 pixels. At final, the MONTHLY POLDER-3 database contains 22 012 BRDFs, i.e. 69% of the theoretic maximal number of pixels. This is a good rate of filling considering that some vegetation types are little or not present (as a thematically homogeneous pixel) in some latitudes. For the YEARLY database, the filling rate is better since it reaches 76% (2 016 different pixels in the database comparing to the theoretic maximum of 2 640 = 22 * 4 * 30).

The IGBP-based MONTHLY and YEARLY POLDER-3 databases contain 14 649, and 13 887 BRDFs, respectively. This is lower than the GLC2000-based databases since the IGBP land cover map contains 16 classes only, against 22 for the GLC2000 land cover.

The methodology of selection of the MONTHLY database consists in keeping the 30 best BRDFs among the 768 (16 GLC_CLASS * 12 months * 4 bands of latitude) classes, what corresponds to 23 040 pixels. At final, the MONTHLY POLDER-3 database contains 14 649 BRDFs, i.e. around 64% of the theoretic maximal number of pixels. For the YEARLY database, the filling rate is a little bit better since it reaches 68% (1 299 different pixels in the database comparing to the theoretic maximum of 1 920 = 16 * 4 * 30). These percentages are lower than for the GLC2000-based databases, which is a consequence of the lower rate of homogeneity of POLDER pixels in terms of IGBP land cover classes.

Some BRDFs are common to MONTHLY and YEARLY databases. Table 5 and Table 6 give the number of BRDFs of the YEARLY database which are also present in the MONTHLY database, for the GLC2000-based database and for the IGBP-based database, respectively.

In a general way, the highest (lowest) percentages are for the classes which represent the less (most) important part of the thematically-homogeneous pixels (Table 3). For other classes, the figures of Table 5 and Table 6 result of the combination of:

- The representativeness of a biome in each band of latitude: least numerous are the pixels, more important is the probability that the same ones are selected in MONTHLY and YEARLY databases.
- The variability of the BRDFs quality during the year: if a pixel has good BRDFs all along the year, it has strong probability to be selected in both databases. The quality of the BRDF depends on many factors and can not be generalized.

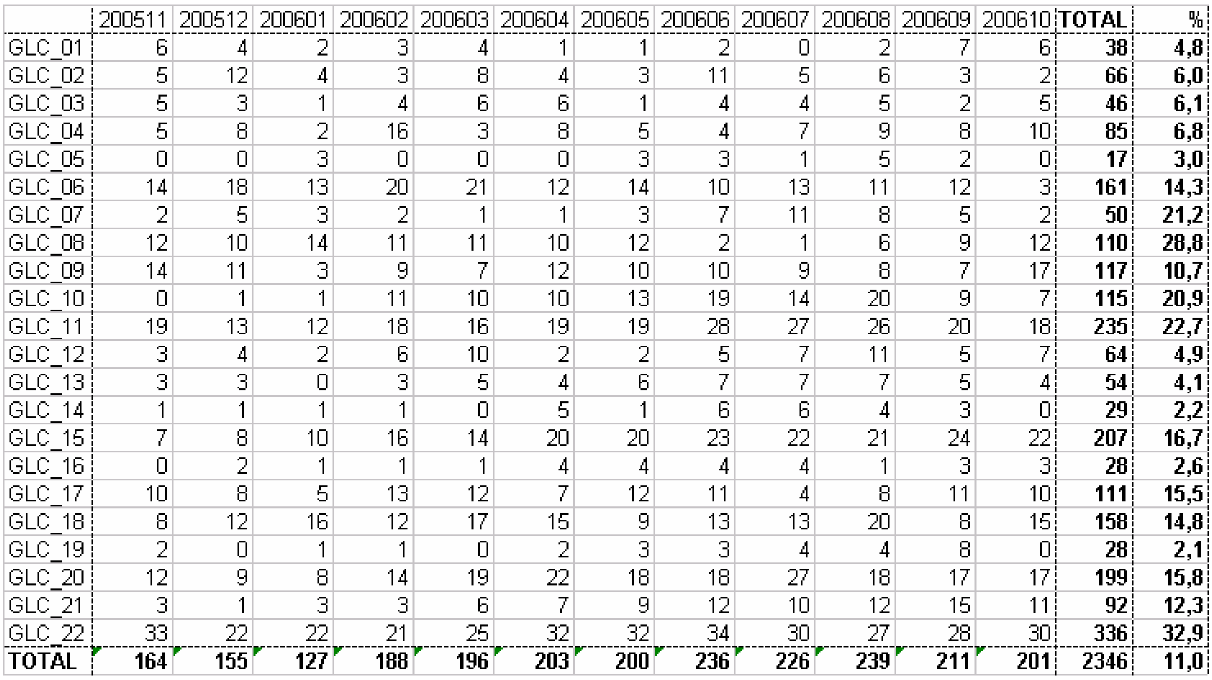

	200511	200512	200601	200602	200603	200604	200605	200606	200607	200608	200609	200610	TOTAL	%
GLC_01	6	4	2	3	4	1	1	2	0	2	7	6	**38**	**4,8**
GLC_02	5	12	4	3	8	4	3	11	5	6	3	2	**66**	**6,0**
GLC_03	5	3	1	4	6	6	1	4	4	5	2	5	**46**	**6,1**
GLC_04	5	8	2	16	3	8	5	4	7	9	8	10	**85**	**6,8**
GLC_05	0	0	3	0	0	0	3	3	1	5	2	0	**17**	**3,0**
GLC_06	14	18	13	20	21	12	14	10	13	11	12	3	**161**	**14,3**
GLC_07	2	5	3	2	1	1	3	7	11	8	5	2	**50**	**21,2**
GLC_08	12	10	14	11	11	10	12	2	1	6	9	12	**110**	**28,8**
GLC_09	14	11	3	9	7	12	10	10	9	8	7	17	**117**	**10,7**
GLC_10	0	1	1	11	10	10	13	19	14	20	9	7	**115**	**20,9**
GLC_11	19	13	12	18	16	19	19	28	27	26	20	18	**235**	**22,7**
GLC_12	3	4	2	6	10	2	2	5	7	11	5	7	**64**	**4,9**
GLC_13	3	3	0	3	5	4	6	7	7	7	5	4	**54**	**4,1**
GLC_14	1	1	1	1	0	5	1	6	6	4	3	0	**29**	**2,2**
GLC_15	7	8	10	16	14	20	20	23	22	21	24	22	**207**	**16,7**
GLC_16	0	2	1	1	1	4	4	4	4	1	3	3	**28**	**2,6**
GLC_17	10	8	5	13	12	7	12	11	4	8	11	10	**111**	**15,5**
GLC_18	8	12	16	12	17	15	9	13	13	20	8	15	**158**	**14,8**
GLC_19	2	0	1	1	0	2	3	3	4	4	8	0	**28**	**2,1**
GLC_20	12	9	8	14	19	22	18	18	27	18	17	17	**199**	**15,8**
GLC_21	3	1	3	3	6	7	9	12	10	12	15	11	**92**	**12,3**
GLC_22	33	22	22	21	25	32	32	34	30	27	28	30	**336**	**32,9**
TOTAL	**164**	**155**	**127**	**188**	**196**	**203**	**200**	**236**	**226**	**239**	**211**	**201**	**2346**	**11,0**

Table 5 : Number of BRDFs of the YEARLY database which are also present in the MONTHLY database (GLC2000-based).

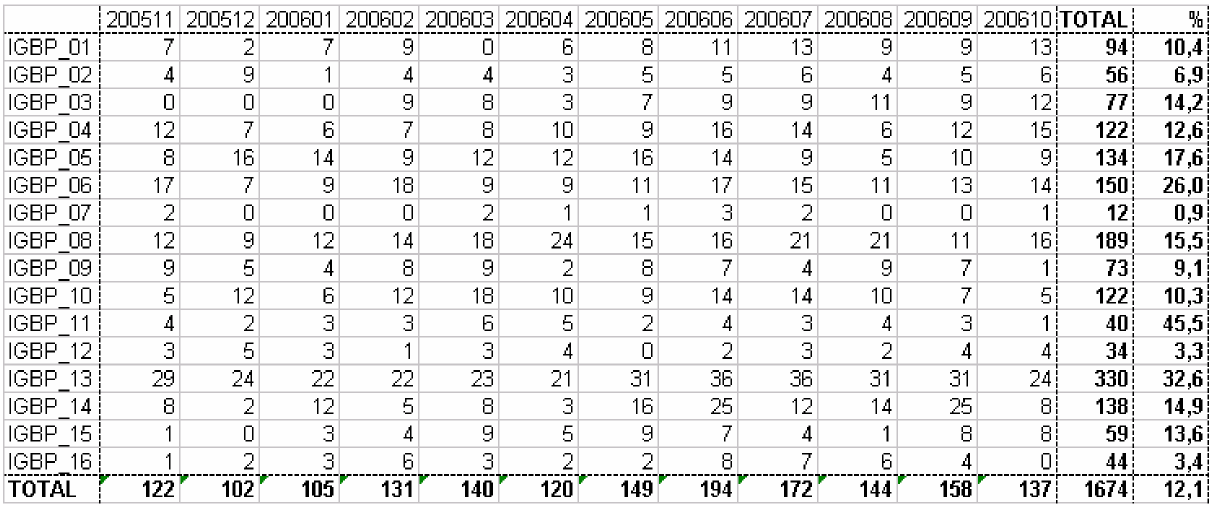

	200511	200512	200601	200602	200603	200604	200605	200606	200607	200608	200609	200610	TOTAL	%
IGBP_01	7	2	7	9	0	6	8	11	13	9	9	13	**94**	**10,4**
IGBP_02	4	9	1	4	4	3	5	5	6	4	5	6	**56**	**6,9**
IGBP_03	0	0	0	9	8	3	7	9	9	11	9	12	**77**	**14,2**
IGBP_04	12	7	6	7	8	10	9	16	14	6	12	15	**122**	**12,6**
IGBP_05	8	16	14	9	12	12	16	14	9	5	10	9	**134**	**17,6**
IGBP_06	17	7	9	18	9	9	11	17	15	11	13	14	**150**	**26,0**
IGBP_07	2	0	0	0	2	1	1	3	2	0	0	1	**12**	**0,9**
IGBP_08	12	9	12	14	18	24	15	16	21	21	11	16	**189**	**15,5**
IGBP_09	9	5	4	8	9	2	8	7	4	9	7	1	**73**	**9,1**
IGBP_10	5	12	6	12	18	10	9	14	14	10	7	5	**122**	**10,3**
IGBP_11	4	2	3	3	6	5	2	4	3	4	3	1	**40**	**45,5**
IGBP_12	3	5	3	1	3	4	0	2	3	2	4	4	**34**	**3,3**
IGBP_13	29	24	22	22	23	21	31	36	36	31	31	24	**330**	**32,6**
IGBP_14	8	2	12	5	8	3	16	25	12	14	25	8	**138**	**14,9**
IGBP_15	1	0	3	4	9	5	9	7	4	1	8	8	**59**	**13,6**
IGBP_16	1	2	3	6	3	2	2	8	7	6	4	0	**44**	**3,4**
TOTAL	**122**	**102**	**105**	**131**	**140**	**120**	**149**	**194**	**172**	**144**	**158**	**137**	**1674**	**12,1**

Table 6 : Number of BRDFs of the YEARLY database which are also present in the MONTHLY database (IGBP-based).

3 006 BRDFs are common to the GLC2000-based and IGBP-based MONTHLY databases, whereas only 243 BRDFs are common to the GLC2000-based and IGBP-based YEARLY databases.

Table 7 gives the number and the percentage of common BRDFs in the MONTHLY databases identified as similar ecosystems in both land cover maps. The percentage is high for the very well located biomes as urban surfaces (100%), snowy areas, and bare soils

(>94%). The agreement between the 2 land cover maps is good for the broadleaf evergreen forests (>96%), needleleaf evergreen forest (89%), and crop and cultivated regions (>76%). At the opposite, only 21% of BRDFs identified as herbaceous areas in the GLC2000 land cover map (GLC_13) selected in the IGBP-based database, belongs to the corresponding IGBP class (IGBP_10). None BRDF of GLC_03 (Open Broadleaf Deciduous Forest) selected in the IGBP-based database is classified in IGBP_04. Most of them (82%) are identified as Woody Savanna (IGBP_08).

Among the 243 pixels common to GLC_based and IGBP_based YEARLY database, 3 belongs to GLC_02 (Closed Broadleaf Deciduous Forest), and only 1 is identified as IGBP_04 (Broadleaf Deciduous Forest). Only 9 pixels are classified as Open Broadleaf Deciduous Forest (GLC_03), but they are identified as Woody savannas (IGBP_08) or Savannas (IGBP_09) on the IGBP land cover map. Likewise, only 1 of the 9 pixels classified as GLC_13 (Herbaceous cover) selected also in the IGBP_based YEARLY database are identified as grassland (IGBP_10), others are identified as Open shrubland (IGBP_07).

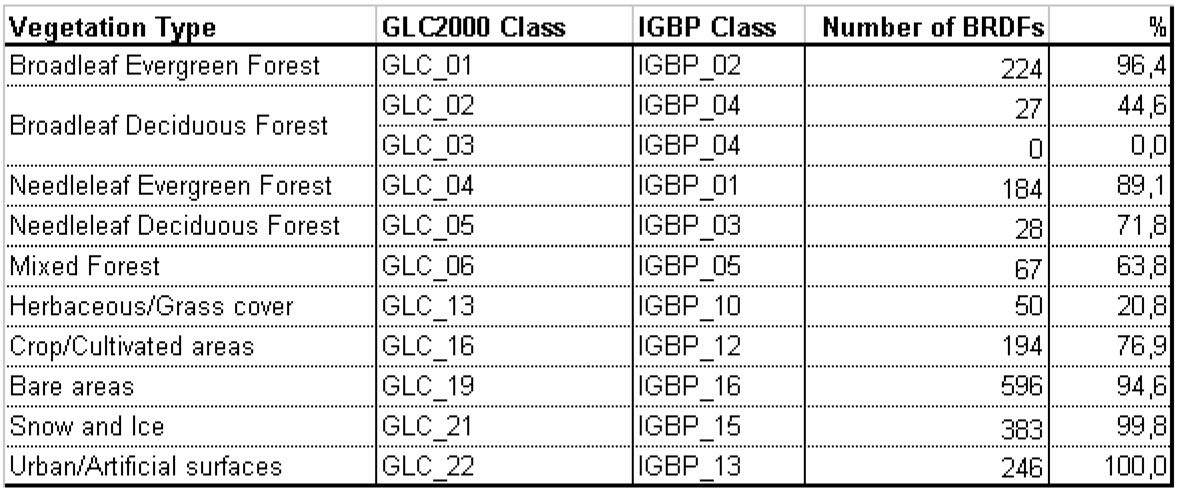

Vegetation Type	GLC2000 Class	IGBP Class	Number of BRDFs	%
Broadleaf Evergreen Forest	GLC_01	IGBP_02	224	96,4
Broadleaf Deciduous Forest	GLC_02	IGBP_04	27	44,6
	GLC_03	IGBP_04	0	0,0
Needleleaf Evergreen Forest	GLC_04	IGBP_01	184	89,1
Needleleaf Deciduous Forest	GLC_05	IGBP_03	28	71,8
Mixed Forest	GLC_06	IGBP_05	67	63,8
Herbaceous/Grass cover	GLC_13	IGBP_10	50	20,8
Crop/Cultivated areas	GLC_16	IGBP_12	194	76,9
Bare areas	GLC_19	IGBP_16	596	94,6
Snow and Ice	GLC_21	IGBP_15	383	99,8
Urban/Artificial surfaces	GLC_22	IGBP_13	246	100,0

Table 7 : Common BRDFs to both MONTHLY databases for some vegetation types. The last column gives the percentage of BRDFs of the GLC2000 class which belong to the corresponding IGBP class.

6.2. Spatial distribution of selected pixels

The 22 012 BRDFs of the GLC2000-based MONTHLY database and the 21 262 BRDFs of the GLC2000-based YEARLY database are shared between the 22 GLC2000 classes and the 12 months as presented in Table 8 and Table 9, respectively. 120 (30 * 4 bands of latitude) is the maximum of BRDFs that can be selected per month and per vegetation class. This happens at least one month for almost half of the GLC_2000 classes, especially during the spring and the summer of the Northern hemisphere. 90 BRDFs in a month means that this vegetation class is probably not present (as thematically homogeneous pixel) in one band of latitude. At the opposite, there are few cases with less than 30 pixels per month: it happens for GLC_07, all the year, GLC_08 (regularly flooded forests) and GLC_10 (Burnt areas). This is reliable since these vegetation types are minority biomes at global scale (Table 3).

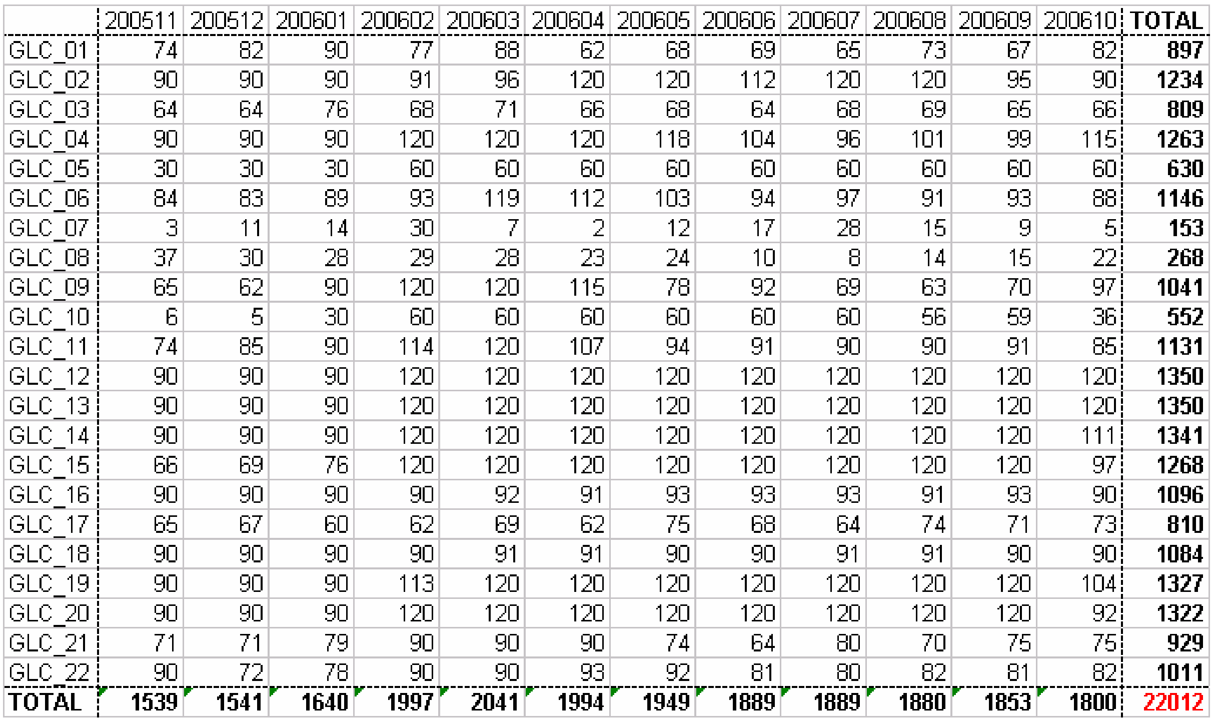

	200511	200512	200601	200602	200603	200604	200605	200606	200607	200608	200609	200610	**TOTAL**
GLC_01	74	82	90	77	88	62	68	69	65	73	67	82	**897**
GLC_02	90	90	90	91	96	120	120	112	120	120	95	90	**1234**
GLC_03	64	64	76	68	71	66	68	64	68	69	65	66	**809**
GLC_04	90	90	90	120	120	120	118	104	96	101	99	115	**1263**
GLC_05	30	30	30	60	60	60	60	60	60	60	60	60	**630**
GLC_06	84	83	89	93	119	112	103	94	97	91	93	88	**1146**
GLC_07	3	11	14	30	7	2	12	17	28	15	9	5	**153**
GLC_08	37	30	28	29	28	23	24	10	8	14	15	22	**268**
GLC_09	65	62	90	120	120	115	78	92	69	63	70	97	**1041**
GLC_10	6	5	30	60	60	60	60	60	60	56	59	36	**552**
GLC_11	74	85	90	114	120	107	94	91	90	90	91	85	**1131**
GLC_12	90	90	90	120	120	120	120	120	120	120	120	120	**1350**
GLC_13	90	90	90	120	120	120	120	120	120	120	120	120	**1350**
GLC_14	90	90	90	120	120	120	120	120	120	120	120	111	**1341**
GLC_15	66	69	76	120	120	120	120	120	120	120	120	97	**1268**
GLC_16	90	90	90	90	92	91	93	93	93	91	93	90	**1096**
GLC_17	65	67	60	62	69	62	75	68	64	74	71	73	**810**
GLC_18	90	90	90	90	91	91	90	90	91	91	90	90	**1084**
GLC_19	90	90	90	113	120	120	120	120	120	120	120	104	**1327**
GLC_20	90	90	90	120	120	120	120	120	120	120	120	92	**1322**
GLC_21	71	71	79	90	90	90	74	64	80	70	75	75	**929**
GLC_22	90	72	78	90	90	93	92	81	80	82	81	82	**1011**
TOTAL	**1539**	**1541**	**1640**	**1997**	**2041**	**1994**	**1949**	**1889**	**1889**	**1880**	**1853**	**1800**	**22012**

Table 8 : Distribution of BRDFs of the MONTHLY database per GLC2000 class and per month

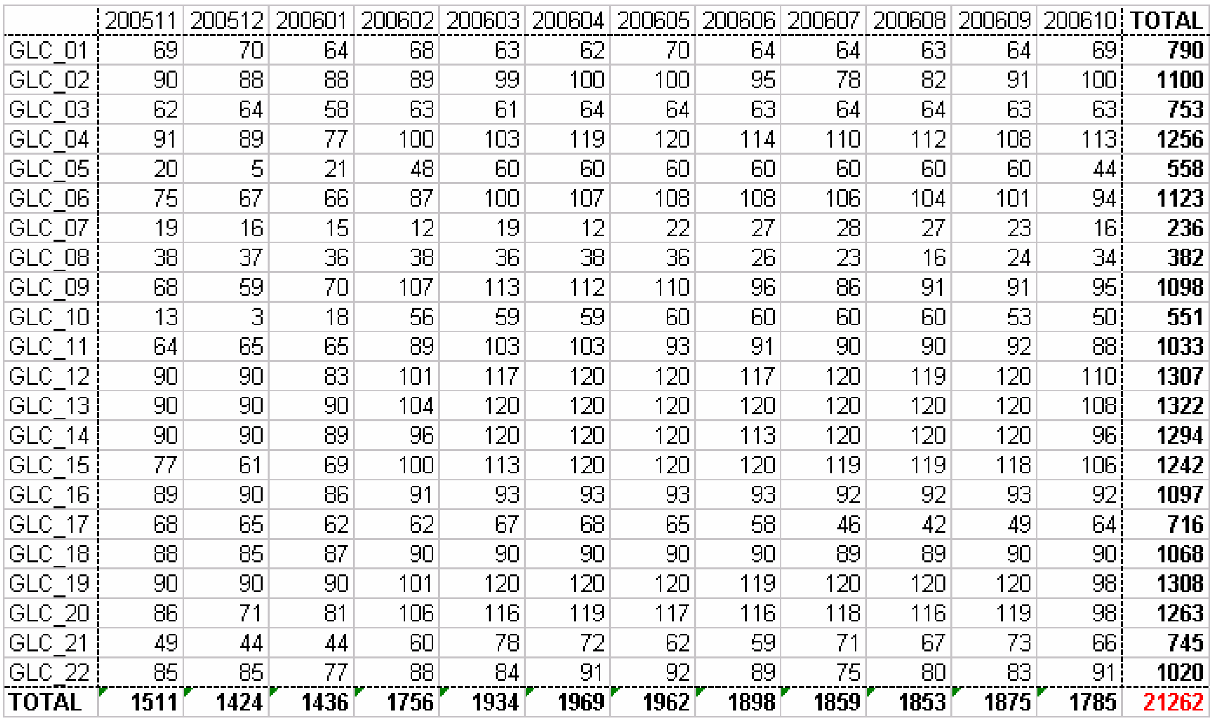

	200511	200512	200601	200602	200603	200604	200605	200606	200607	200608	200609	200610	**TOTAL**
GLC_01	69	70	64	68	63	62	70	64	64	63	64	69	**790**
GLC_02	90	88	88	89	99	100	100	95	78	82	91	100	**1100**
GLC_03	62	64	58	63	61	64	64	63	64	64	63	63	**753**
GLC_04	91	89	77	100	103	119	120	114	110	112	108	113	**1256**
GLC_05	20	5	21	48	60	60	60	60	60	60	60	44	**558**
GLC_06	75	67	66	87	100	107	108	108	106	104	101	94	**1123**
GLC_07	19	16	15	12	19	12	22	27	28	27	23	16	**236**
GLC_08	38	37	36	38	36	38	36	26	23	16	24	34	**382**
GLC_09	68	59	70	107	113	112	110	96	86	91	91	95	**1098**
GLC_10	13	3	18	56	59	59	60	60	60	60	53	50	**551**
GLC_11	64	65	65	89	103	103	93	91	90	90	92	88	**1033**
GLC_12	90	90	83	101	117	120	120	117	120	119	120	110	**1307**
GLC_13	90	90	90	104	120	120	120	120	120	120	120	108	**1322**
GLC_14	90	90	89	96	120	120	120	113	120	120	120	96	**1294**
GLC_15	77	61	69	100	113	120	120	120	119	119	118	106	**1242**
GLC_16	89	90	86	91	93	93	93	93	92	92	93	92	**1097**
GLC_17	68	65	62	62	67	68	65	58	46	42	49	64	**716**
GLC_18	88	85	87	90	90	90	90	90	89	89	90	90	**1068**
GLC_19	90	90	90	101	120	120	120	119	120	120	120	98	**1308**
GLC_20	86	71	81	106	116	119	117	116	118	116	119	98	**1263**
GLC_21	49	44	44	60	78	72	62	59	71	67	73	66	**745**
GLC_22	85	85	77	88	84	91	92	89	75	80	83	91	**1020**
TOTAL	**1511**	**1424**	**1436**	**1756**	**1934**	**1969**	**1962**	**1898**	**1859**	**1853**	**1875**	**1785**	**21262**

Table 9 : Distribution of BRDFs of the YEARLY database per GCL2000 class and per month

The 14 649 BRDFs of the IGBP-based MONTHLY database and the 13 887 BRDFs of the IGBP-based YEARLY database are shared between the 16 IGBP classes and the 12 months as presented in Table 10 and Table 11. Only a quarter of the classes display a maximum of BRDFs (120) at least one month in both databases. That never happens for forest classes (IGBP_01 to IGBP_05). Then, there is almost 49% more BRDFs of forests in the GLC-based MONTHLY database than in the IGBP-based MONTHLY database. This is larger than the difference noted on the thematically-homogeneous pixels (§3.1). Likewise, although IGBP displays much more homogeneous shrubland pixels than GLC2000 (Table 3), the number of BRDFs for classes IGBP_06 and IGBP_07 is lesser than the number of BRDFs for corresponding GLC2000 classes (GLC_11 and GLC12). IGBP_07 is a majority class, and IGBP_06 a minority class not present in the Northern latitudes. At the opposite, GLC_11 and GLC_12 are medium classes (in terms of spatial coverage) and are present in all bands of latitude. The methodology of selection, with a number maximum of pixels pre-selected by class and by band of latitude (§3.2), favours the second case.

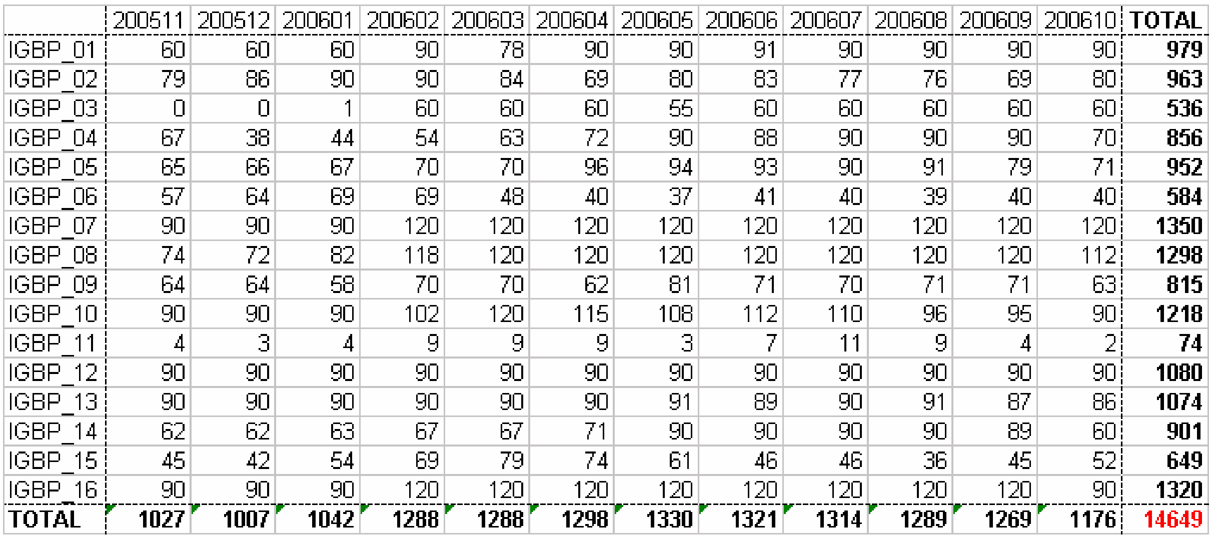

	200511	200512	200601	200602	200603	200604	200605	200606	200607	200608	200609	200610	**TOTAL**
IGBP_01	60	60	60	90	78	90	90	91	90	90	90	90	**979**
IGBP_02	79	86	90	90	84	69	80	83	77	76	69	80	**963**
IGBP_03	0	0	1	60	60	60	55	60	60	60	60	60	**536**
IGBP_04	67	38	44	54	63	72	90	88	90	90	90	70	**856**
IGBP_05	65	66	67	70	70	96	94	93	90	91	79	71	**952**
IGBP_06	57	64	69	69	48	40	37	41	40	39	40	40	**584**
IGBP_07	90	90	90	120	120	120	120	120	120	120	120	120	**1350**
IGBP_08	74	72	82	118	120	120	120	120	120	120	120	112	**1298**
IGBP_09	64	64	58	70	70	62	81	71	70	71	71	63	**815**
IGBP_10	90	90	90	102	120	115	108	112	110	96	95	90	**1218**
IGBP_11	4	3	4	9	9	9	3	7	11	9	4	2	**74**
IGBP_12	90	90	90	90	90	90	90	90	90	90	90	90	**1080**
IGBP_13	90	90	90	90	90	90	91	89	90	91	87	86	**1074**
IGBP_14	62	62	63	67	67	71	90	90	90	90	89	60	**901**
IGBP_15	45	42	54	69	79	74	61	46	46	36	45	52	**649**
IGBP_16	90	90	90	120	120	120	120	120	120	120	120	90	**1320**
TOTAL	**1027**	**1007**	**1042**	**1288**	**1288**	**1298**	**1330**	**1321**	**1314**	**1289**	**1269**	**1176**	**14649**

Table 10 : Distribution of BRDFs of the MONTHLY database per IGBP class and per month

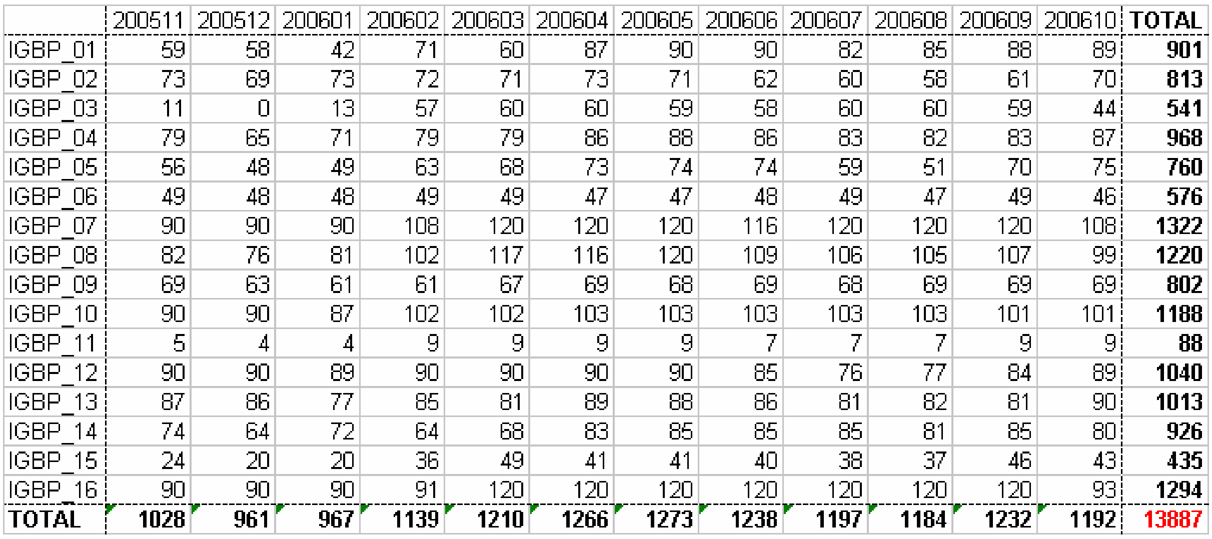

	200511	200512	200601	200602	200603	200604	200605	200606	200607	200608	200609	200610	**TOTAL**
IGBP_01	59	58	42	71	60	87	90	90	82	85	88	89	**901**
IGBP_02	73	69	73	72	71	73	71	62	60	58	61	70	**813**
IGBP_03	11	0	13	57	60	60	59	58	60	60	59	44	**541**
IGBP_04	79	65	71	79	79	86	88	86	83	82	83	87	**968**
IGBP_05	56	48	49	63	68	73	74	74	59	51	70	75	**760**
IGBP_06	49	48	48	49	49	47	47	48	49	47	49	46	**576**
IGBP_07	90	90	90	108	120	120	120	116	120	120	120	108	**1322**
IGBP_08	82	76	81	102	117	116	120	109	106	105	107	99	**1220**
IGBP_09	69	63	61	61	67	69	68	69	68	69	69	69	**802**
IGBP_10	90	90	87	102	102	103	103	103	103	103	101	101	**1188**
IGBP_11	5	4	4	9	9	9	9	7	7	7	9	9	**88**
IGBP_12	90	90	89	90	90	90	90	85	76	77	84	89	**1040**
IGBP_13	87	86	77	85	81	89	88	86	81	82	81	90	**1013**
IGBP_14	74	64	72	64	68	83	85	85	85	81	85	80	**926**
IGBP_15	24	20	20	36	49	41	41	40	38	37	46	43	**435**
IGBP_16	90	90	90	91	120	120	120	120	120	120	120	93	**1294**
TOTAL	**1028**	**961**	**967**	**1139**	**1210**	**1266**	**1273**	**1238**	**1197**	**1184**	**1232**	**1192**	**13887**

Table 11 : Distribution of BRDFs of the YEARLY database per IGBP class and per month

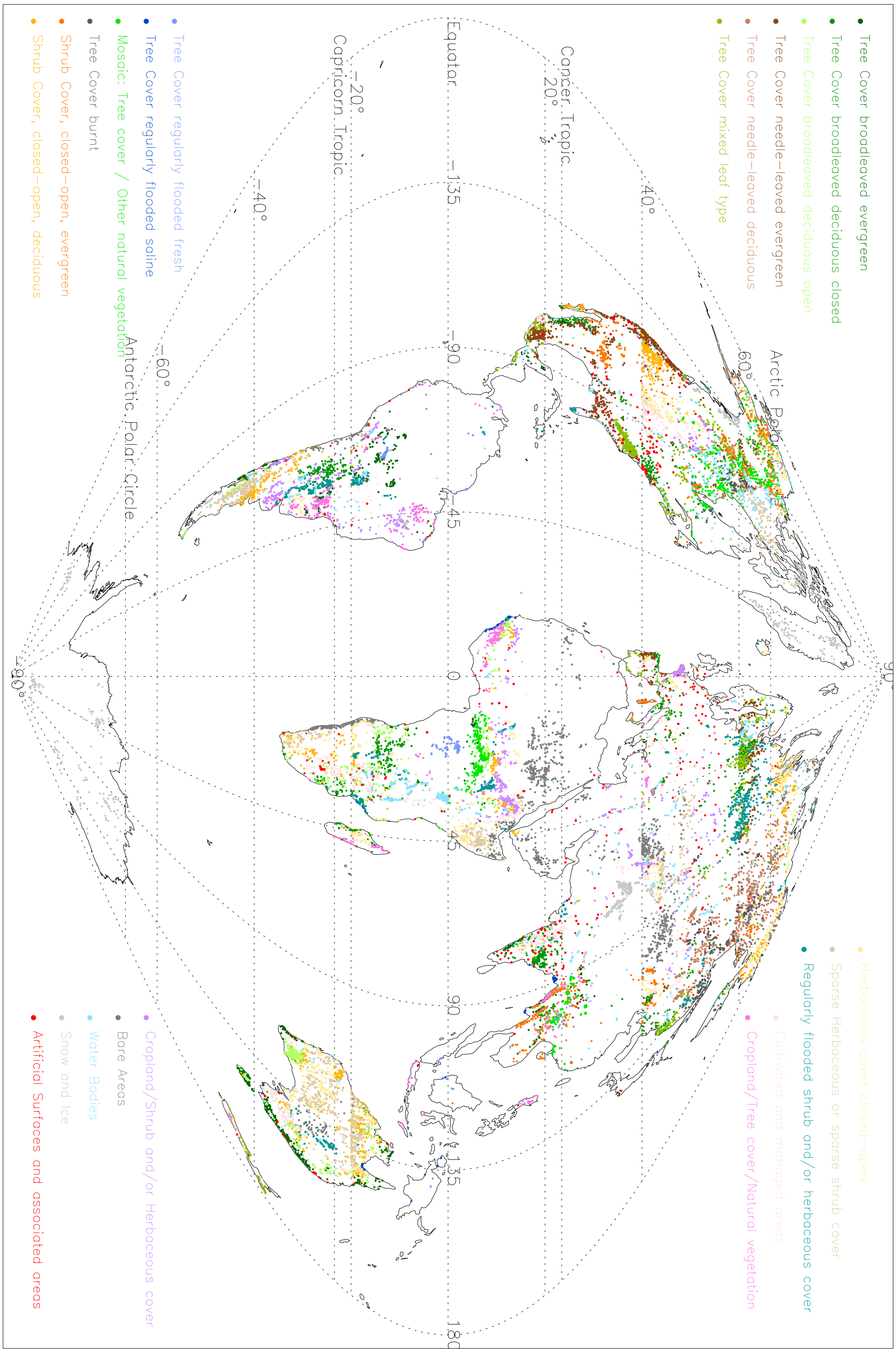
Tree Cover broadleaved evergreen
Tree Cover broadleaved deciduous closed
Tree Cover broadleaved deciduous open
Tree Cover needle−leaved evergreen
Tree Cover needle−leaved deciduous
Tree Cover mixed leaf type
Tree Cover regularly flooded fresh
Tree Cover regularly flooded saline
Mosaic: Tree cover / Other natural vegetation
Tree Cover burnt
Shrub Cover, closed−open, evergreen
Shrub Cover, closed−open, deciduous
Herbaceous cover, closed−open
Sparse Herbaceous or sparse shrub cover
Regularly flooded shrub and/or herbaceous cover
Cultivated and managed areas
Cropland/Tree cover/Natural vegetation
Cropland/Shrub and/or Herbaceous cover
Bare Areas
Water Bodies
Snow and Ice
Artificial Surfaces and associated areas
Arctic Polar Circle
Cancer Tropic
Equator
Capricorn Tropic
Antarctic Polar Circle
60°
40°
20°
−20°
−40°
−60°
90°
−90°
−135
−90
−45
0
45
90
135
180

Figure 6 : Location of the 22 012 pixels of the GLC2000-based MONTHLY database.

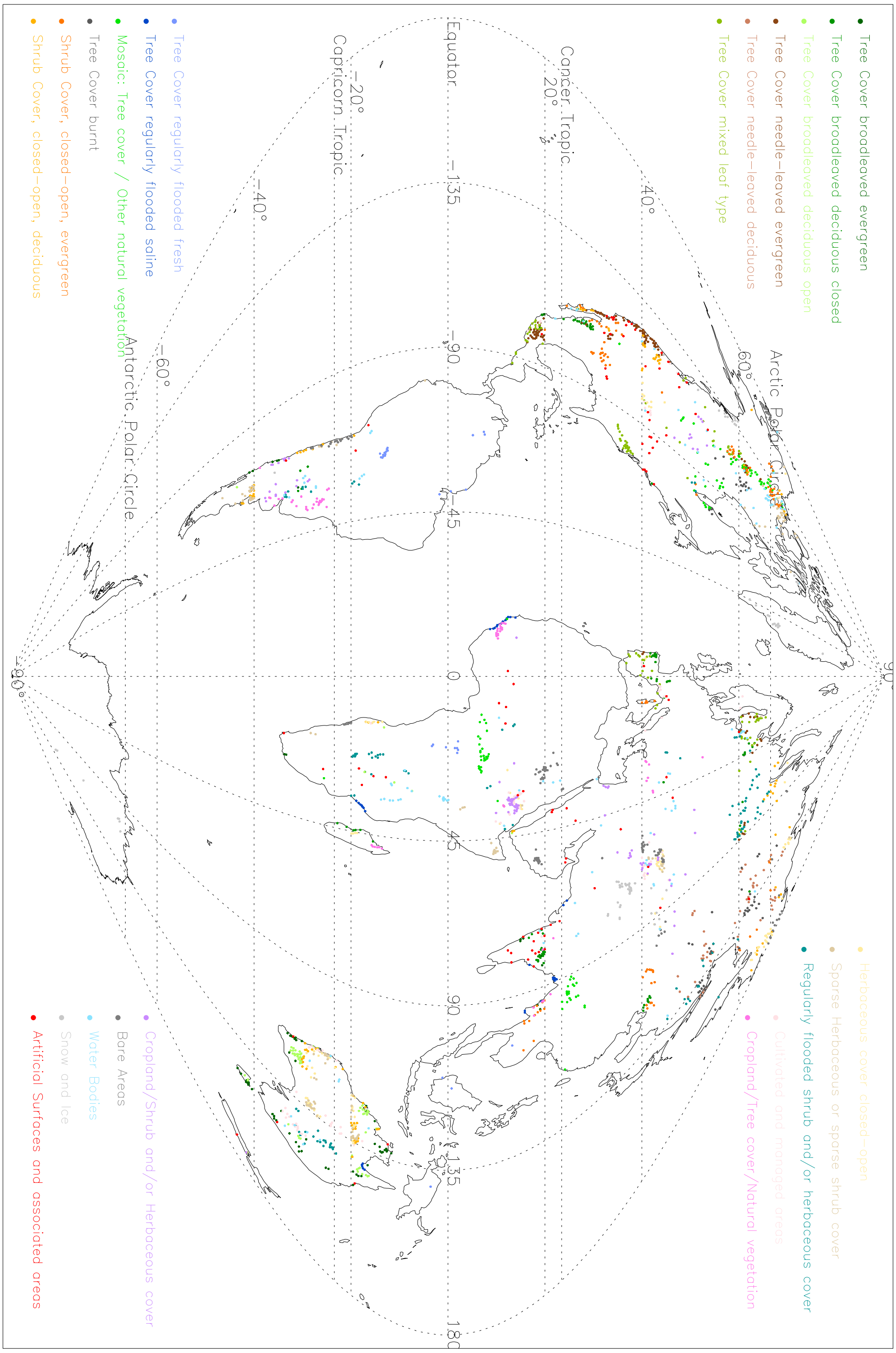
Tree Cover broadleaved evergreen
Tree Cover broadleaved deciduous closed
Tree Cover broadleaved deciduous open
Tree Cover needle-leaved evergreen
Tree Cover needle-leaved deciduous
Tree Cover mixed leaf type
Tree Cover regularly flooded fresh
Tree Cover regularly flooded saline
Mosaic: Tree cover / Other natural vegetation
Tree Cover burnt
Shrub Cover, closed-open, evergreen
Shrub Cover, closed-open, deciduous
Herbaceous cover, closed-open
Sparse Herbaceous or sparse shrub cover
Regularly flooded shrub and/or herbaceous cover
Cultivated and managed areas
Cropland/Tree cover/Natural vegetation
Cropland/Shrub and/or Herbaceous cover
Bare Areas
Water Bodies
Snow and Ice
Artificial Surfaces and associated areas
Arctic Polar Circle
Cancer Tropic
Equator
Capricorn Tropic
Antarctic Polar Circle
60°
40°
20°
−20°
−40°
−60°
90°
−90°
−135
−90
−45
0
45
90
135
180

Figure 7 : Location of the 2 016 different pixels of the GLC2000-based YEARLY database

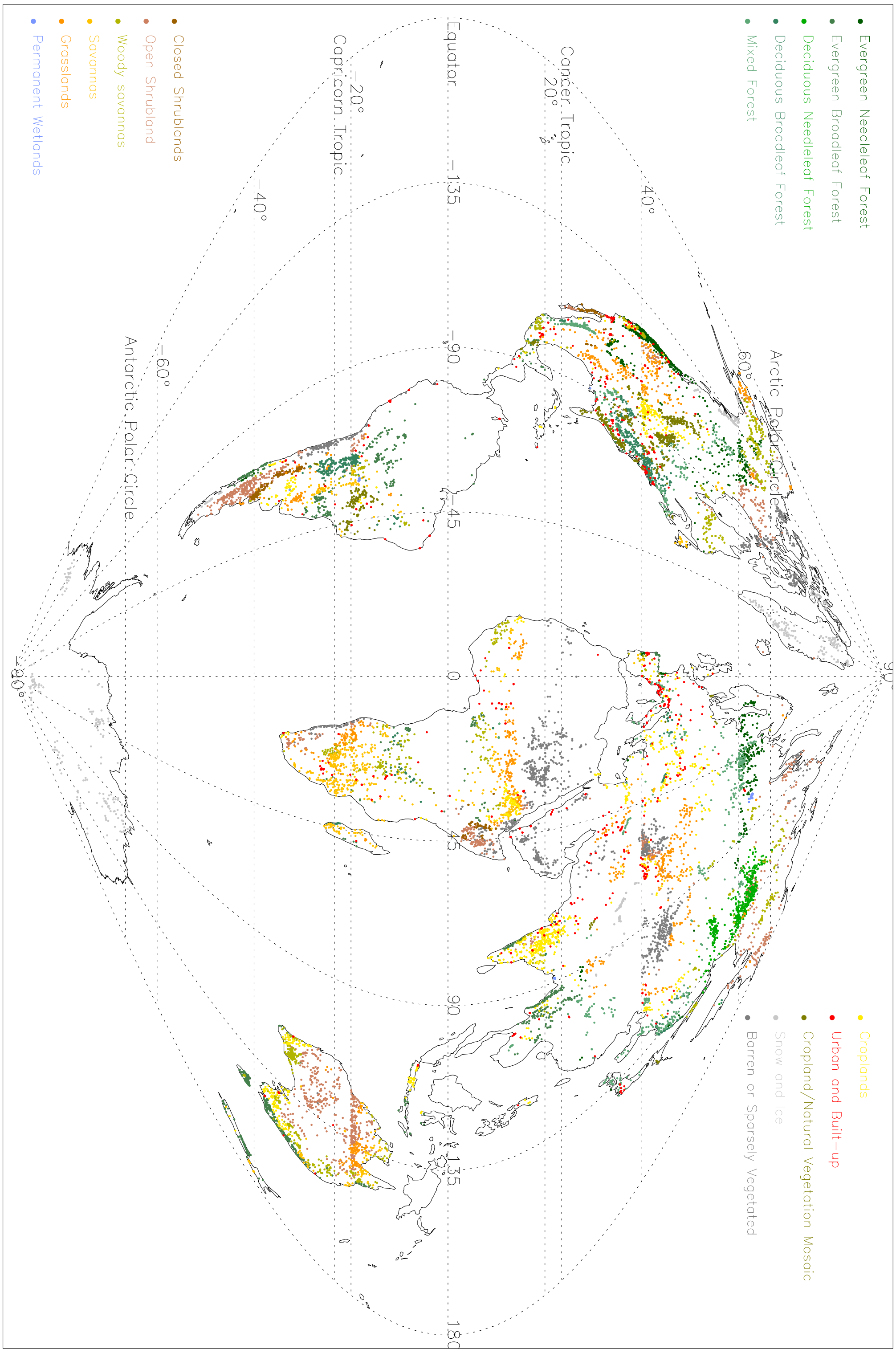
Evergreen Needleleaf Forest
Evergreen Broadleaf Forest
Deciduous Needleleaf Forest
Deciduous Broadleaf Forest
Mixed Forest
Closed Shrublands
Open Shrubland
Woody savannas
Savannas
Grasslands
Permanent Wetlands
Croplands
Urban and Built-up
Cropland/Natural Vegetation Mosaic
Snow and Ice
Barren or Sparsely Vegetated
Arctic Polar Circle
60°
40°
Cancer Tropic
20°
Equator
−20°
Capricorn Tropic
−40°
−60°
Antarctic Polar Circle
−135
−90
−45
0
45
90
135
180
90°
−90°

Figure 8 : Location of the 14 649 pixels of the IGBP-based MONTHLY database.

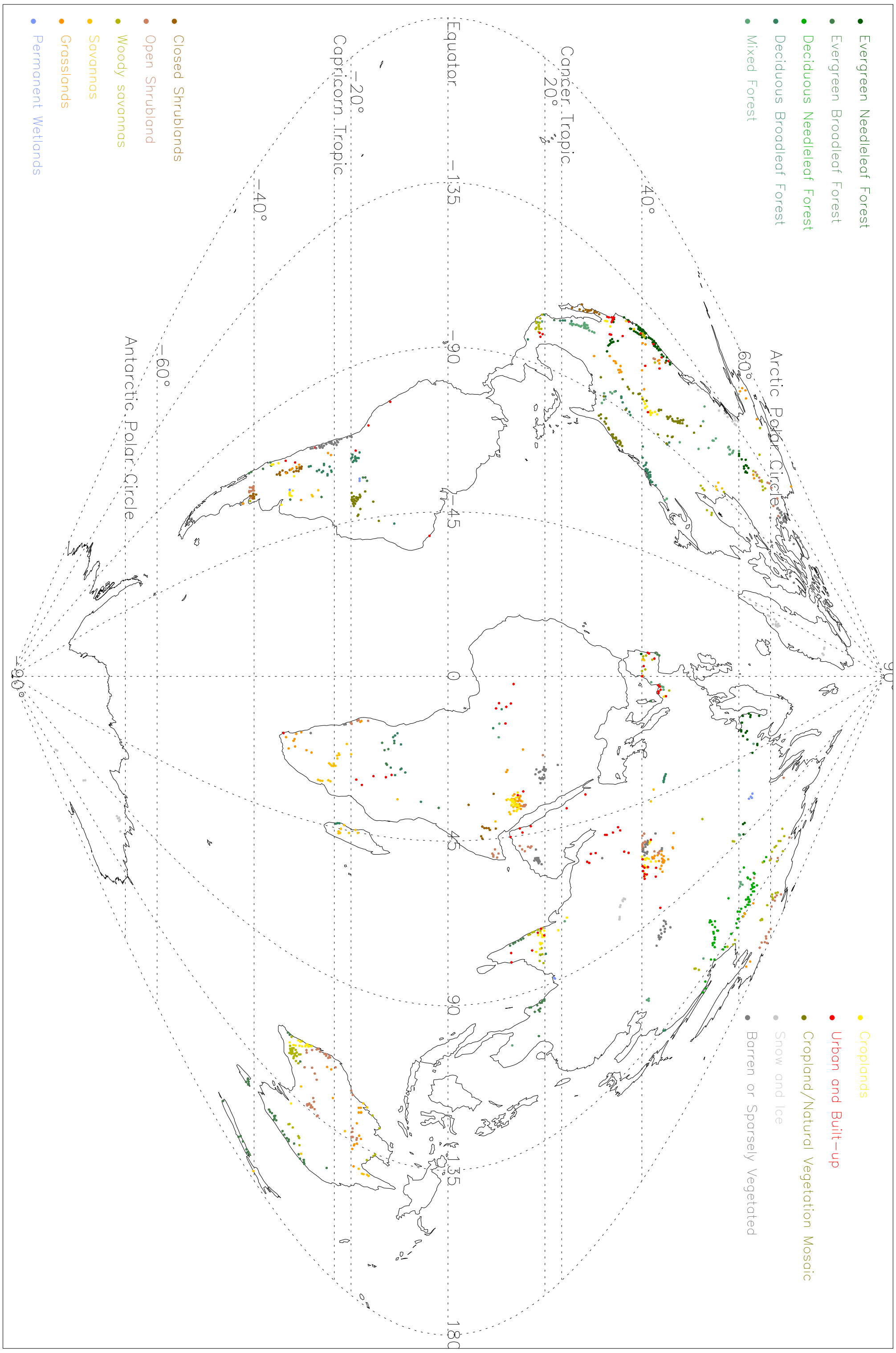
Evergreen Needleleaf Forest
Evergreen Broadleaf Forest
Deciduous Needleleaf Forest
Deciduous Broadleaf Forest
Mixed Forest
Closed Shrublands
Open Shrubland
Woody savannas
Savannas
Grasslands
Permanent Wetlands
Croplands
Urban and Built−up
Cropland/Natural Vegetation Mosaic
Snow and Ice
Barren or Sparsely Vegetated
Arctic Polar Circle
Cancer Tropic
Equator
Capricorn Tropic
Antarctic Polar Circle
90°
60°
40°
20°
−20°
−40°
−60°
−90°
−135
−90
−45
0
45
90
135
180

Figure 9 : Location of the 1 299 different pixels of the IGBP-based YEARLY database.

Figure 6 displays the spatial distribution of the 22 012 selected pixels of the GLC2000-based MONTHLY database. Very few of them are located in the equatorial region because of the cloudiness and of the PARASOL field of view. The band of latitude between the Cancer Tropic and 40°N in Africa and Asia is also under-sampled. At the opposite, the medium and high latitudes are well-sampled, especially in America. In Europe, the under-sampling is related to the non homogeneity of pixels (Figure 2). The discontinuity of the sampling appears at the limits of bands of latitudes like at 60° North in Eurasia, at 40° North in USA and 20° South in Australia. The same comments are generally valid for the spatial distribution of the 14 649 BRDFs of the IGBP-based MONTHLY database (Figure 8), the 2 016 different pixels of the GLC2000-based YEARLY database (Figure 7), and the 1 299 different pixels of the IGBP-based YEARLY database (Figure 9).

6.3. Temporal distribution of selected pixels

Some pixels of the GLC2000-based and IGBP-based MONTHLY databases are selected at several months. For all the vegetation classes, the percentage of pixels having at least 2 BRDFs reaches 10% in the both MONTHLY databases. It is not appropriate to perform relevant analysis to monitor the temporal evolution of the surface. That's why the YEARLY databases have been elaborated. They contain all the available (according to the criteria described in Section 3) monthly BRDFs of 2 016 different pixels (GLC2000-based database) and 1 299 different pixels (IGBP-based database) acquired during one year.

Table 12 and Table 13 analyse the temporal distribution of the BRDFs of the GLC2000-based and IGBP-based YEARLY databases, respectively. Only IGBP_03 (Deciduous Needleleaf forest) have no pixels with 12 BRDFs, i.e. one per month, describing a complete vegetative cycle. Only GLC_07 (forest regularly flooded by fresh water), GLC_09 (Mosaic: tree/other natural vegetation), IGBP_02 (Evergreen Broadleaf Forest), and IGBP_15 (Snow and Ice) contain pixels having only 5 BRDFs which is the minimum required by the method of selection. At the opposite, the GLC_18 (Mosaic: crop/shrub/grass), GLC_03 (Broadleaf Deciduous Open Forest), and IGBP_06 (Closed Shrubland) are the vegetation types with the best temporal sampling. IGBP_15 (Snow and Ice), GLC_07 (forest regularly flooded by fresh water), IGBP_02 (Evergreen Broadleaf Forest) contain numerous pixels (~20%, ~17%, and ~16%, respectively) with no BRDF during a long period (more than 5 months).

We can also note that 1 IGBP class (IGBP_06: Closed Shrubland), and 2 GLC classes (GLC_03: Broadleaf Deciduous Open Forest and GLC_18: Mosaic crop/shrub and/or grass) contains no pixels without BRDF during more than 2 successive months. 3 IGBP classes (IGBP_06, IGBP_09: savannas, IGBP_11: permanent wetland), and only 2 GLC classes (GLC_18, GLC_03: Broadleaf Deciduous Open forest) contain pixels having N BRDFs with $9 \leq N < 12$. Finally, 9 IGBP classes (IGBP_03, IGBP_04: Deciduous Braodleaf Forest, IGBP_06, IGBP_07: Open shrubland, IGBP_09, IGBP_10: grassland, IGBP_11, IGBP_12: cropland, IGBP_16: Barren and sparsely vegetated), and 10 GLC classes (GLC_03, GLC_05: Needleleaf deciduous forest, GLC_10: Burnt tree cover; GLC_12: Deciduous shrubland; GLC_13: Herbaceous cover; GLC_14: Sparse herbaceous or sparse shrubland, GLC_15: regularly flooded shrub and/or grass, GLC_16: cultivated and managed areas, GLC_18,GLC_19: bare areas) contain no pixels without BRDF during more than 5 months.

This general result has to be detailed with a comparison per thematic class. Table 14 gives the best database considering each criterium for similar vegetation types. For the majority of comparisons, the GLC2000-based YEARLY database presents the best temporal sampling, especially for the forest classes.

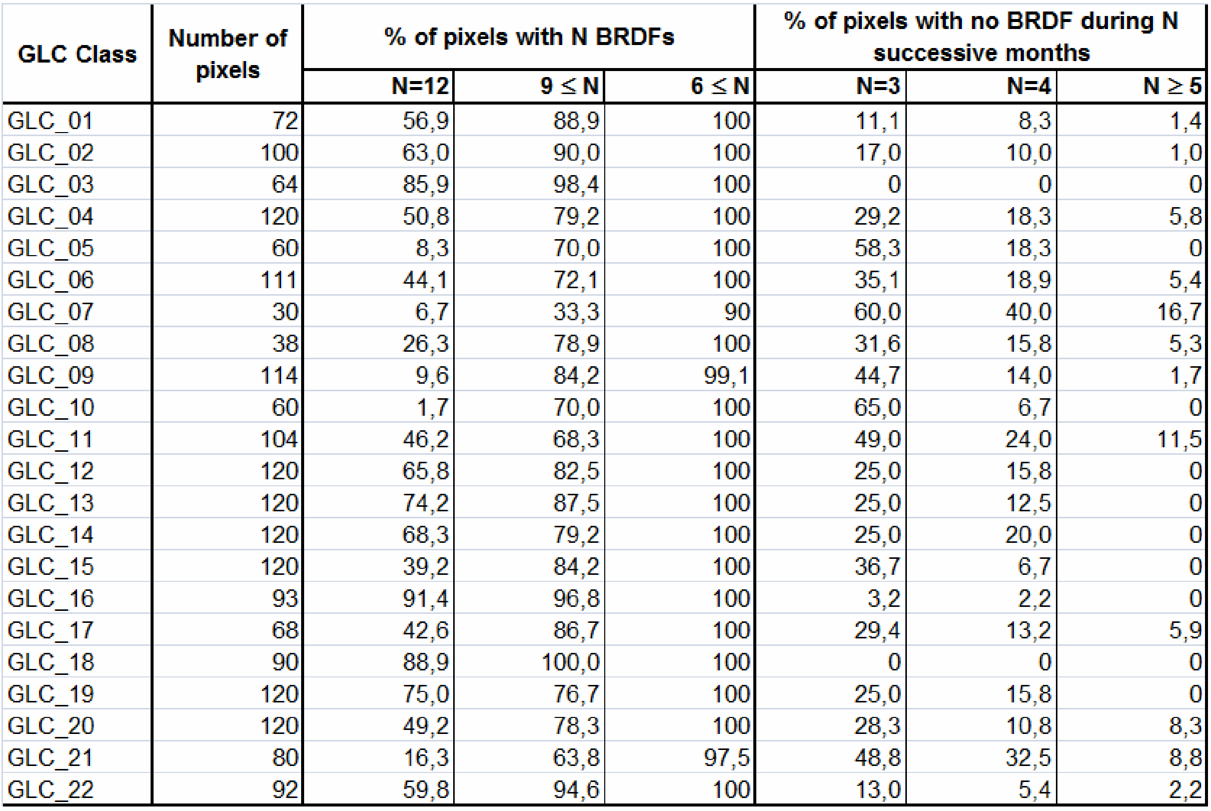

GLC Class	Number of pixels	% of pixels with N BRDFs			% of pixels with no BRDF during N successive months		
		N=12	9 ≤ N	6 ≤ N	N=3	N=4	N ≥ 5
GLC_01	72	56,9	88,9	100	11,1	8,3	1,4
GLC_02	100	63,0	90,0	100	17,0	10,0	1,0
GLC_03	64	85,9	98,4	100	0	0	0
GLC_04	120	50,8	79,2	100	29,2	18,3	5,8
GLC_05	60	8,3	70,0	100	58,3	18,3	0
GLC_06	111	44,1	72,1	100	35,1	18,9	5,4
GLC_07	30	6,7	33,3	90	60,0	40,0	16,7
GLC_08	38	26,3	78,9	100	31,6	15,8	5,3
GLC_09	114	9,6	84,2	99,1	44,7	14,0	1,7
GLC_10	60	1,7	70,0	100	65,0	6,7	0
GLC_11	104	46,2	68,3	100	49,0	24,0	11,5
GLC_12	120	65,8	82,5	100	25,0	15,8	0
GLC_13	120	74,2	87,5	100	25,0	12,5	0
GLC_14	120	68,3	79,2	100	25,0	20,0	0
GLC_15	120	39,2	84,2	100	36,7	6,7	0
GLC_16	93	91,4	96,8	100	3,2	2,2	0
GLC_17	68	42,6	86,7	100	29,4	13,2	5,9
GLC_18	90	88,9	100,0	100	0	0	0
GLC_19	120	75,0	76,7	100	25,0	15,8	0
GLC_20	120	49,2	78,3	100	28,3	10,8	8,3
GLC_21	80	16,3	63,8	97,5	48,8	32,5	8,8
GLC_22	92	59,8	94,6	100	13,0	5,4	2,2

Table 12 : Distribution over the year of BRDFs in the GLC2000-based YEARLY database.

Annex2 displays examples of multi-temporal BRDFs of pixels selected in both YEARLY databases. They allows following the evolution of the BRDF shape according to the vegetation cycle and the changes of the surface properties. The hot spot effect is well marked by a strong increase of the spectral reflectances (Annex2_1, Annex2_2, Annex2_4), whereas the minimum of reflectance in the forward directions is also clearly displayed on vegetated areas. The BRDFs of snowy areas present very high reflectances, with maximum values in the forward directions (Annex2_ 8). The pixels located in highest latitudes, Northern or Southern, do not have BRDFs during the winter time due to permanent cloud coverage (Annex2_1, Annex2_3, Annex2_ 8). We can also see the presence of snow mixed with vegetation on the multi-temporal BRDF of needleleaf forests located over 50°N (Annex2_1, Annex2_3).

IGBP Class	Number of pixels	% of pixels with N BRDFs			% of pixels with no BRDF during N successive months		
		N=12	9 ≤ N	6 ≤ N	N=3	N=4	N ≥ 5
IGBP_01	90	25,6	76,7	100	35,5	20,0	10,0
IGBP_02	80	43,8	68,8	98,8	30,0	27,5	16,3
IGBP_03	60	0,0	71,7	100	68,3	5,0	0
IGBP_04	88	51,1	94,3	100	9,1	4,5	0
IGBP_05	75	29,3	84,0	100	36,0	13,3	4,0
IGBP_06	49	83,7	100,0	100	0	0	0
IGBP_07	120	71,7	88,3	100	25,0	10,0	0
IGBP_08	120	42,5	75,8	100	40,0	18,3	1,7
IGBP_09	69	71,0	100,0	100	1,4	0	0
IGBP_10	103	84,5	96,1	100	12,6	1,0	0
IGBP_11	9	11,1	100,0	100	66,7	0	0
IGBP_12	90	83,3	94,4	100	6,7	4,4	0
IGBP_13	90	70,0	93,3	100	12,2	5,6	2,2
IGBP_14	85	60,0	89,4	100	14,1	7,1	3,5
IGBP_15	51	9,8	47,1	96,1	72,5	49,0	19,6
IGBP_16	120	75,0	75,0	100	25,0	24,2	0

Table 13 : Distribution over the year of BRDFs in the IGBP-based YEARLY database.

Thematic Classes	% of pixels with N BRDFs	% of pixels with no BRDF during N successive months
GLC_01 vs IGBP_02	GLC	GLC
GLC_02+GLC_03 vs IGBP_04	GLC	GLC
GLC_04 vs IGBP_01	GLC	GLC
GLC_05 vs IGBP_03	GLC	IGBP
GLC_06 vs IGBP_05	IGBP	IGBP
GLC_13 vs IGBP_10	IGBP	IGBP
GLC_16 vs IGBP_12	GLC	GLC
GLC_19 vs IGBP_16	GLC	GLC
GLC_21 vs IGBP_15	GLC	GLC
GLC_22 vs IGBP_13	IGBP	IGBP

Table 14 : Summary of comparison for similar GLC and IGBP vegetation classes

6.4. Thematic content of the selected pixels

In the POLDER-2 database, we noted that some pixels are clearly misclassified: the BRDF features and the NDVI values did not agree with the vegetation class (Lacaze, 2006). Here, in the POLDER-3 databases, these cases are reduced because of the criterium on the pixel homogeneity (§ 3.1). For example, 7% (8,3%) of the pixels identified as bare soils in the GLC2000-based MONTHLY database (IGBP-based MONTHLY database) display NDVI values larger than 0.2. Likewise, only 5.3% (0.1%) of pixels identified as broadleaf evergreen forest in the GLC2000-based MONTHLY database (IGBP-based MONTHLY database) give an NDVI lesser than 0.5. Although that improvement, some misclassifications still exist. The easiest ones to detect concern the “Snow and Ice” areas, and the “Water Bodies”. Some typical examples are presented in Annex3.

Annex3_ 1 and Annex3_ 2 show the multi-temporal BRDF of 2 pixels identified as “Snow and Ice” by IGBP and GLC2000, respectively, which are obviously not permanent snowy areas. The BRDFs give the seasonal variations of the surface. For the first one, the snow which fully covers the surface in winter, melts slowly in May and June to make way to tundra vegetation, likely. For the second one, located in the Rockies, the BRDFs, which do not indicate the presence of snow for the full year, is typical of a vegetation with a well-marked vegetative cycle (the NDVI is larger than 0.7 in May and June).

Annex3_ 3 shows the multi-temporal BRDF of a pixel identified as “Water Bodies” by GLC2000 and located in Australia. The reflectance values are high, the BRDF displays a strong hot spot peak but no glitter effect which is the typical feature translating the water presence on the surface. The pixel could be an area of bright soil covered by sparse vegetation (the NDVI varies from 0.1 to 0.4). On Annex3_ 4, we can see the multi-temporal BRDFs of a mixed (water + vegetation) pixel, which displays both a strong hot spot phenomenon and a glitter effect in the forward direction. Even if there is a water pond on the pixel surface, the directional signature and the magnitude of reflectance are clearly driven by the vegetation contribution.

6.5. Analysis of the BPDF

The shape of BPDF is similar for all types of surfaces: at a given sun angle, the polarized reflectance increases from the backscattering directions to the forward scattering directions. The minimum around the backscattering direction is due to the fact that polarization is mostly generated by specular reflection, whose degree of polarization is null for a nadir incidence. Note however that negative polarization (i.e. polarization parallel to the scattering plane) is observed, which can not be explained by single reflectance or scattering process.

The polarized reflectance is low, even negative in the back-scattering direction (Annex4_ 1, Annex4_ 2, Annex4_ 7). Its magnitude, for the given angular conditions, is larger for bare soil (Annex4_ 6) than for vegetated areas (Annex4_ 1, Annex4_ 4,

Annex4_ 5). When polarizing surfaces as water ponds or lakes are present in the pixel, the BPDF display a “glitter” effect in the specular direction (Annex4_ 1 bottom, Annex4_ 3 top, Annex4_ 6 bottom). We can note that the maximum of polarized reflectance is obtained in the specular direction over a snowy pixel (Annex4_ 7).

6.6. Some potential uses of the databases

The BRDFs of the databases provide detailed information about the angular properties of the land surface ecosystems. Measurements acquired in the principal plane, where the

BRDFs display its sharpest features, show the great potential of these data. As examples, Figure 10, and Figure 11 present spectral directional signatures of 8 various ecosystems at different time periods. The graphs show that reflectances at 565nm are higher than reflectances at 670nm for well vegetated areas (forests, cropland) where NDVI is high. When the influence of soil background increases, the reflectance at 670nm is close (cropland) or higher (shrubland, grassland) than the reflectance at 565nm. The principal plane displays the main patterns of the BRDF: the peak of reflectance in the hot spot direction, and the glitter effect, when water is located in the pixel, with a magnitude almost equal to the hot spot intensity. The BRDF of “Snow and Ice” pixels exhibits well distinct spectral profiles with maximum of reflectances at 490nm and minimum at 1020nm. The specific bowl shape shows an increase of reflectance in the forward direction, which translates the presence of a thin layer of water at the surface. As we have already noted on the BRDF showed in Annexes, the signatures in the principal plane are very smooth. This is due to the removal of disturbed orbit during the procedure of selection.

Such directional measurements can be very useful for many applications. They have already used to investigate the retrieval of structural parameters of the vegetation or to quantify the spatial distribution of major elements of landscape (Lacaze et al., 2002; Chen et al., 2003) in order to improve the assessment of the leaf area index (Chen et al., 2005), which is a biophysical parameter of major interest for many environmental applications. These databases are also unique and essential tools for testing the abilities of radiative transfer models to simulate the directional effects.

The POLDER-3 BRDF databases are essential tools for testing the abilities of radiative transfer models to simulate the directional properties of the surface with the aim, for instance, to correct the bi-directional effects. Such application can be achieved with the linear reflectance model of Maignan et al. (2004), used for selecting these BRDFS, and also used in the POLDER-3/PARASOL Land Surface operational processing line to normalise the directional measurements. Annex5 presents examples of the measured BRDF, the simulated one after inversion of the Maignan model, and a scatter-plot comparing the both for 3 wavebands. The quality of the inversion depends on the ecosystem and its specificities. The model reproduces very well the sharp peak of reflectance of the hot spot phenomenon (e.g.Annex5_ 1, Annex5_ 3, Annex5_ 5, Annex5_ 8, Annex5_ 9, Annex5_ 10, Annex5_ 11, Annex5_ 12) because of the hotspot module (Bréon et al., 2002) merged with the Ross_thick kernel. The model cannot simulate the glitter effect when some water is on the surface (Annex5_ 13). The model is well adapted to reproduce the directional signature of discontinuous landscapes (Annex5_ 8, Annex5_ 9, Annex5_ 10). The best results of the inversion are obtained in the near infrared channel where the multiple scattering smoothes the directional features of the BRDF.

Thanks to the instrumental concept of the POLDER sensor, the view zenith angles at surface level are ± 61° along track and ± 50° across track (± 70° in the matrix diagonal). The POLDER-3 BRDFs databases are irreplaceable tools to test the ability of reflectance models to reproduce the BRDF shape at large viewing angles, and to determine which model could be the best to improve the assessment of surface albedo, considering that the contribution of radiation at large angles is not negligible.

The YEARLY databases provide a unique opportunity to analyse the temporal variability of directional signatures as a function of vegetation cover type. The availability of a full vegetative cycle improves the usefulness of these databases comparing to the 8 months of the POLDER-1 measurements used by Bacour and Bréon (2005) to elaborate standard BRDFs used to perform the correction of directional effects in AVHRR reflectance time series (Bacour et al., 2006). However, the information about the vegetation type has to be used carefully. As shown in Table 7, the agreement between the land cover maps depends on the ecosystem: it can be very good for urban areas, and quite bad for the open deciduous broadleaf forests of GLC2000 which are identified at 82% as woody savannas by IGBP. Then, it would be more recommended to use only pixels common to both databases, and identified as similar vegetation types.

Nadal and Bréon (1999) have used the polarized reflectances measured by POLDER-1 to generate empirical surface BPDFs of eleven surface types defined by the IGBP classification and the NDVI. For each surface type, an empirical function with two parameters has been fitted to the observations. The primary use of these functions is the correction of TOA polarized reflectance measurements for an estimate of aerosol characteristics over land surfaces. They are currently use in the operational Land Surface processing line to carry out the tropospheric aerosol correction (Lacaze and Maignan, 2007).

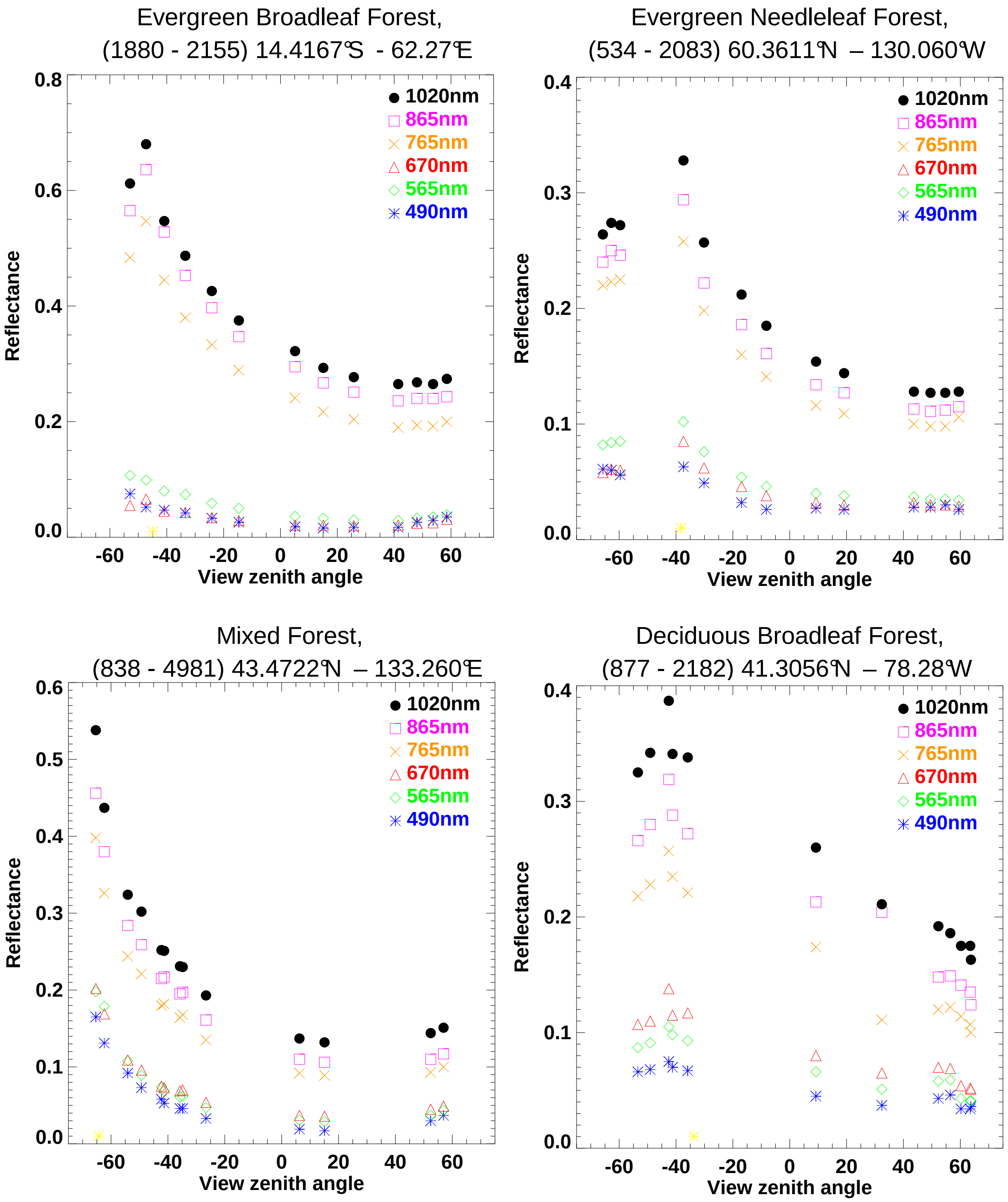

Figure 10 : Directional signatures measured by POLDER-3 in the principal plane over an Evergreen Broadleaf forest (up-left), an Evergreen Needleleaf forest (up-right), a mixed forest (bottom-left), and a Deciduous Broadleaf forest (bottom-right). These pixels are selected in both MONTHLY databases.

Open Deciduous Shrubland,
(2159 - 5159) 29.9167°S – 122.98°E)

Grassland/Herbaceous areas,
(1355 - 3632) 14.75°N – 22.49°E

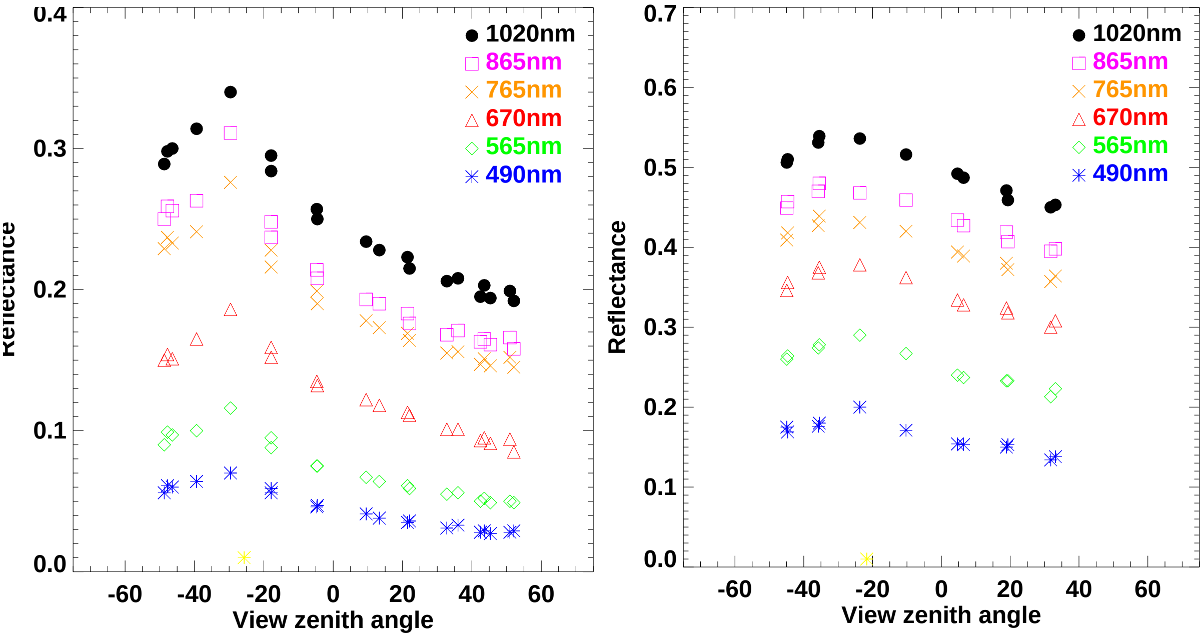

Cropland/Cultivated areas,
(870 - 1737) 41.6944°N – 111.880°W

Snow and Ice,
(2847 - 3666) 68.1389°S – 63.51°E

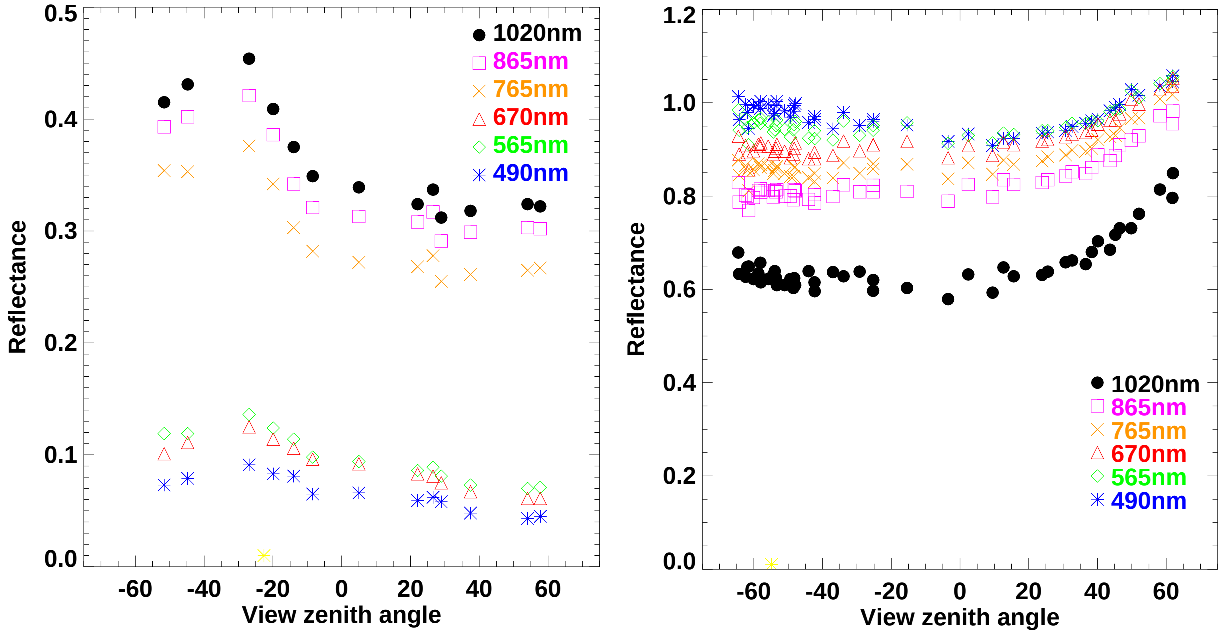

Figure 11 : Directional signatures measured by POLDER-3 in the principal plane over shrubland (top-left), herbaceous area (top-right), a Cultivated and Managed region (bottom-left), and Snow and Ice (bottom-right). These pixels are selected in both MONTHLY databases.

7. Conclusion

The POSTEL Service Centre provides 4 BRDF databases gathering POLDER-3/PARASOL measurements selected using a new methodology developed by the LSCE. They also contains the polarized reflectance measured at 865nm.

The criteria of selection, which rely on the RMS resulting of a reflectance model inversion against observations, favour the smoothest BRDFs. The selection is done per month (MONTHLY databases) and on the whole year (YEARLY databases) for each class of the GLC2000 land cover map (GLC2000-based databases), and of the IGBP land cover map (IGBP-based databases). These databases are dedicated to modelling activities with a specific focus on the impact of surface seasonal variations on the BRDF features.

Comparing to the existing POLDER-1 and POLDER-2 BRDF databases, the POLDER-3/PARASOL databases present many improvements. One year of acquisitions allow to monitor the variations of BRDF over a full vegetative cycle. The orbital cycle of PARASOL, longer than the ADEOS-2 one, provides a better angular sampling of the BRDF. Observations under larger viewing angles (up to 70°) give the opportunity to investigate the ability of models to simulate the BRDF sides, with the aim to improve the albedo assessment.

Used carefully regarding to the information on the vegetation type (due to the disagreement between the both land cover maps), these databases are an exceptional collection of bi-directional reflectances measured from space, providing exclusive information about the anisotropy of the continental ecosystems.

8. References

Global Land Cover 2000 database. European Commission, Joint Research Centre, 2003, www3.

Abuelgasin, A., S. Gopal, J. R. Irons, and A. H. Strahler, Classification of ASAS multiangle and multispectral measurements using artificial neural networks, *Remote Sensing of Environment, 57, 79-87,* 1996.

Bacour, C. and F.M. Bréon, Variability of biome reflectance directional signature as seen by POLDER, *Remote Sensing of Environment, 98, 80-95*, 2005.

Bacour, C., F.M. Bréon, and F. Maignan, Normalisation of the directional effect on NOAA-AVHRR reflectances measurements for an improved monitoring of vegetation cycles, *Remote Sensing of Environment, 102, 402-413*, 2006.

Bicheron, P., M. Leroy, O. Hautecoeur, and F. M. Bréon, Enhanced discrimination of boreal forest covers with directional reflectances from the airborne polarization and directionality of Earth Reflectances (POLDER) instrument, *Journal of Geophysical Research, 102, 29,517-29,528,* 1997.

Bicheron, P. and M. Leroy, A method of biophysical parameter retrieval at global scale by inversion of a vegetation reflectance model, *Remote Sensing of Environment, 67, 251-266,* 1999.

Bicheron, P. and M. Leroy, Bidirectional reflectance distribution function signatures of major biomes observed from space, *Journal of Geophysical Research, 105, 21, 26,669-26,681,* 2000.

Bréon, F.M. , F. Maignan, M. Leroy, and I. Grant, Analysis of the hot spot directional signatures measured from space, *Journal of geophysical research, 107, (16), 4,282-4,296,* 2002.

Bréon, F.M. and the Cnes PARASOL Team, PARASOL Level-1 Product Data Format and User Manual, *Issue 1, Revision 1,* May, 26th 2005 (www55).

Cabot, F. and G. Dedieu, Surface albedo from space: Coupling bidirectional models and remotely sensed measurements, *Journal of Geophysical research, 102, 19,645-19,664,* 1997.

Capderou, M. , Determination of the shortwave anisotropic function for clear sky desert scenes from ScaRab data: Comparison with models issued from other satellite data, *Journal of Applied Meteorology, 37, 1398-1411,* 1998.

Chen, J.M., J. Liu, S.G. Leblanc, R. Lacaze, and J.L. Roujean, Multi-angular optical remote sensing for assessing vegetation structure and carbon absorption, *Remote Sensing of Environment, 84, Issue 4, 516-525*, 2003.

Chen, J.M., C.H. Menges, and S.G. Leblanc, Global mapping of foliage clumping index using multi-angular satellite data, *Remote Sensing of Environment, 97, 447-457*, 2005.

Deering, D. W., T. F. Eck and T. Grier, Shinnery oak bidirectional reflectance properties and canopy model inversion, *IEEE Transaction in Geoscience and Remote Sensing, 30, 339-348,* 1992.

Di Gregorio, A. and Jansen, L., Land Cover classification system, classification concepts and user manual, *Food and Agriculture Organisation of the United Nations: Rome,* 2000.

Eidenshink, J.C. and Faundeen, J.L., The 1 km AVHRR global land data set-first stages in implementation: *International Journal of Remote Sensing , v. 15, no. 17, p. 3,443-3,462,* 1994.

Godsalve, C., Bidirectional reflectance sampling by ATSR-2: A combined orbit and scan model, *International Journal of Remote Sensing, 16, 269-300,* 1995.

Gutman, G. G., the derivation of vegetation indices from AVHRR data, *International Journal of Remote Sensing, 8, 1235-1243,* 1987.

Hautecoeur, O. and M. Leroy, Surface bidirectional reflectance distribution function observed at global scale by OLDER/ADEOS, *Geophysical Research Letter, 25, 4197-4200,* 1998.

Hyman, A. H., and M. J. Barnsley, On the potential for land cover mapping from multiple view angle (MVA) remotely sensed information, *International Journal of Remote Sensing, 18, 2471-1475,* 1997.

Irons, J. R., K. J. Ranson, D. L. Williams, R. R. Irish, and F. G. Huegel, An off-nadir pointing imaging spectroradiometer for terrestrial ecosystem studies, *IEEE Transaction in Geoscience and Remote Sensing, 29, 66-74,* 1991.

Kimes, D. S., Dynamics of directional reflectance factor distributions for vegetation canopies, *Applied Optics, 22, 1364-1373,* 1983.

Knyazikhin, Y., J. V. Martonchik, D. J. Diner, R. B. Myneni, M. M. Verstraete, B. Pinty, and N. Gobron, Estimation of vegetation canopy leaf area index and fraction of absorbed photosynthetically active radiation from atmosphere-corrected MISR data, *Journal of Geophysical Research, 103, 32,239-32,256,* 1998.

Lacaze, R., J. M. Chen, J. L. Roujean and S. G. Leblanc, Retrieval of vegetation clumping index using hot spot signatures measured by POLDER instrument, *Remote Sensing of Environment, 79, 84-95,* 2002.

Lacaze, R. POLDER-1 BRDF Database – User Document, *POSTEL Service Centre, Issue 2, Revision 2*, July 3rd 2006a (www4).

Lacaze, R. POLDER-2 BRDF Database – User Document, *POSTEL Service Centre, Issue 1, Revision 1*, July 3rd 2006b (www4).

Lacaze, R, and F. Maignan, POLDER-3/PARASOL Land Surface Algorithm Description, *POSTEL Service Centre, Issue 3, Revision 1*, June 13th 2007 (www4).

Leroy, M and J. L. Roujean, Sun and view angle corrections on reflectances derived from NOAA/AVHRR data, *IEEE Transaction in Geoscience and Remote Sensing, 32, 684-697,* 1994.

Leroy, M. and F. M. Bréon, Surface reflectance angular signatures from airborne POLDER data, *Remote sensing of environment, 57, 97-107,* 1996.

Loveland, T. R. and A. S. Belward, The IGBP-DIS global 1-km land cover data set DISCover: first results*, International Journal of Remote Sensing, 18, 3289-3295*, 1997.

Maignan, F., F.M. Bréon, et R. Lacaze, Bidirectional reflectance of Earth targets : evaluation of analytical models using a large set of spaceborne measurements with emphasis of the hot spot, *Remote Sensing of Environment, vol.90, 210-220*, 2004.

Manalo-Smith, N., G. L. Smith, S. N. Tiwari, and F. W. Taylor, Analytic form of bidirectional reflectance functions for application to Earth radiation budget studies, *Journal of Geophysical Research, 103, 19,733-19,751,* 1998.

Nadal, F. et F.M. Bréon, Parametrization of surface polarized reflectance derived ffrom POLDER spaceborne measurements, *IEEE Transactions on Geoscience and Remote Sensing, 37, 1709-1718*, 1999.

Wanner, W., A. H. Strahler, B. Hu, P. Lewis, J. P. Muller, X. Li, C. L. Barker Schaaf, and M. J. Barnsley, Global retrieval of bidirectional reflectance and albedo over land from EOS MODIS and MISR data: Theory and algorithm, *Journal of Geophysical Research, 102, 17,143-17,161,* 1997.

Wu, A., Z. Li and J. Cilhar, Effects of land cover type and greenness on advanced very high radiometer bidirectional reflectances: Analysis and removal, *Journal of Geophysical Research, 100, 9179-9192,* 1995.

Zhu, Z., and Yang, L., Characteristics of the 1-km AVHRR data set for North America: *International Journal of Remote Sensing , v. 17, p. 1,915-1,924*, 1996.

www1 : http://postel.mediasfrance.org/en/DOWNLOAD/Biogeophysical-Products/
www2 : http://LPDAAC.usgs.gov/glcc/globe_int.php
www3 : http://www-gvm.jrc.it/glc2000/
www4 : http://postel.mediasfrance.org/en/DOWNLOAD/Documents/
www5 : http://www-icare.univ-lille1.fr/parasol/

9. Acknowledgment and contact

The BRDFs databases are a product of POSTEL, the French Thematic Centre on Land Surfaces.

The LSCE (Laboratoire des Sciences du Climat et de l'Environnement), one of the Expertise Centre of POSTEL, has defined the methodology of the BRDF selection, and produced the databases from the original Level-1 POLDER-3/PARASOL data provided by Cnes. The analysis has been carried out by the POSTEL Service Centre at MEDIAS-France.

The tool called Visu_BRDF, used to test the potential of the BRDF database for model inversion, has been developed by F.M. Bréon (CEA/LSCE).

The BRDF databases, and Visu_BRDF, are available for downloading on the POSTEL web site at the address: http://postel.mediasfrance.org.

In any publication using the POLDER-3/PARASOL BRDF databases, please include the following citation:

“The POLDER-3/PARASOL BRDFs databases are elaborated by the LSCE, and provided by the POSTEL Service Centre. The POLDER-3/PARASOL data are from Cnes.”

For any question, please contact:

Dr. Roselyne Lacaze
POSTEL Service Centre / MEDIAS-France
Cnes Bpi 2102
18 avenue Edouard Belin
31 401 Toulouse Cedex 9
France
Phone: 33 – 5 – 61 – 27 – 31 – 21
Fax: 33 – 5 – 61 – 28 – 29 – 05
Email : roselyne.lacaze@medias.cnes.fr

Annex1 : POLDER full resolution reference grid

The POLDER reference grid is based on the sinusoidal equal area projection (Sanson-Flamsted). The step is constant along a meridian with a resolution of 1/18° degrees. Thus, there are 180 x 18 = 3240 lines from pole to pole. Along a parallel, the step is chosen in order to have a resolution as constant as possible. The number of pixel from 180°W to 180°E is chosen equal to 2 x NINT[3240 COS(latitude)] where NINT stands for *nearest integer*.

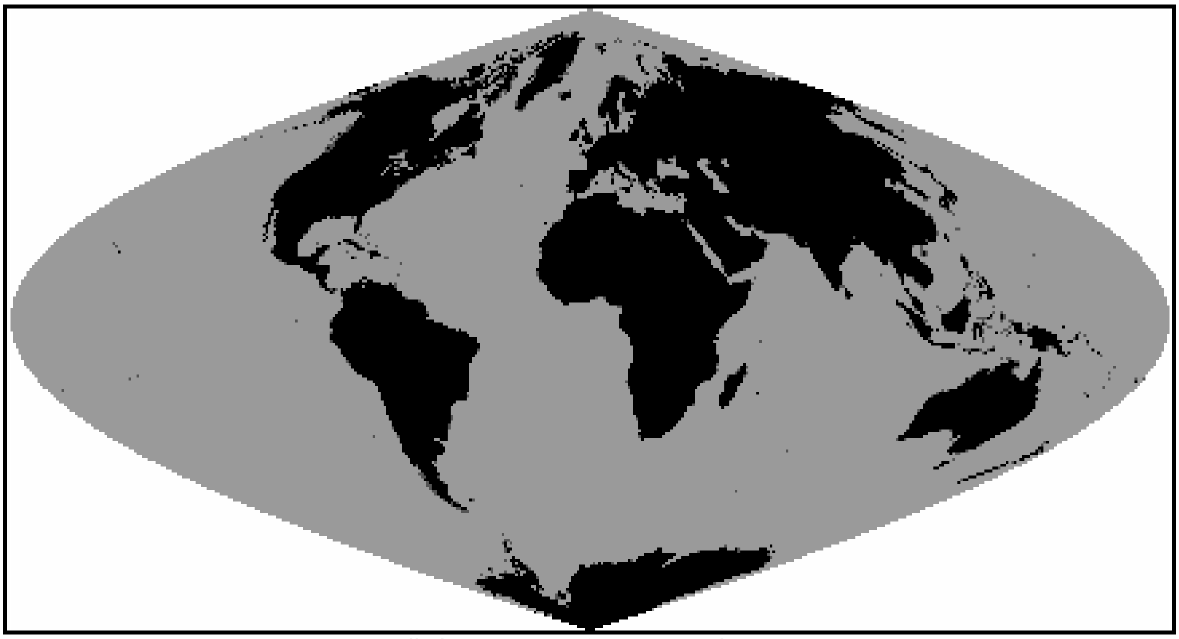

lin is 1 to 3240 from top to bottom
col is 1 to 6480 from left to right

Note that, in the real world, the coordinates of the neighbors of a given pixel (*lin, col*) are ***not*** necessarily given by (*lin* ± 1, *col* ± 1). It is necessary to account for the deformation of the projection with the longitude.

The following equations yield the latitude and longitude of a pixel given by its (*lin*, *col*) coordinates in the POLDER reference grid:

$$lat = 90 - \frac{lin - 0.5}{18}$$

$$N_i = \mathrm{NINT}[3240\cos(lat)]$$

$$lon = \frac{180}{N_i}(col - 3240.5)$$

The following equations yield the (*lin*, *col*) coordinates in the POLDER reference grid for a pixel of given latitude and longitude:

$$lin = \mathrm{NINT}[18(90 - lat) + 0.5]$$

$$N_i = \mathrm{NINT}[3240\sin(\frac{lin - 0.5}{18})]$$

$$col = \mathrm{NINT}[3240.5 + \frac{N_i}{180}lon]$$

Note that, in the equation above, it is assumed $-180 \leq lon < 180$

This POLDER reference grid is centered on the Greenwich meridian. For the extraction and visualization of POLDER data close to the 180° longitude line, it may be easier to work with a similar grid centered on this meridian. A simple formula allows switching from one (*lin*, *col*) coordinate system to the other (*lin'*, *col'*):

$$lin' = lin$$

$$N_i = \mathrm{NINT}[3240\sin(\frac{lin - 0.5}{18})]$$

$$col' = 3241 - N_i + \mathrm{MOD}_{2N_i}(col + 2N_i - 3241)$$

where MOD2Ni returns the remainder of the integer division by 2Ni.

Annex2 : Multi-temporal BRDFs of the YEARLY databases

(Reflectances are expressed in %)

The pixels presented in the following figures are selected in both databases.

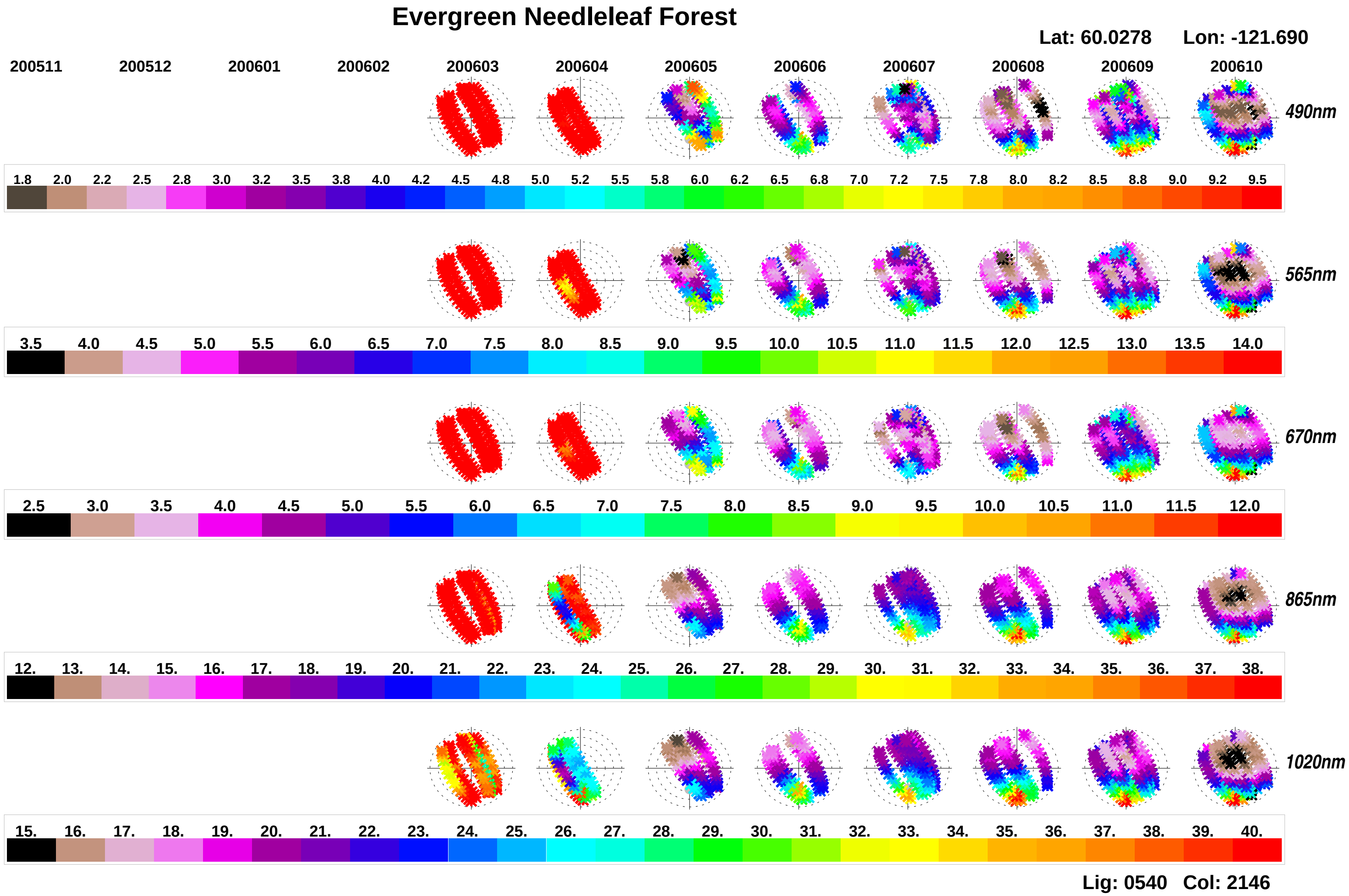

Annex2_1: Multi-temporal BRDF of an Evergreen Needleleaf Forest located in Northern Territory, Canada.

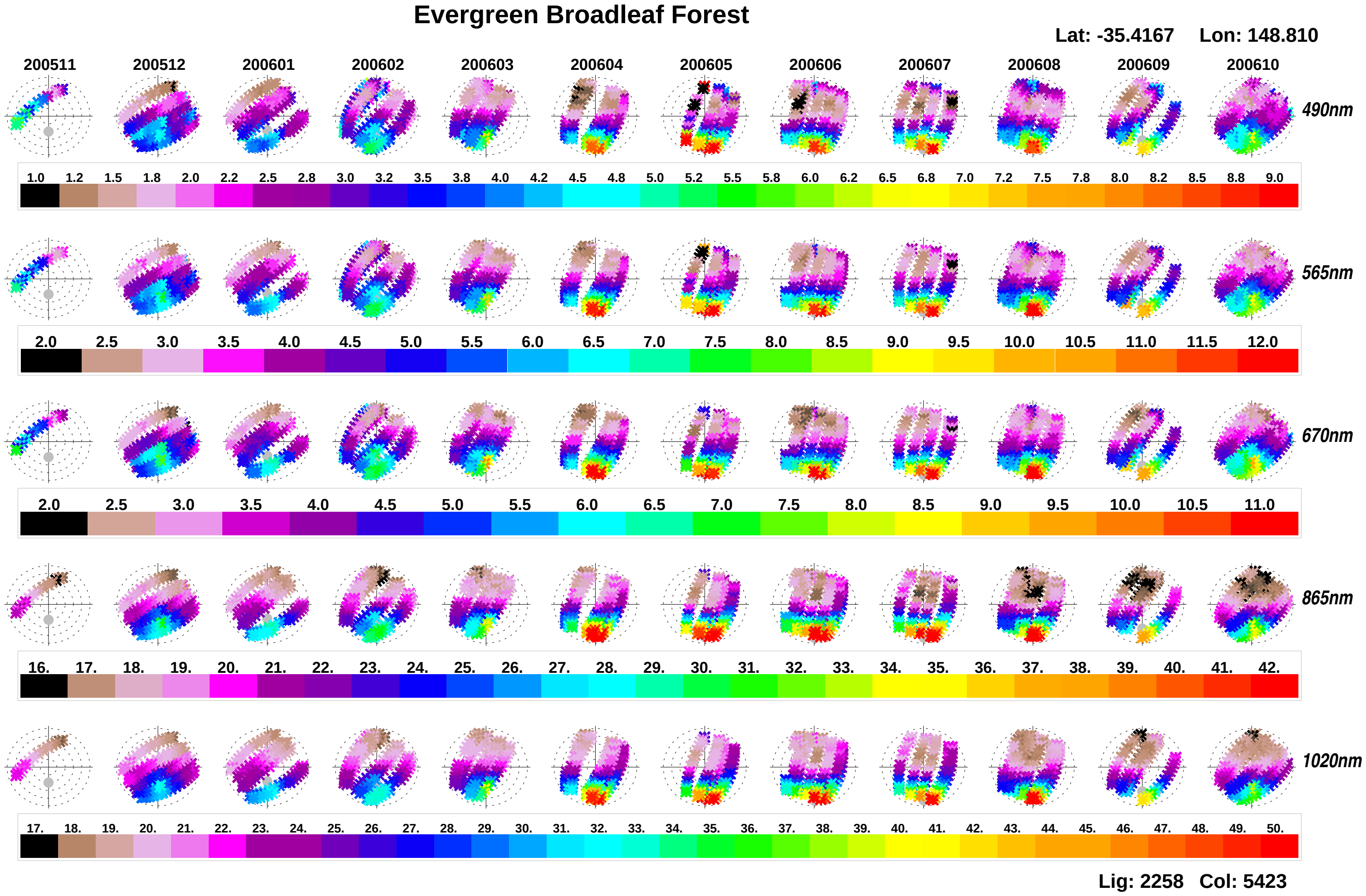

Annex2_2 : Multi-temporal BRDF of an Evergreen Broadleaf Forest located in Australia.

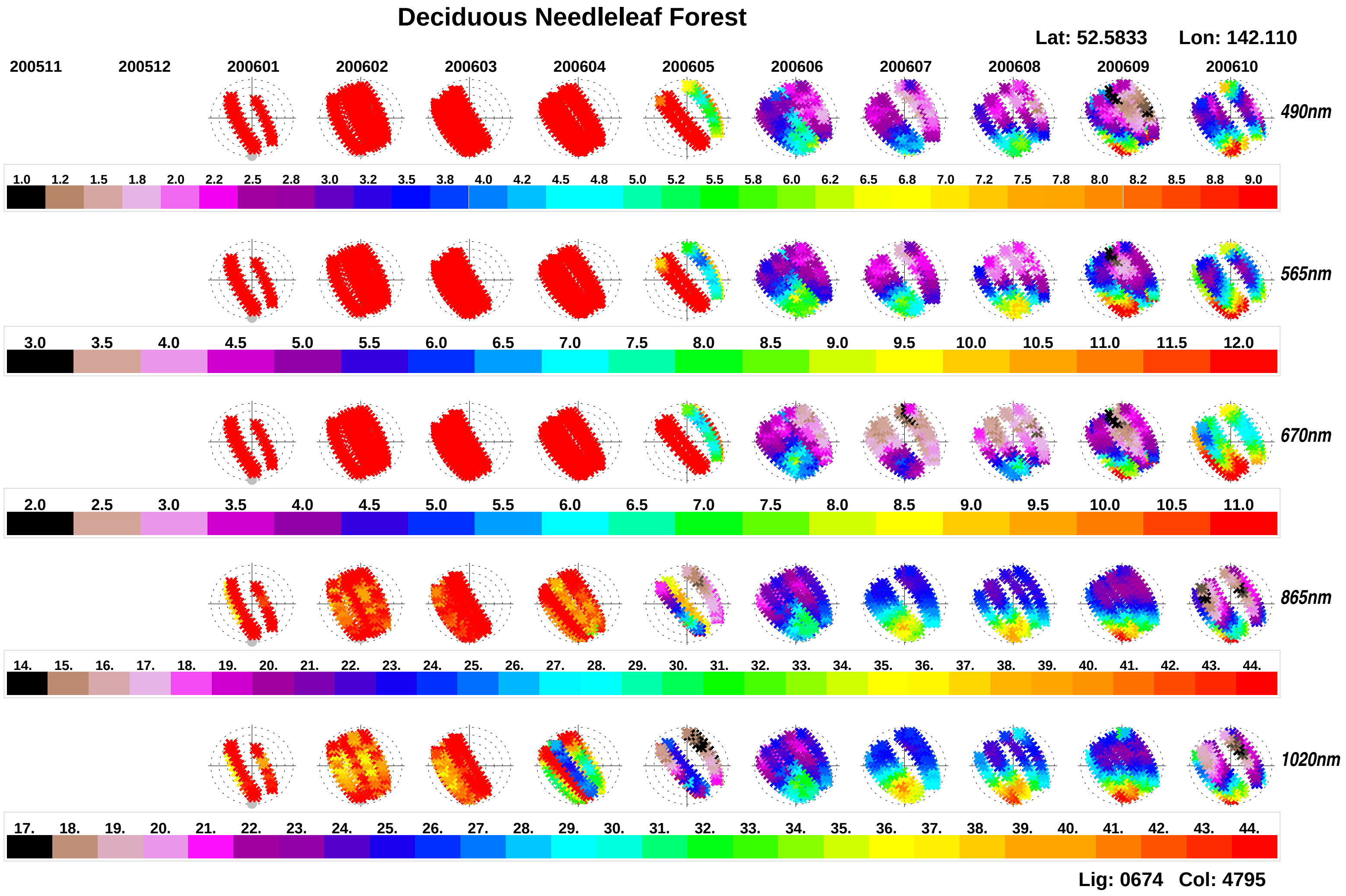

Annex2_3 : Multi-temporal BRDF of a Deciduous Needleleaf Forest located in Sakhalin Island.

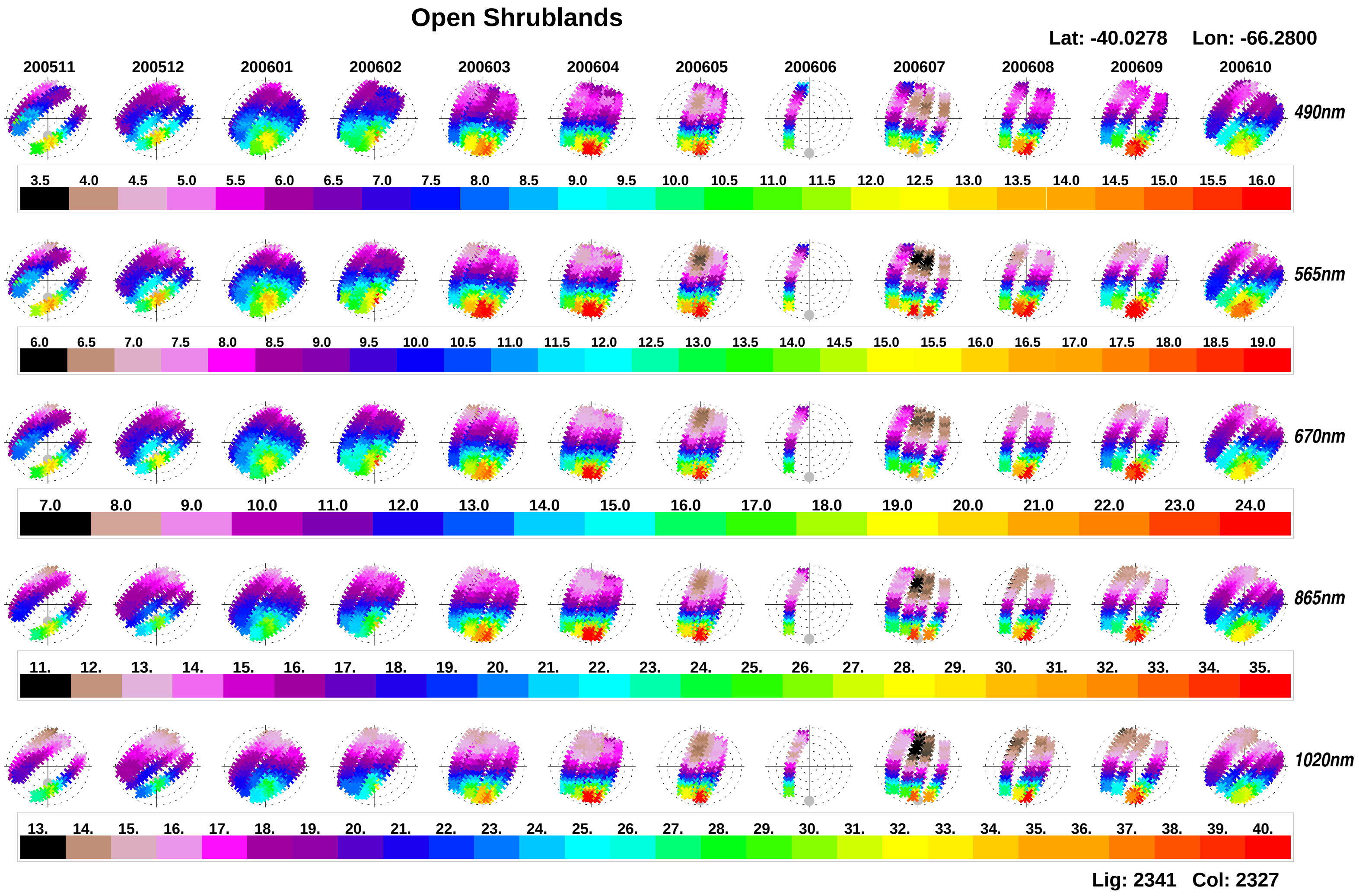

Annex2_4 : Multi-temporal BRDF of a Shrubland located in Argentina.

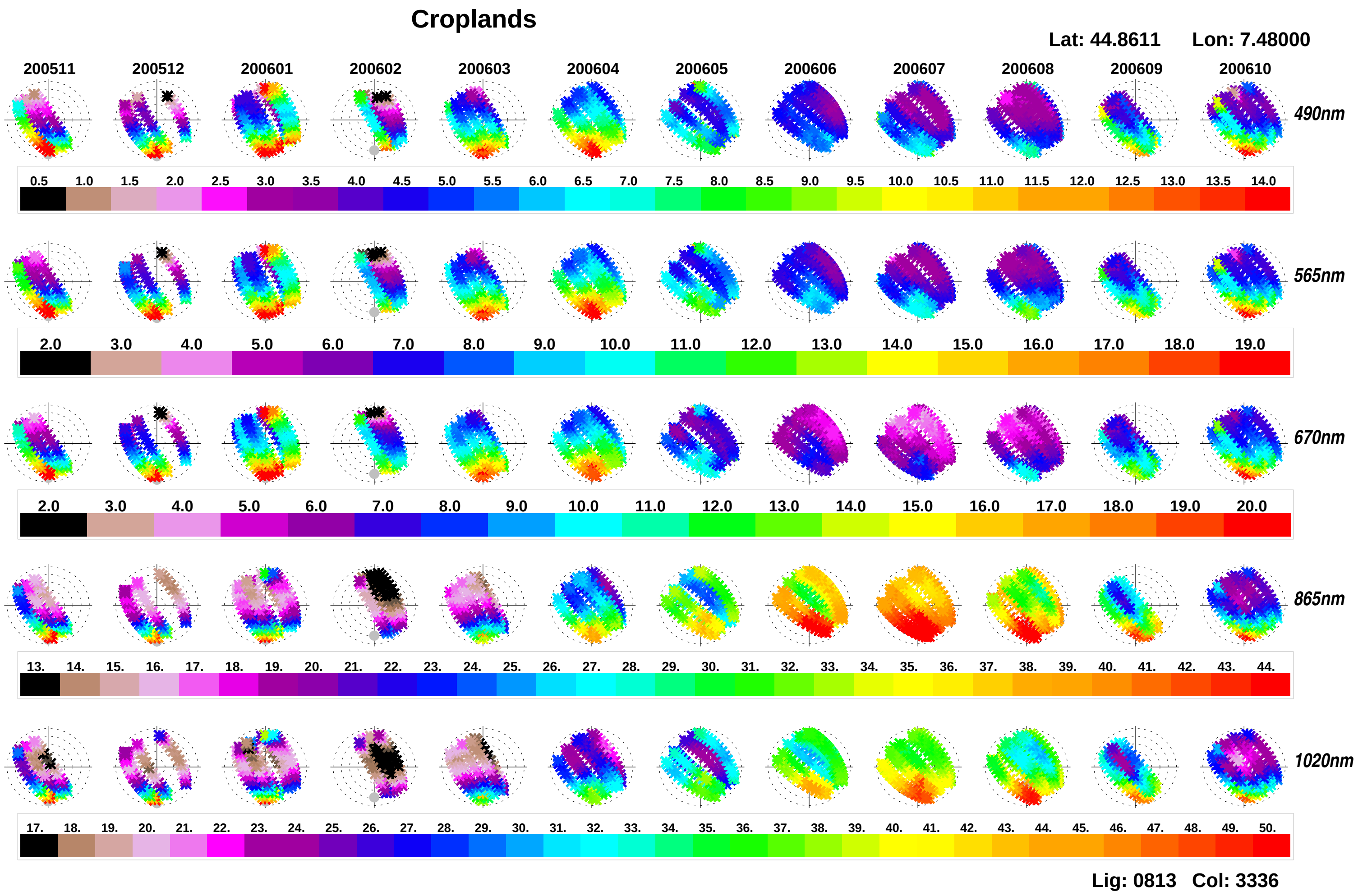

Annex2_5 : Multi-temporal BRDF of cropand area located in the Po valley in Italy.

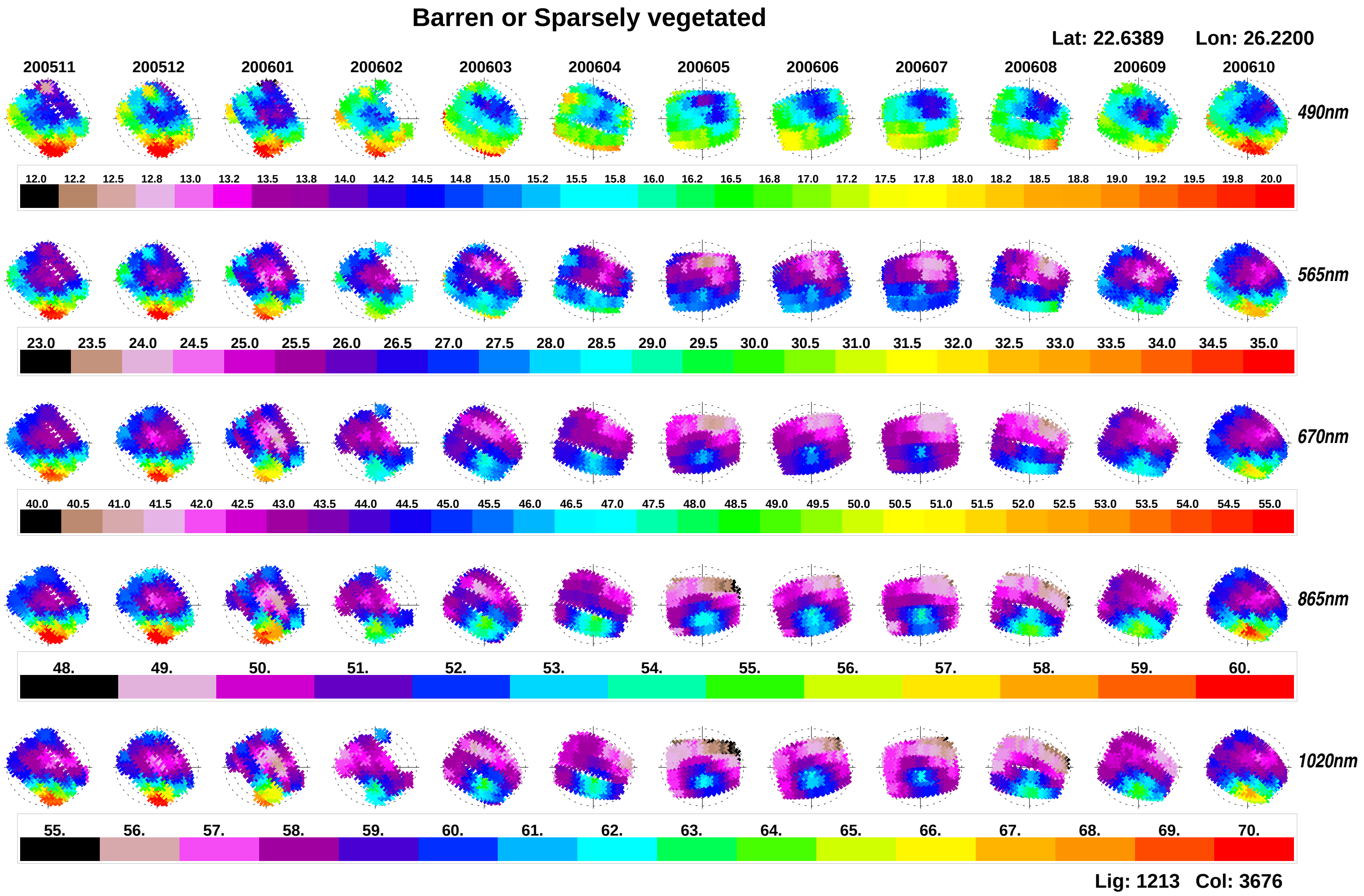

Annex2_ 6 : Multi-temporal BRDF of a bare area localed in Libya.

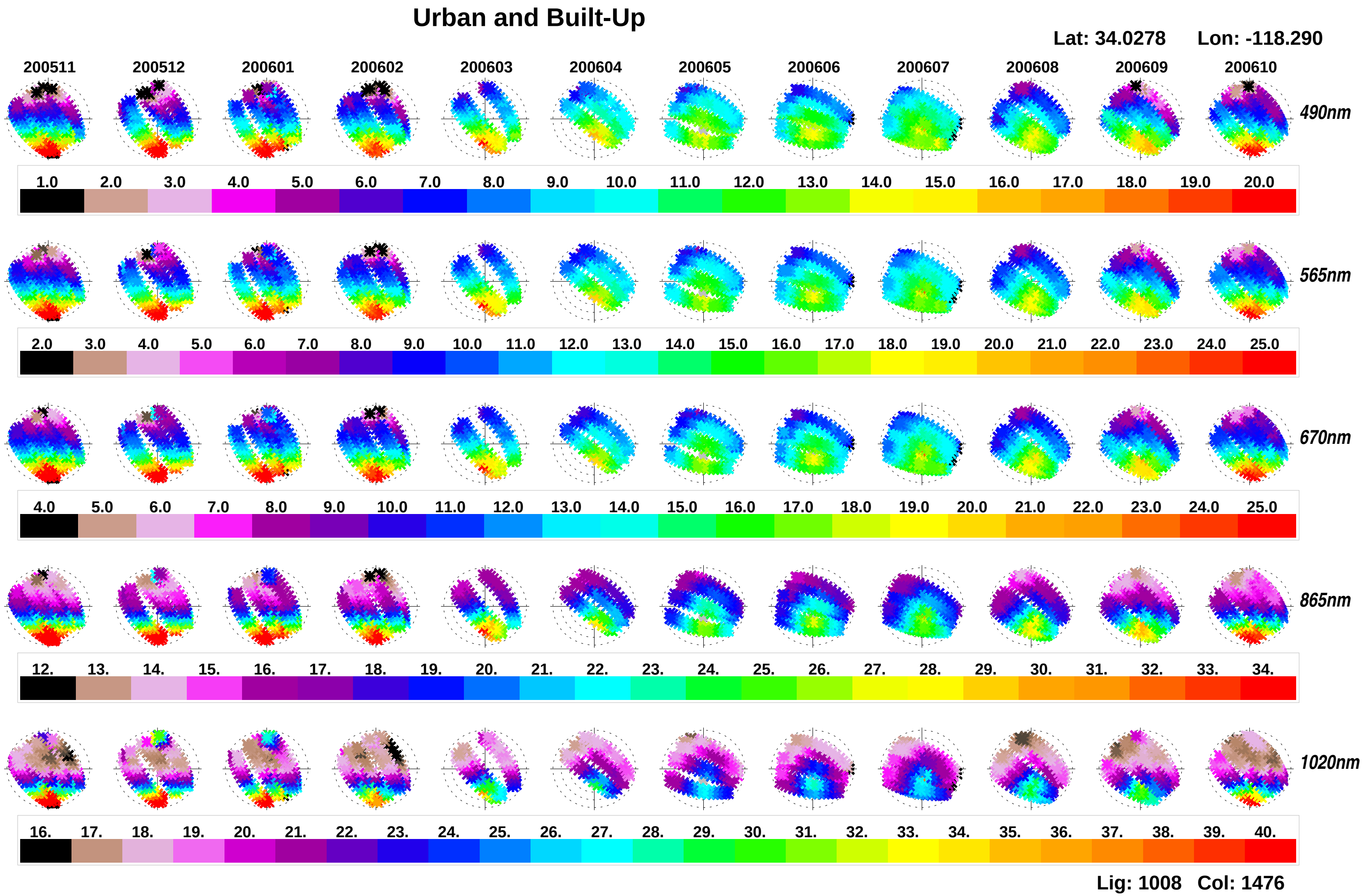

Annex2_7 : Multi-temporal BRDF of a urban pixel located in Los Angeles area.

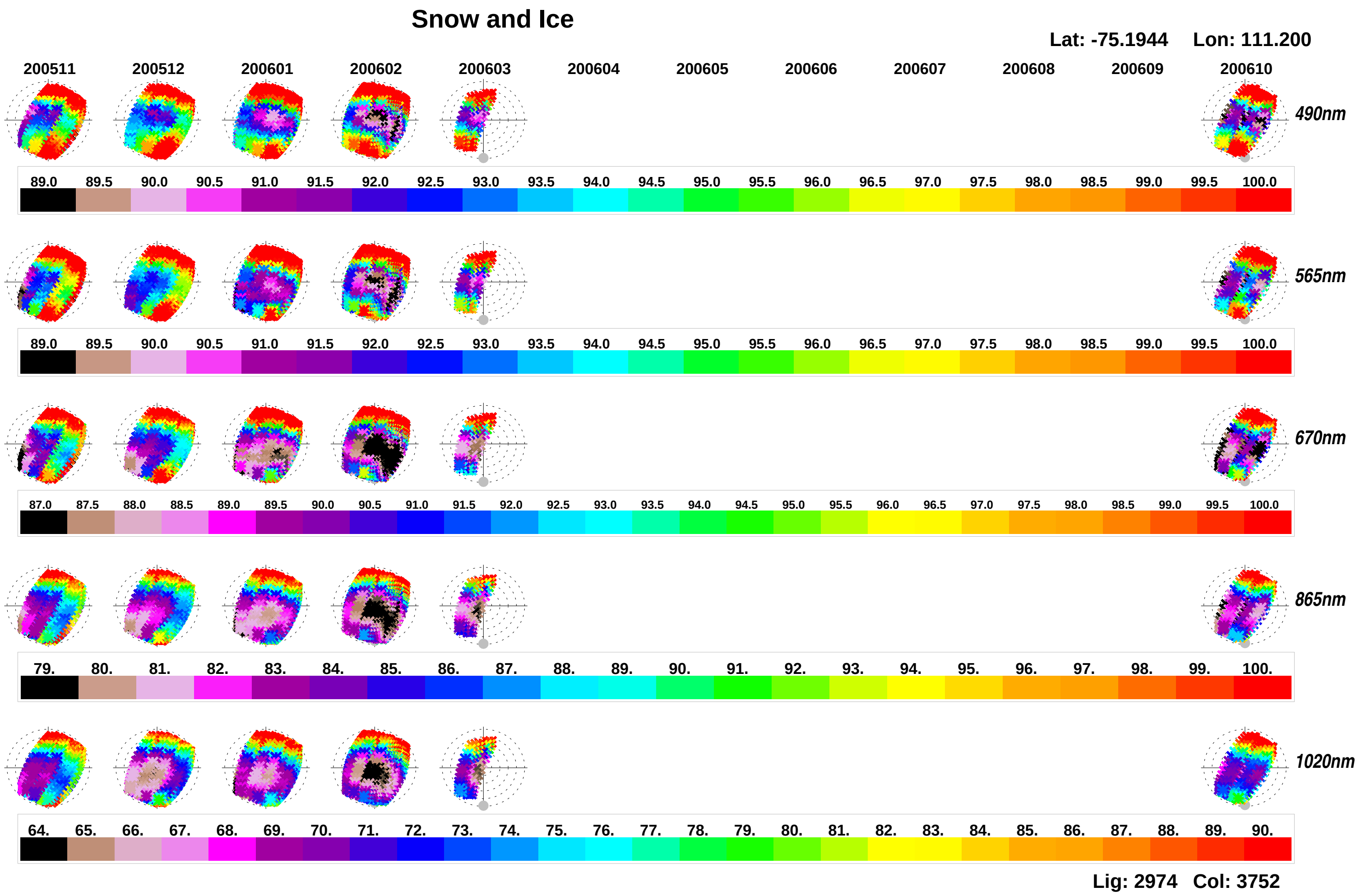

Annex2_ 8 : Multi-temporal BRDF of a snowy area located in Antarctica.

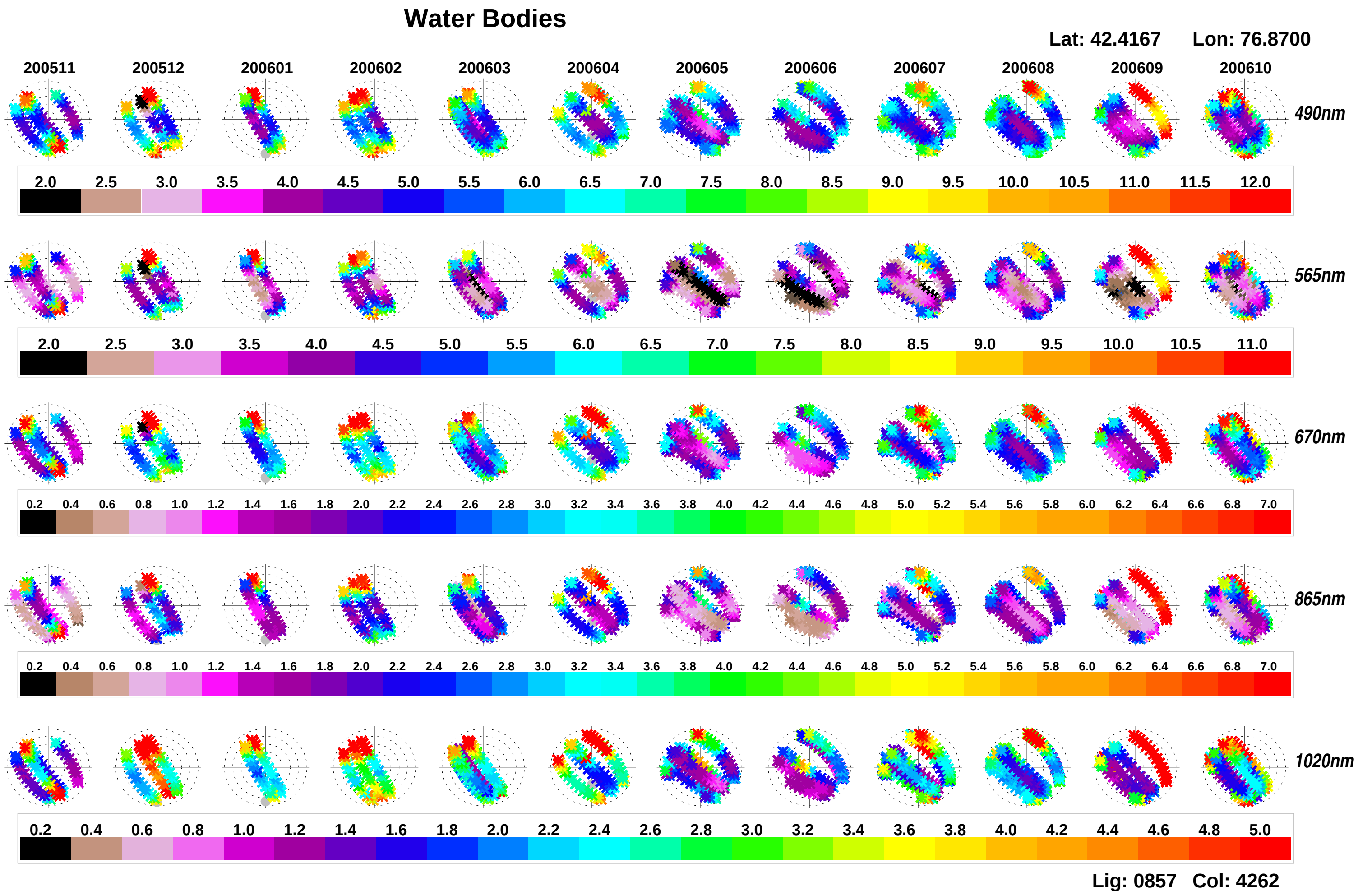

Annex2_ 9 : Multi-temporal BRDF of a water pixel located in Lake Ysik-Köl inKirghizistan.

Annex3 : BRDFs of misclassified or mixed pixels

(Reflectances are expressed in %)

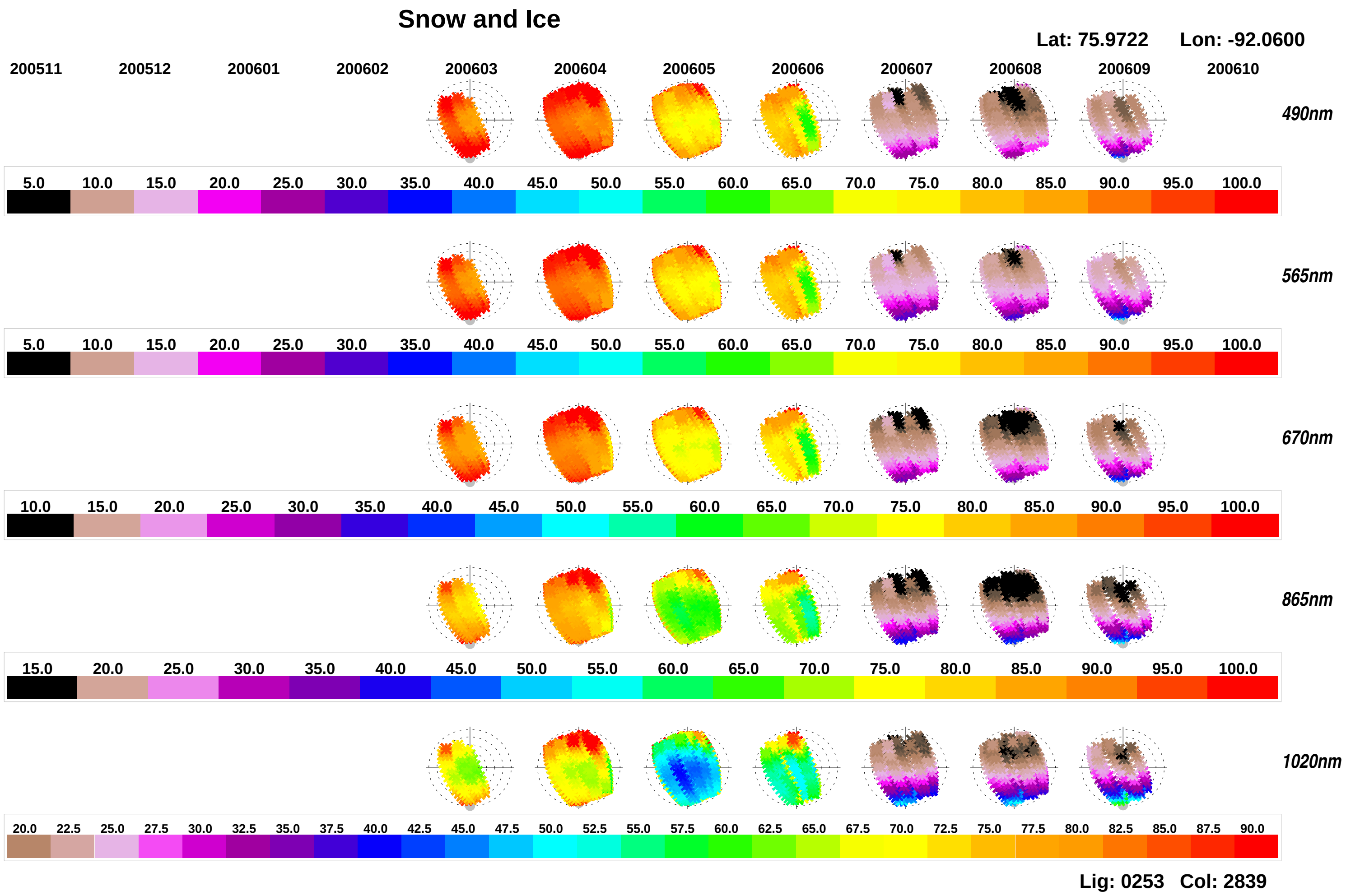

Annex3_1 : Multi-temporal BRDF of a pixel identified as « Snow and Ice » by IGBP located in Northern Canada.

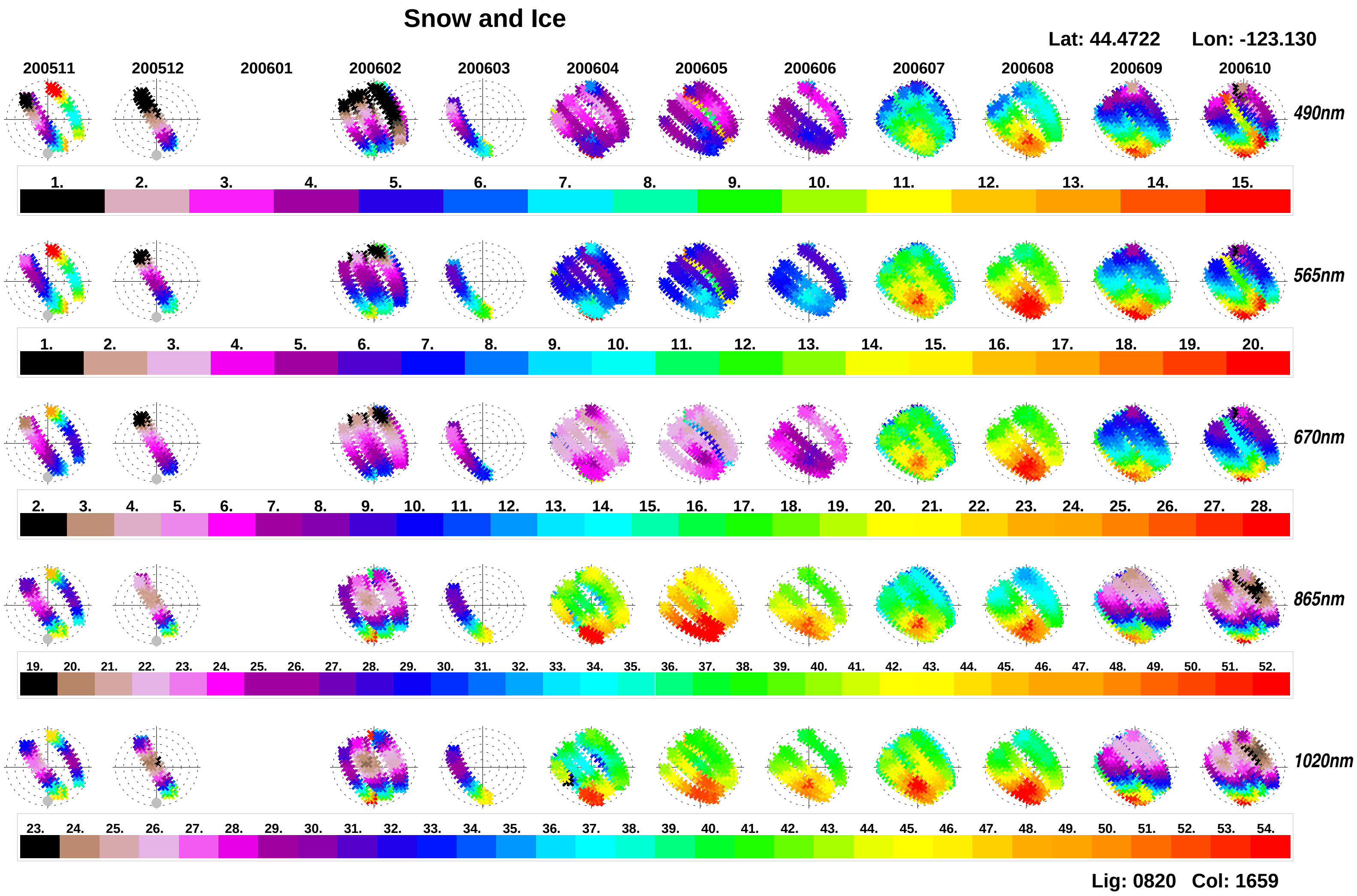

Annex3_ 2 : Multi-temporal BRDF of a pixel identified as "Snow and ice" by GLC2000 located in the US Rocky mountains.

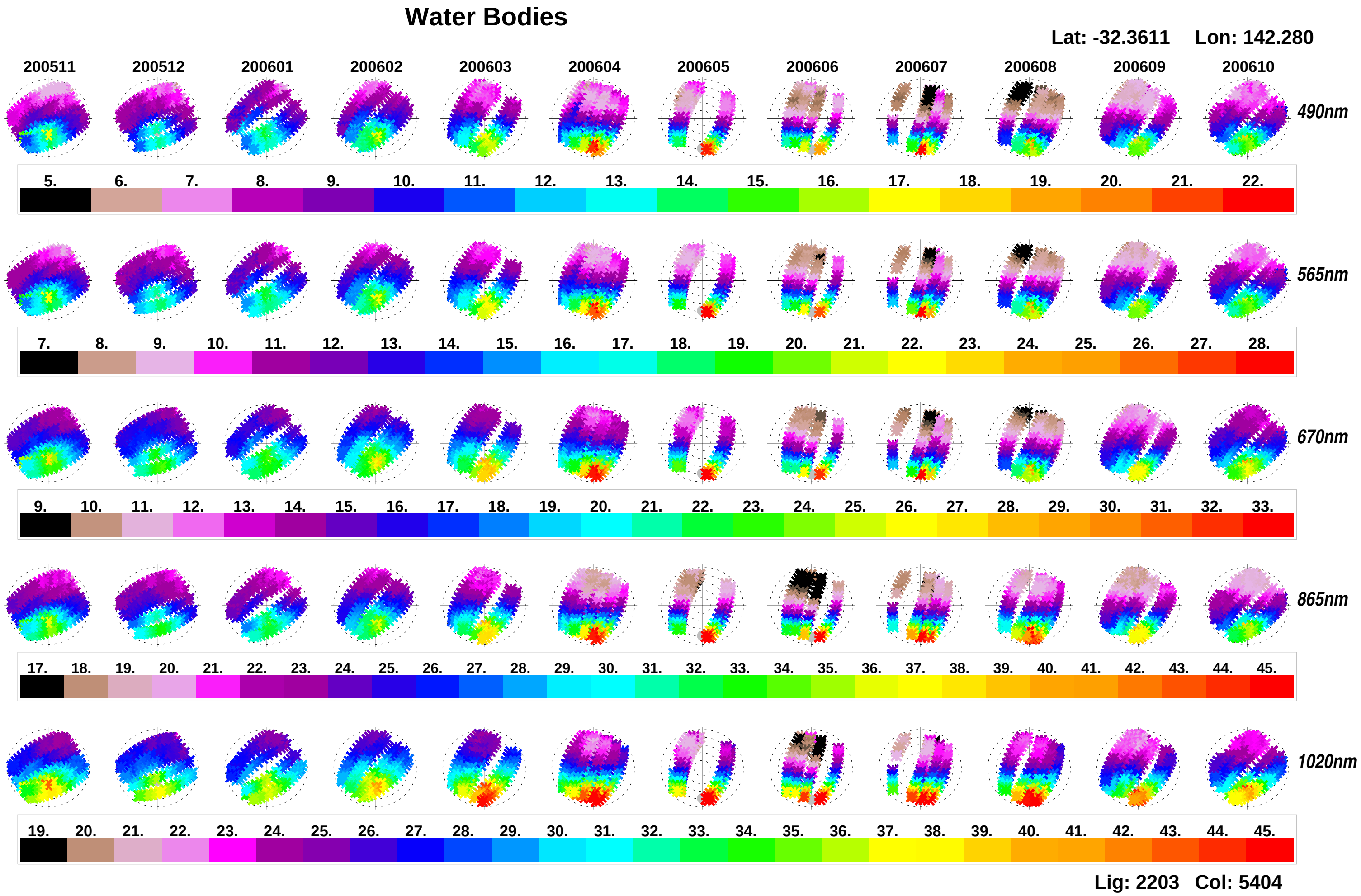

Annex3_ 3 : Multi-temporal BRDF of a pixel identified as « Water Bodies » by GLC2000 located in Australia.

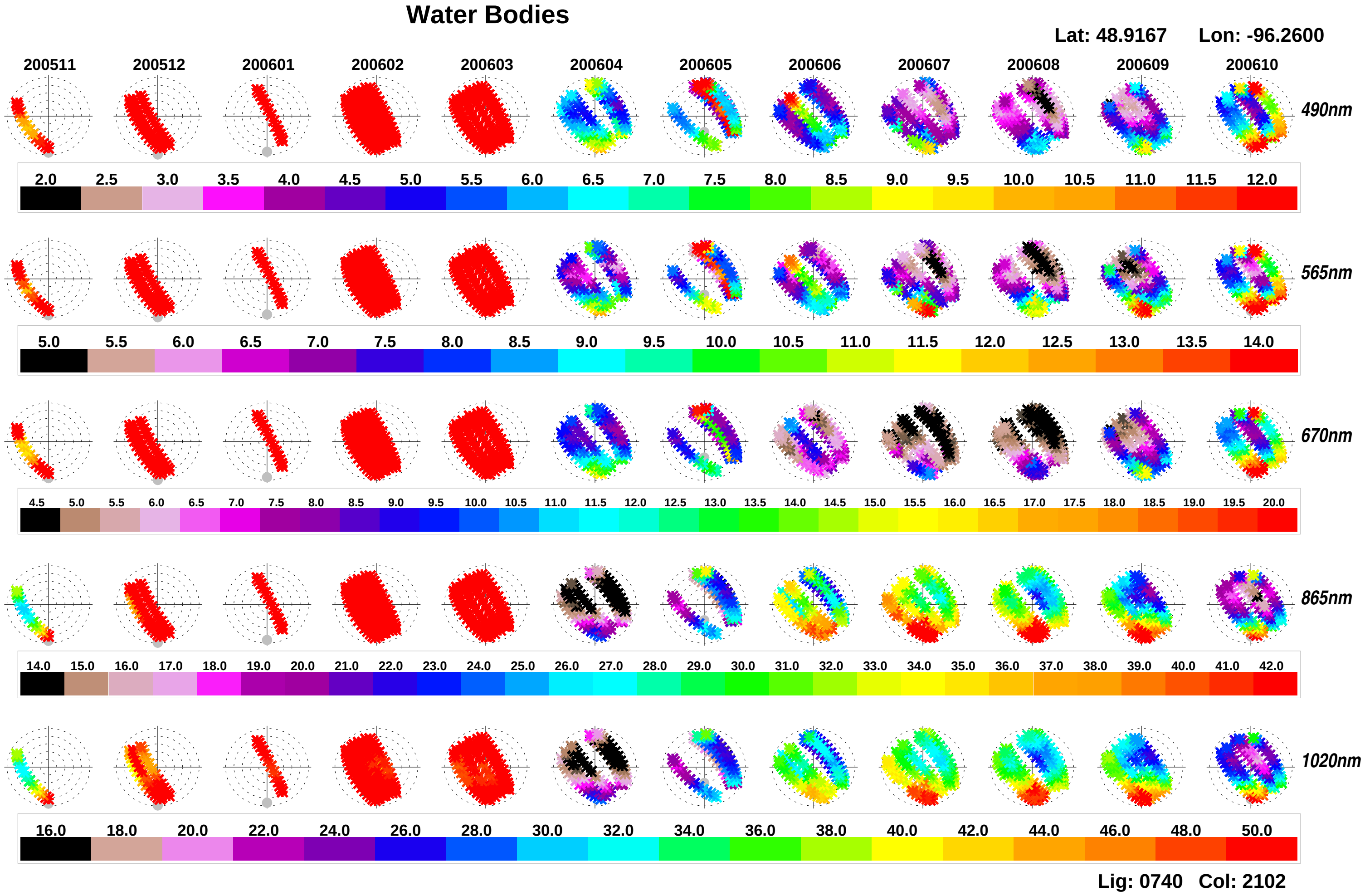

Annex3_ 4 : Multi-temporal BRDF of a pixel identifed as « Water Bodies » by GLC2000 located in Minnesota, USA.

Annex4 : Examples of BPDF measured at 865nm

(All reflectances are expressed in %)

The following pixels are selected in the MONTHLY or in the YEARLY GLC2000-based database.

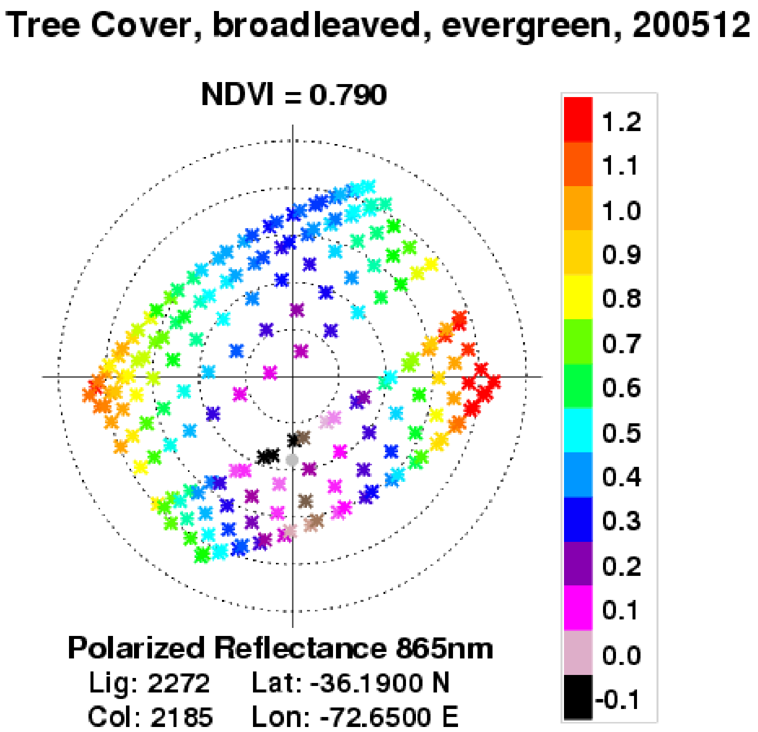

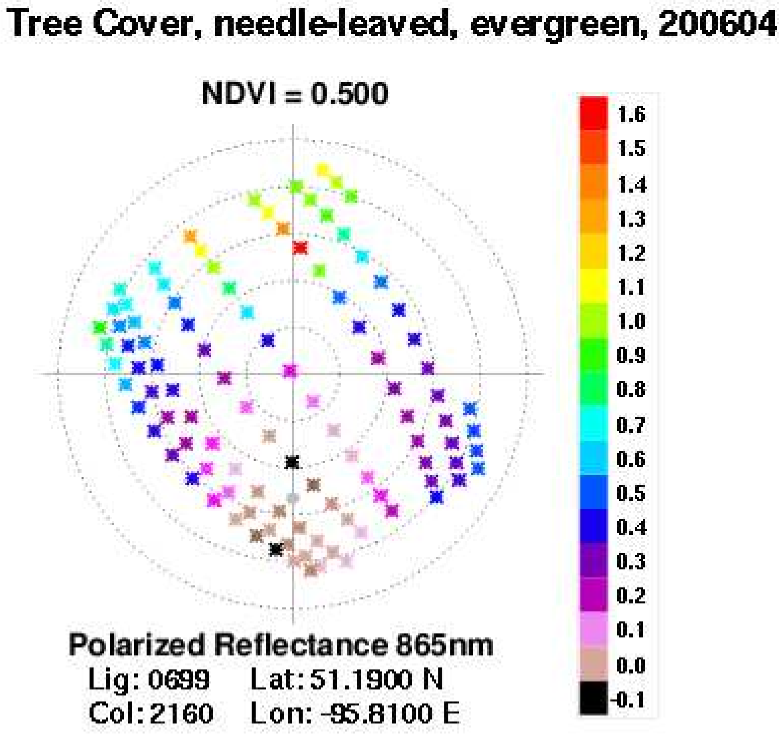

Annex4_ 1 : Polarized reflectance measured at 865nm over a broadleaf evergreen forest located in Argentina (top), and over a needleleaf evergreen forests located in Canada (bottom)

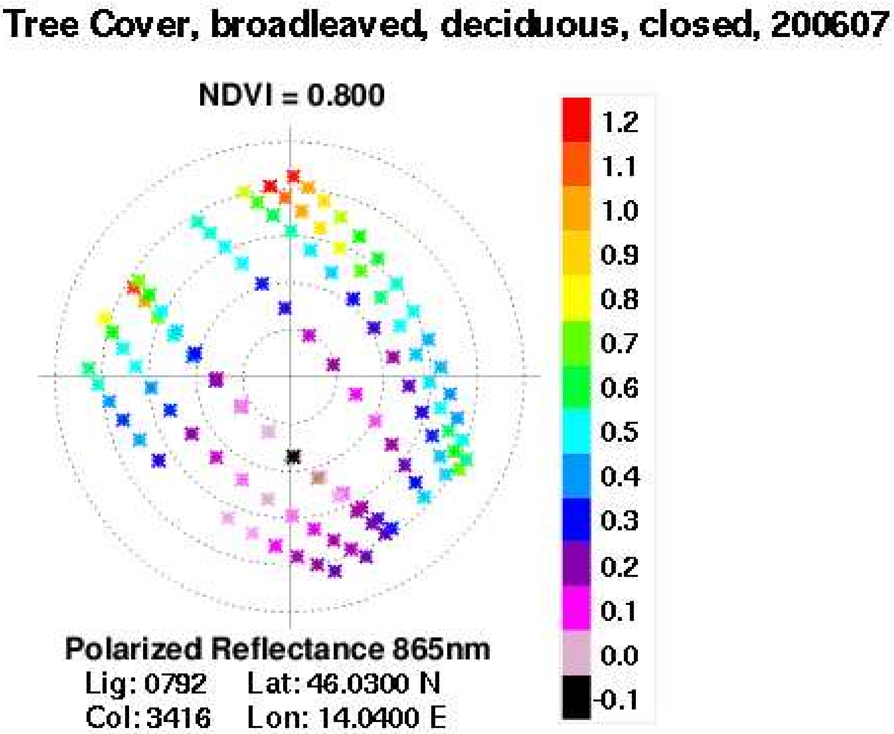

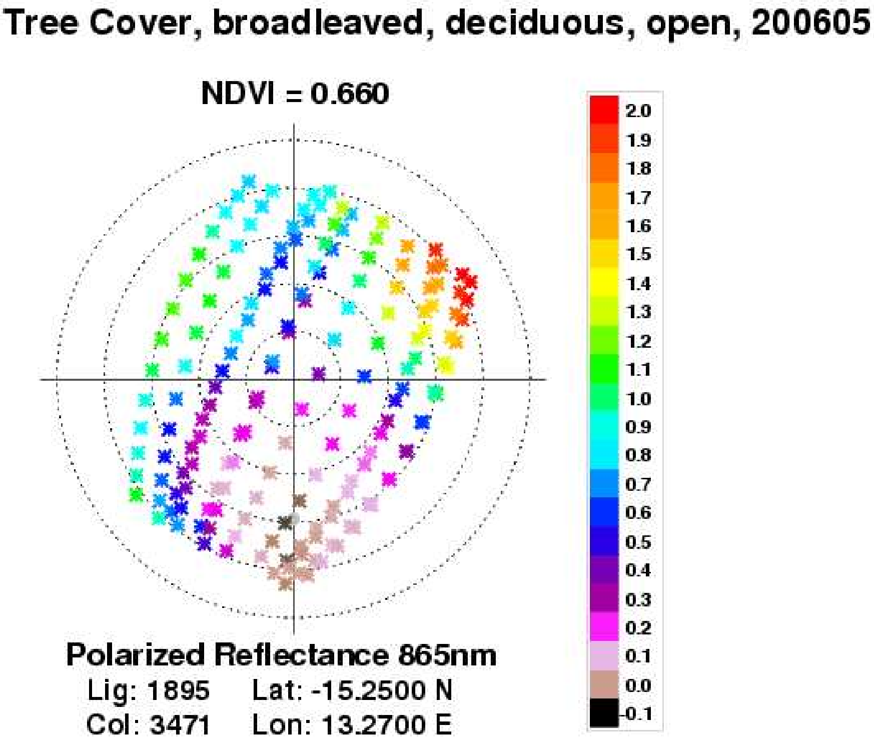

Annex4_ 2 : Polarized reflectance measured at 865nm over broadleaf deciduous forests located in Slovenia (top) and Angola (bottom)

Tree Cover, mixed leaf type, 200607

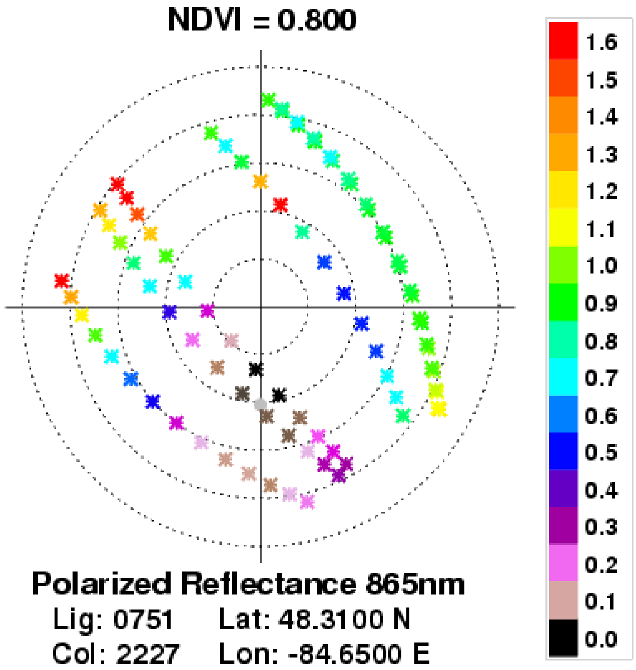

Mosaic: Tree cover / Other natural vegetation, 200512

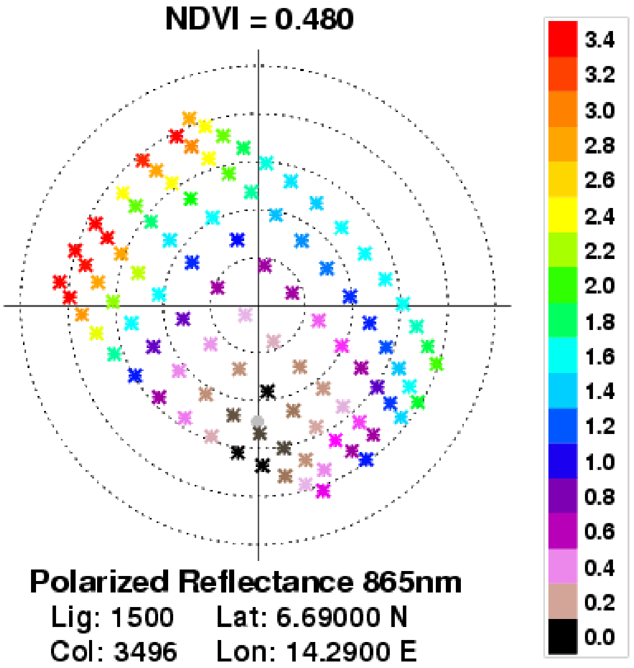

Annex4_ 3 : Polarized reflectance measured at 865nm over a mixed forest located in Canada (top), and over a mosaic vegetation pixel located in Cameroon (bottom).

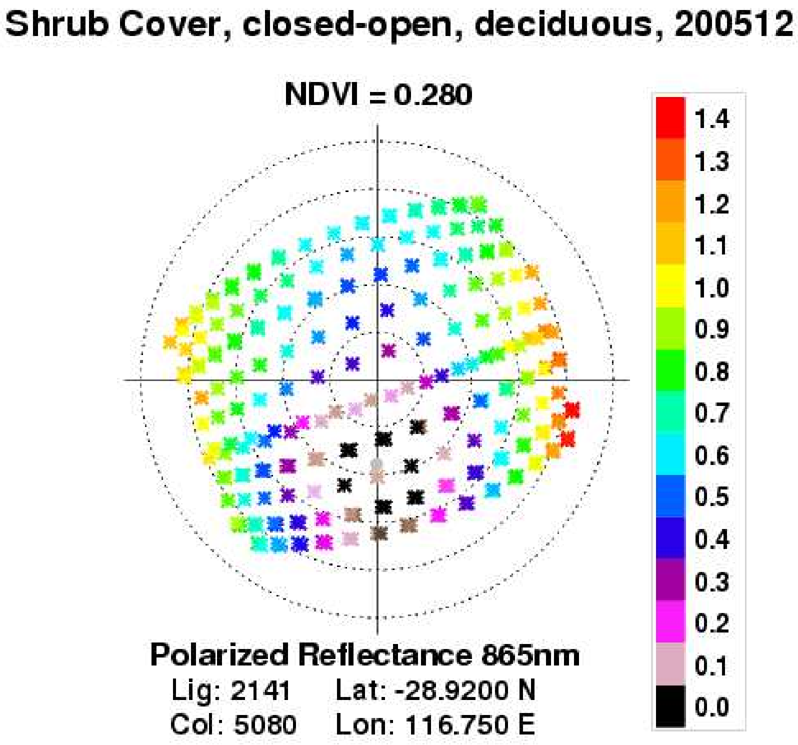

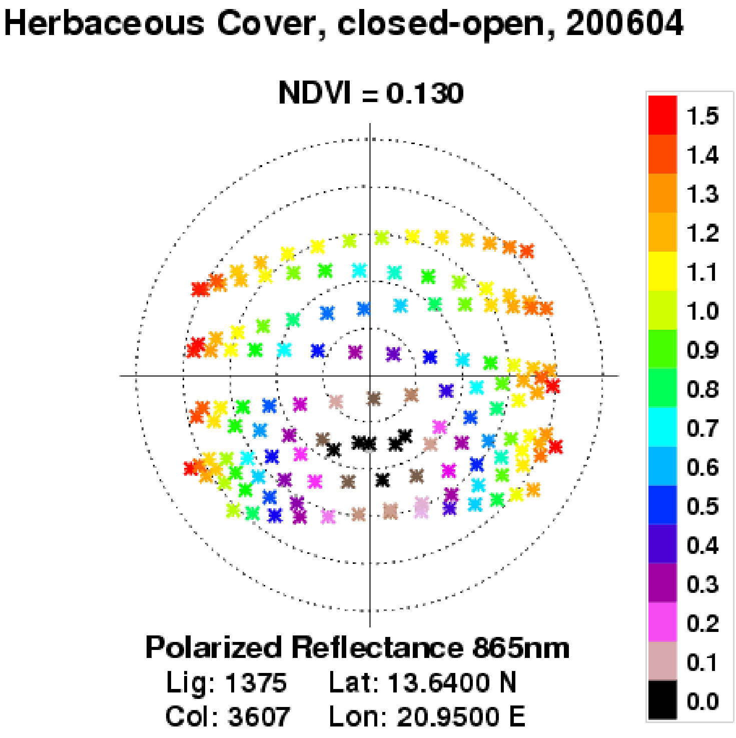

Annex4_ 4 : Polarized reflectance measured at 865nm over a shrubland pixel located in Australia (top), and a herbaceous area located in Chad (bottom)

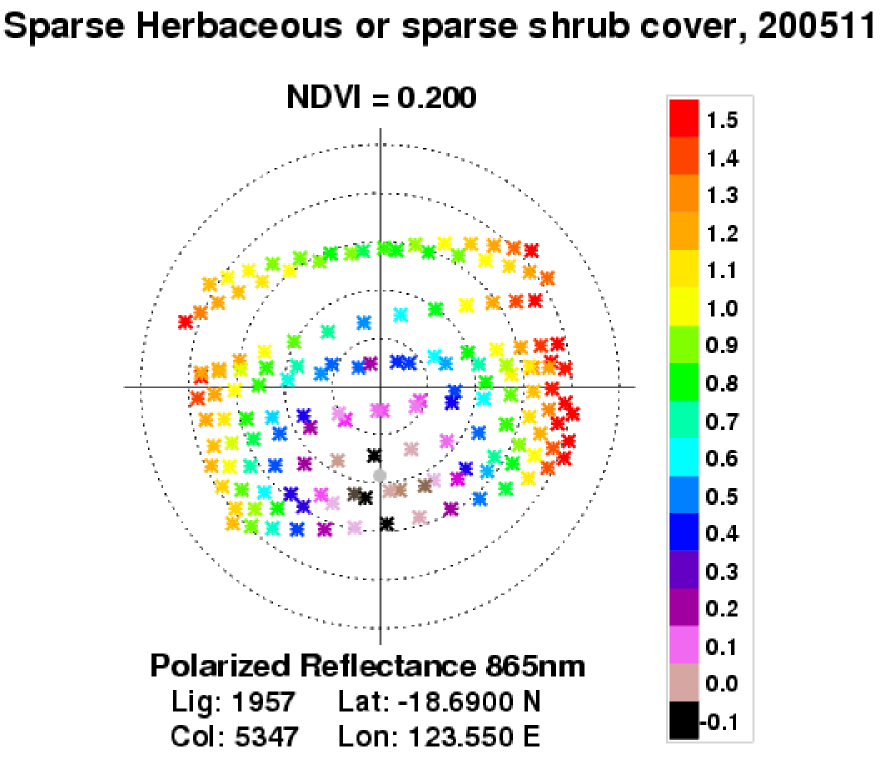

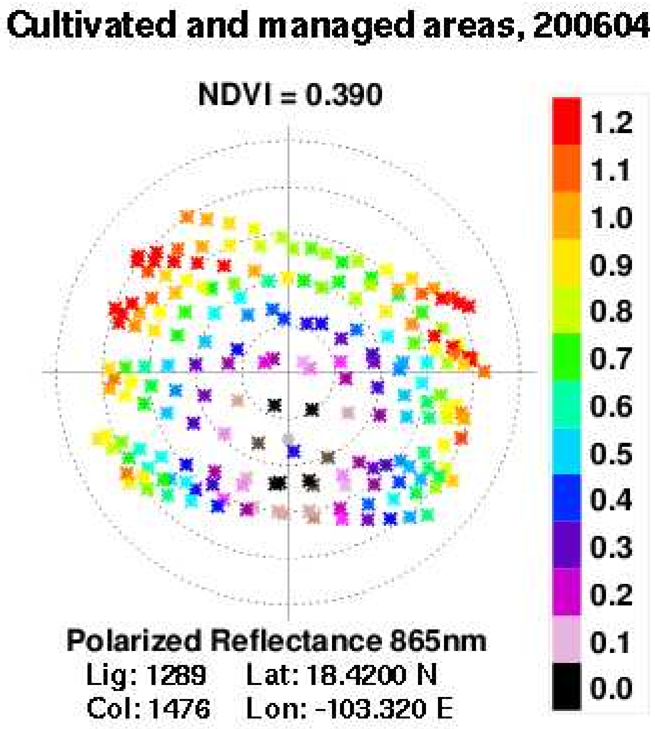

Annex4_ 5 : Polarized reflectance measured at 865nm over a sparse vegetated area located in Australia (top), and over a cropland pixel located in Mexico (bottom).

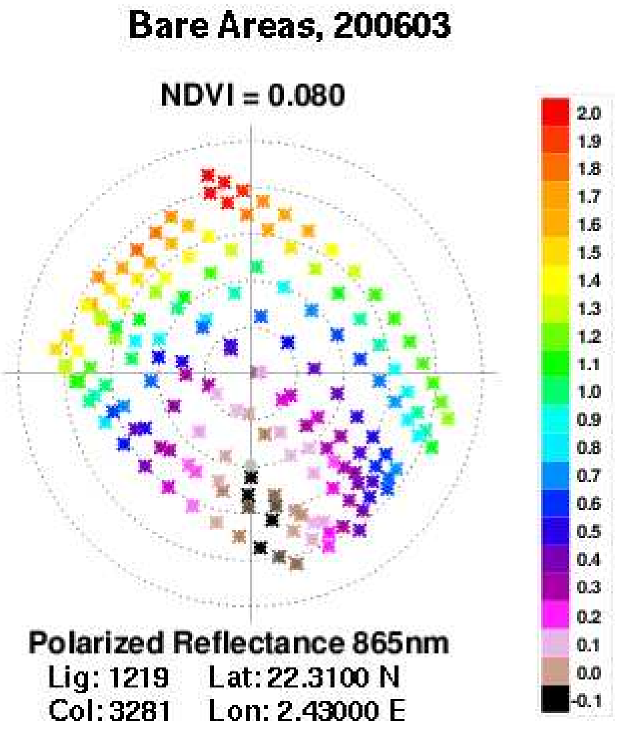

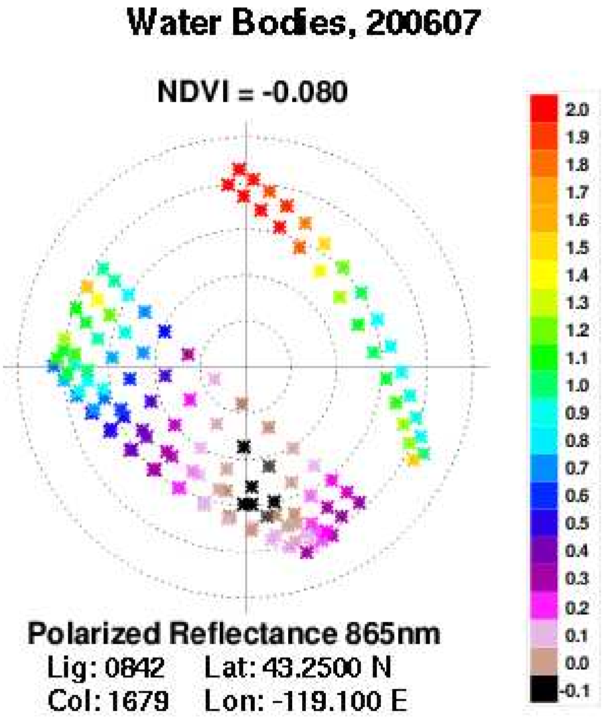

Annex4_ 6 : Polarized reflectance measured at 865nm over a bare area located in Algeria (top), and a water body located in Oregon (USA) (bottom).

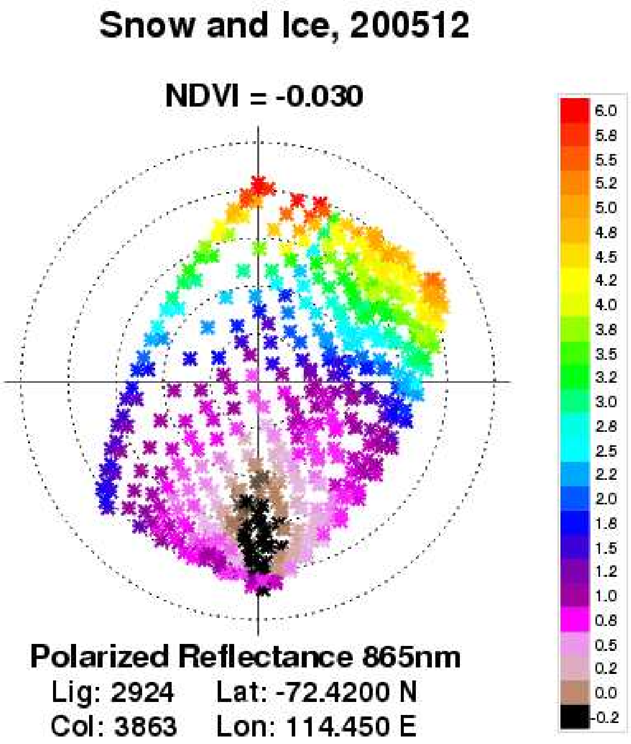

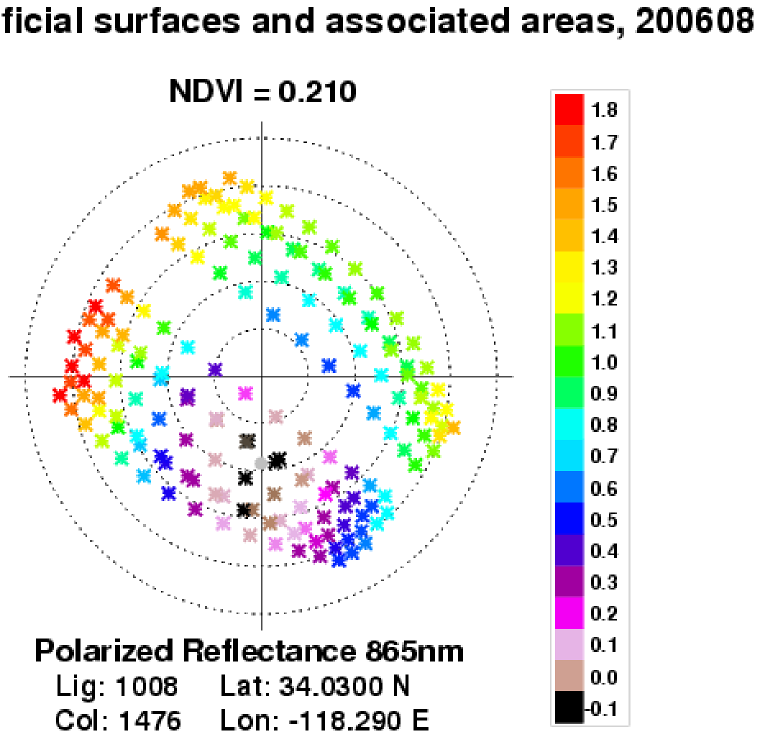

Annex4_ 7 : Polarized reflectance measured at 865nm over a snowy pixel located in Antarctica (top), and an urban pixel located in Los Angeles area (bottom)

Annex5 : Examples of measured and simulated BRDF

(All reflectances are expressed in %)

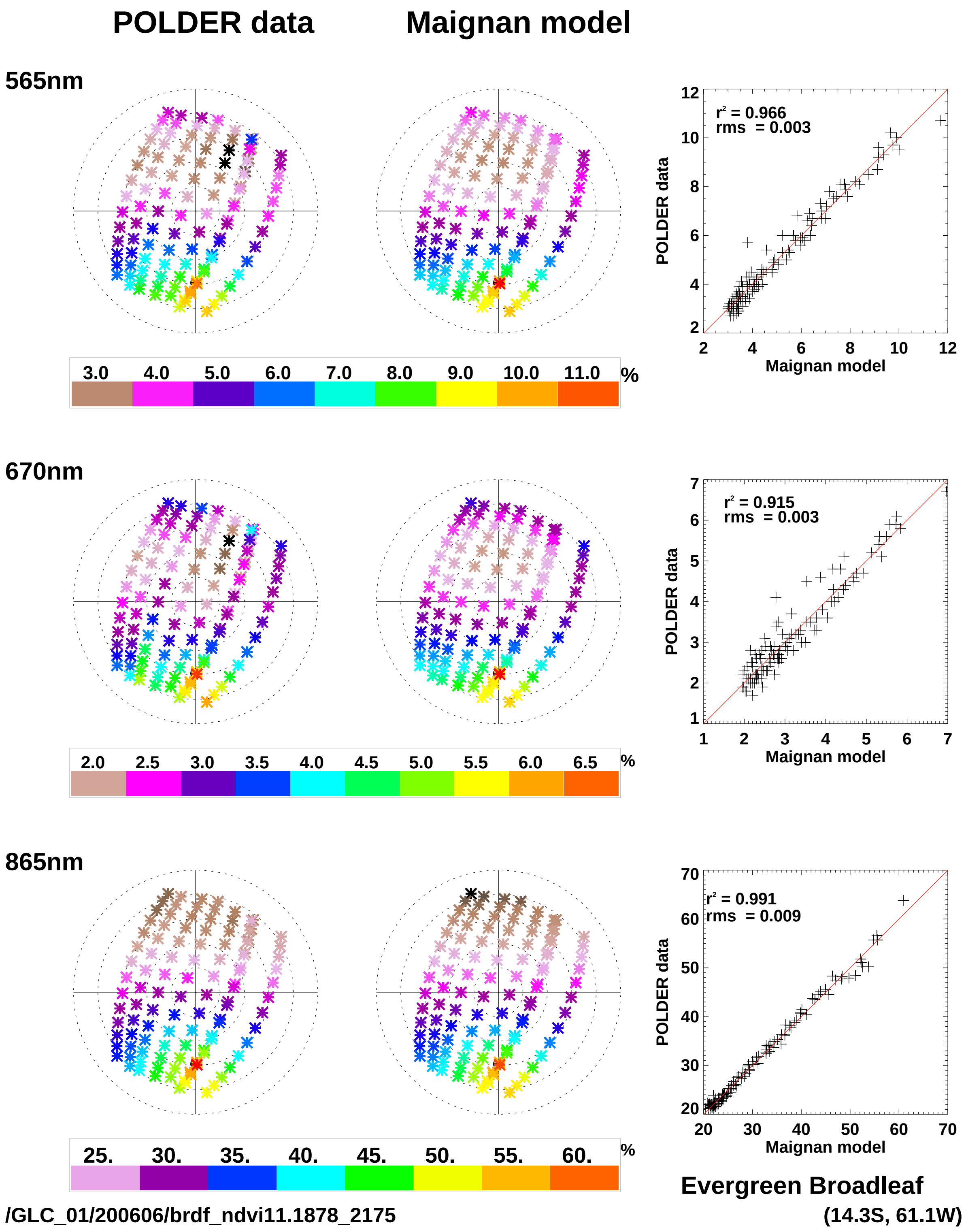

Annex5_ 1 : Measured BRDF (at left), simulated BRDF by the Maignan model (at center), and comparison of the both (at right) for an evergreen broadleaf forest located in Amazonia.

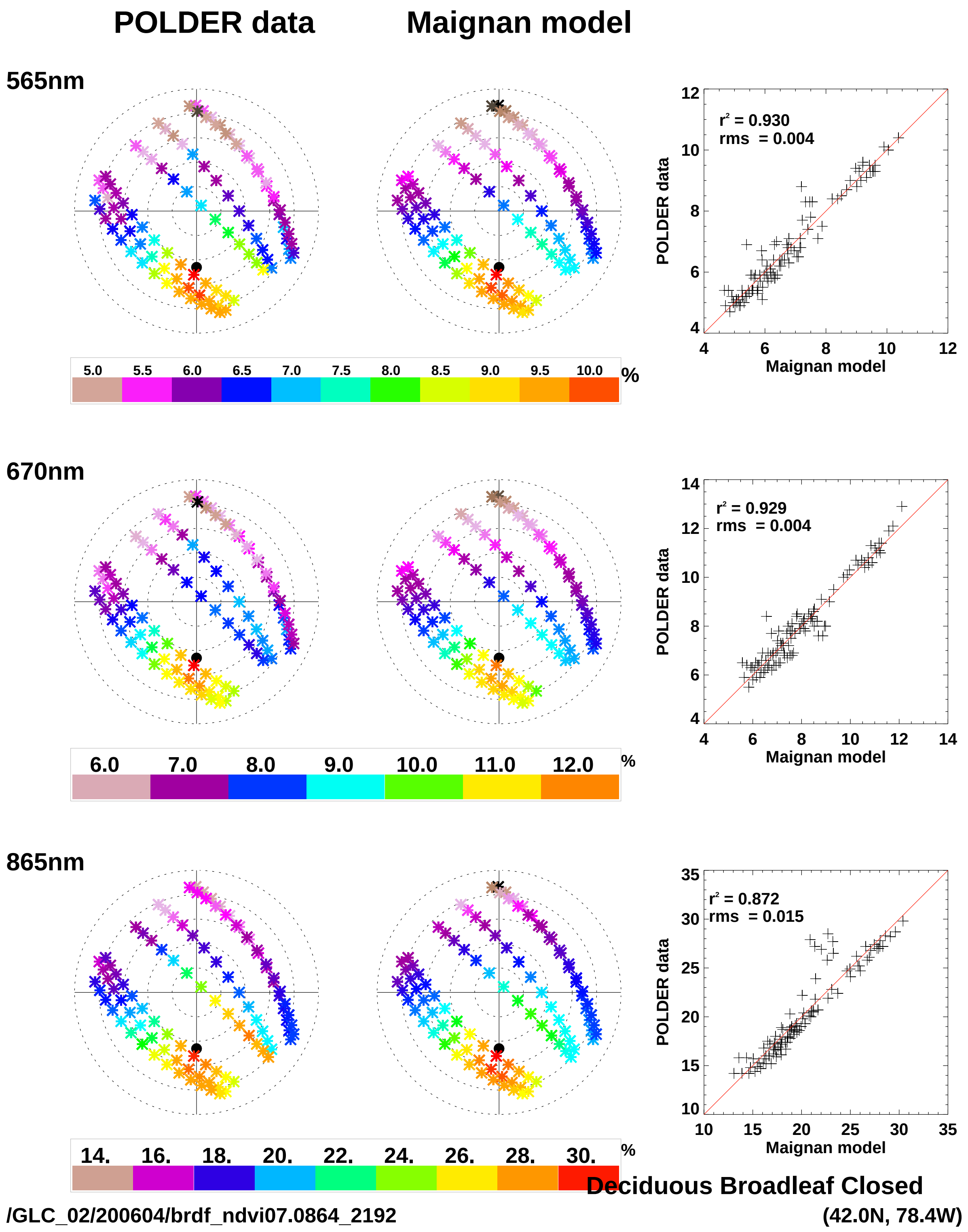

Annex5_ 2 : Measured BRDF (at left), simulated BRDF by the Maignan model (at center), and comparison of the both (at right) for a broadleaf deciduous forest located in USA.

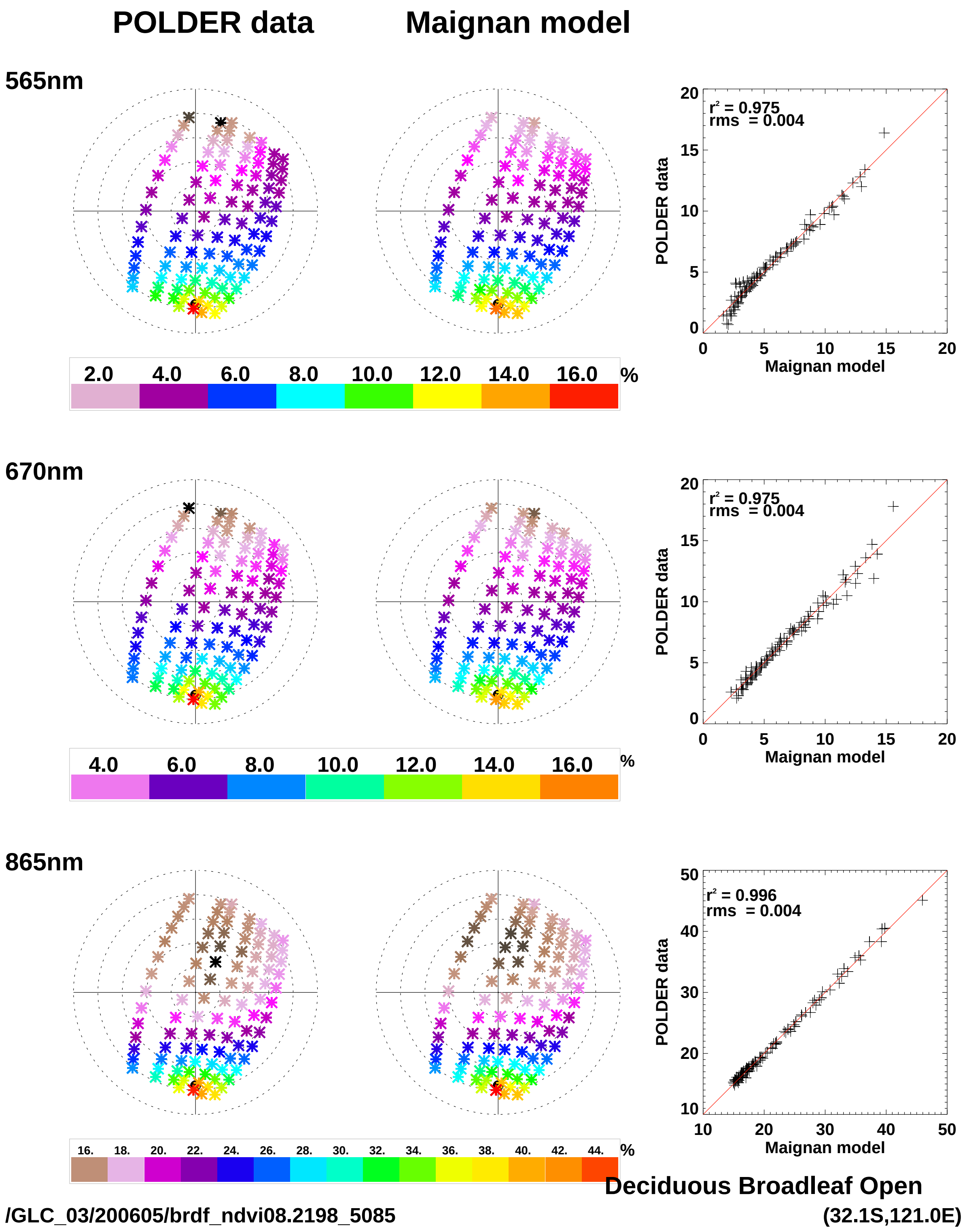

Annex5_ 3 : Measured BRDF (at left), simulated BRDF by the Maignan model (at center), and comparison of the both (at right) for an open deciduous broadleaf forest (as GLC2000) and a woody savanna (as IGBP) located in Australia.

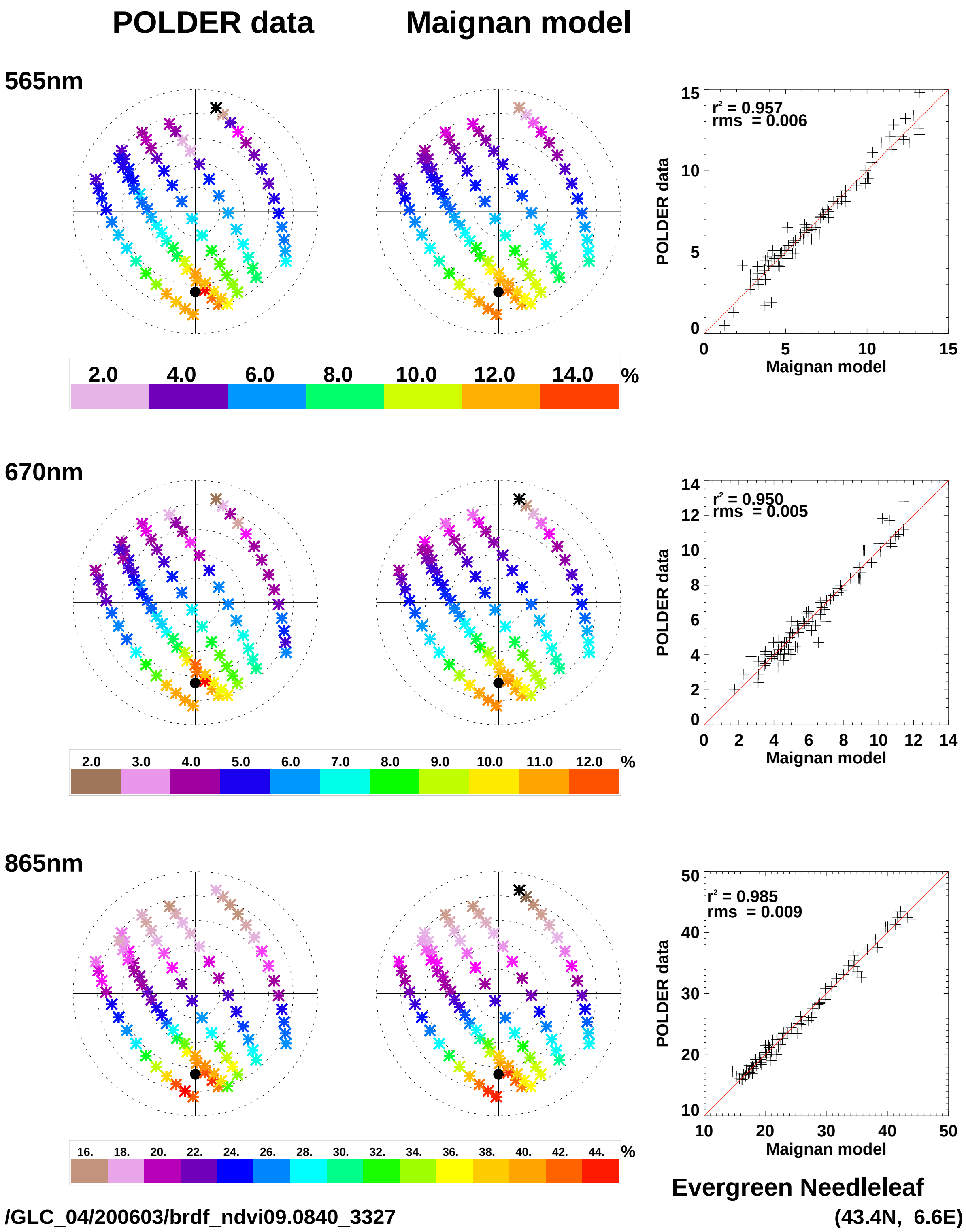

Annex5_ 4 : Measured BRDF (at left), simulated BRDF by the Maignan model (at center), and comparison of the both (at right) for an evergreen needleleaf forest located in French Alps.

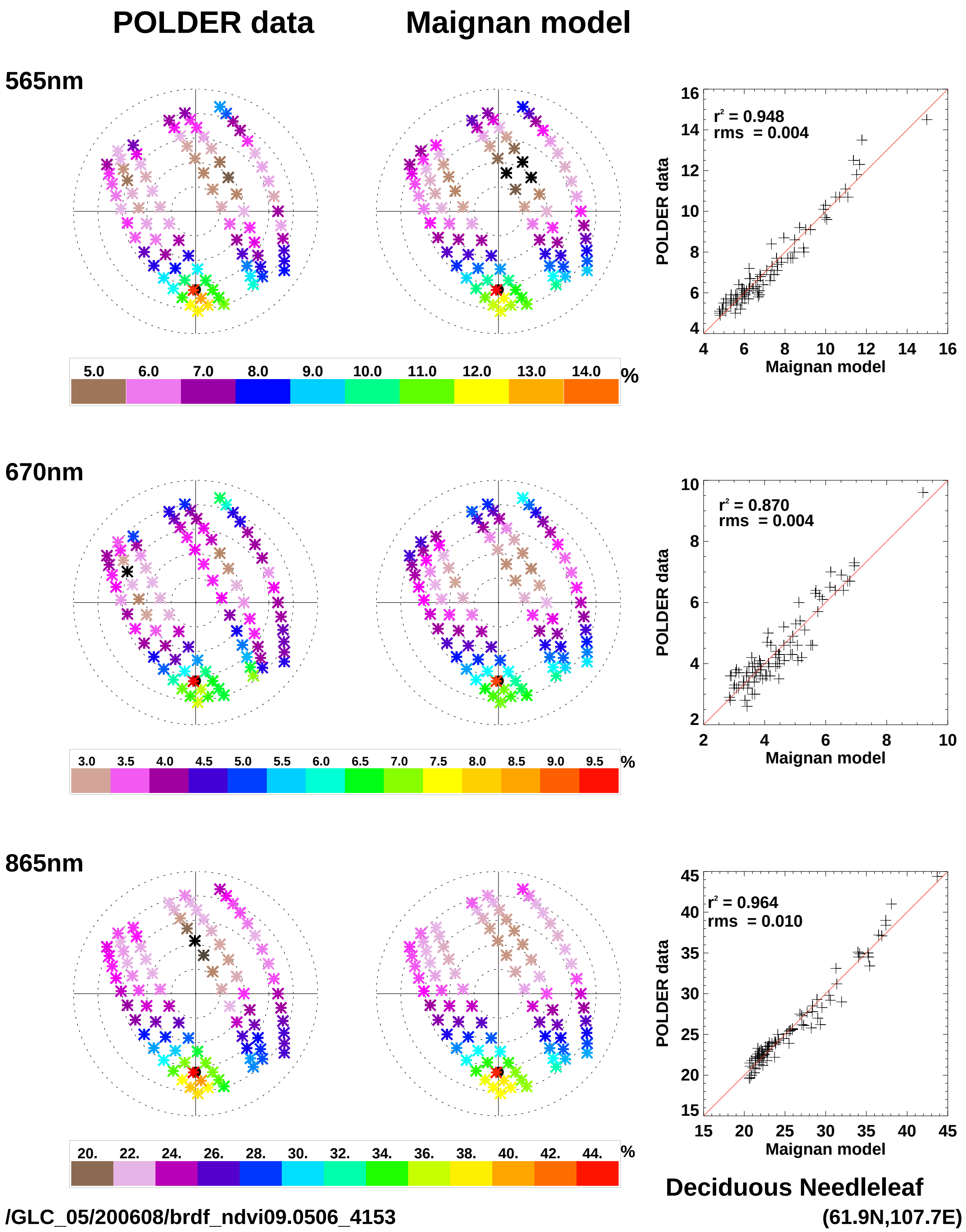

Annex5_ 5 : Measured BRDF (at left), simulated BRDF by the Maignan model (at center), and comparison of the both (at right) for a deciduous needleleaf forest located in Siberia.

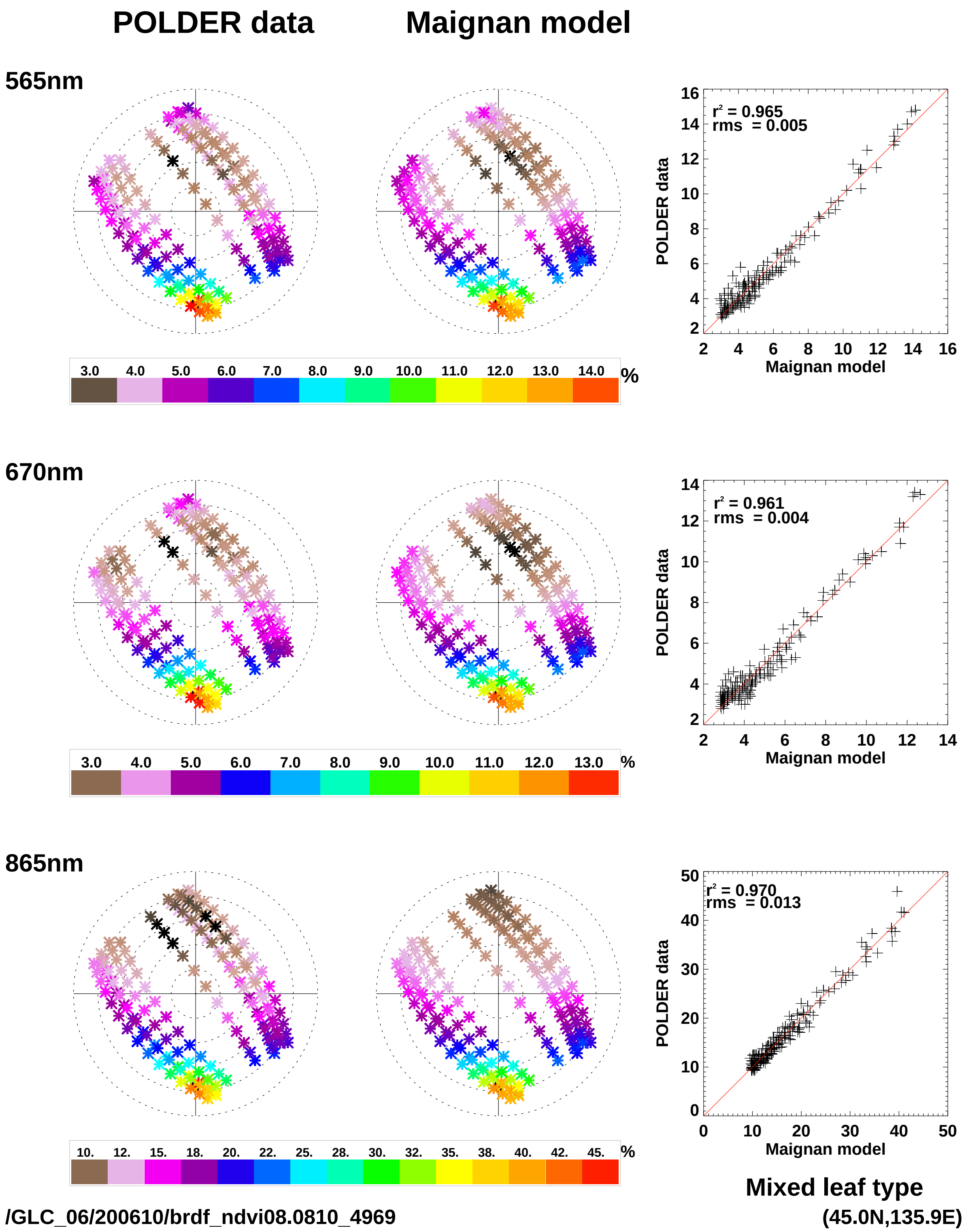

Annex5_ 6 : Measured BRDF (at left), simulated BRDF by the Maignan model (at center), and comparison of the both (at right) for a mixed forest located in Eastern Russia.

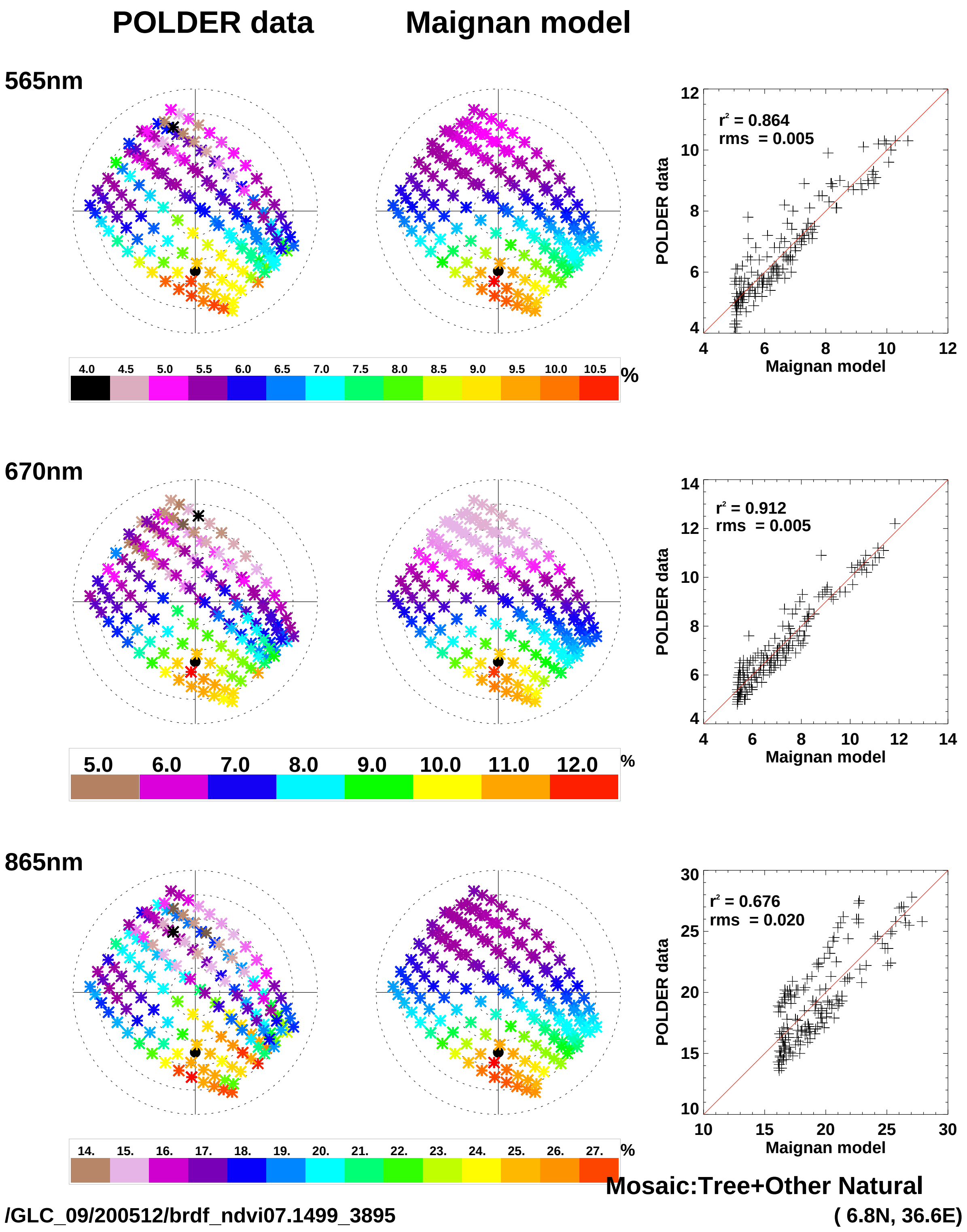

Annex5_ 7 : Measured BRDF (at left), simulated BRDF by the Maignan model (at center), and comparison of the both (at right) for a mosaic tree+other natural vegetation (as GLC2000) or a woody savanna (as IGBP) located in Cameroon.

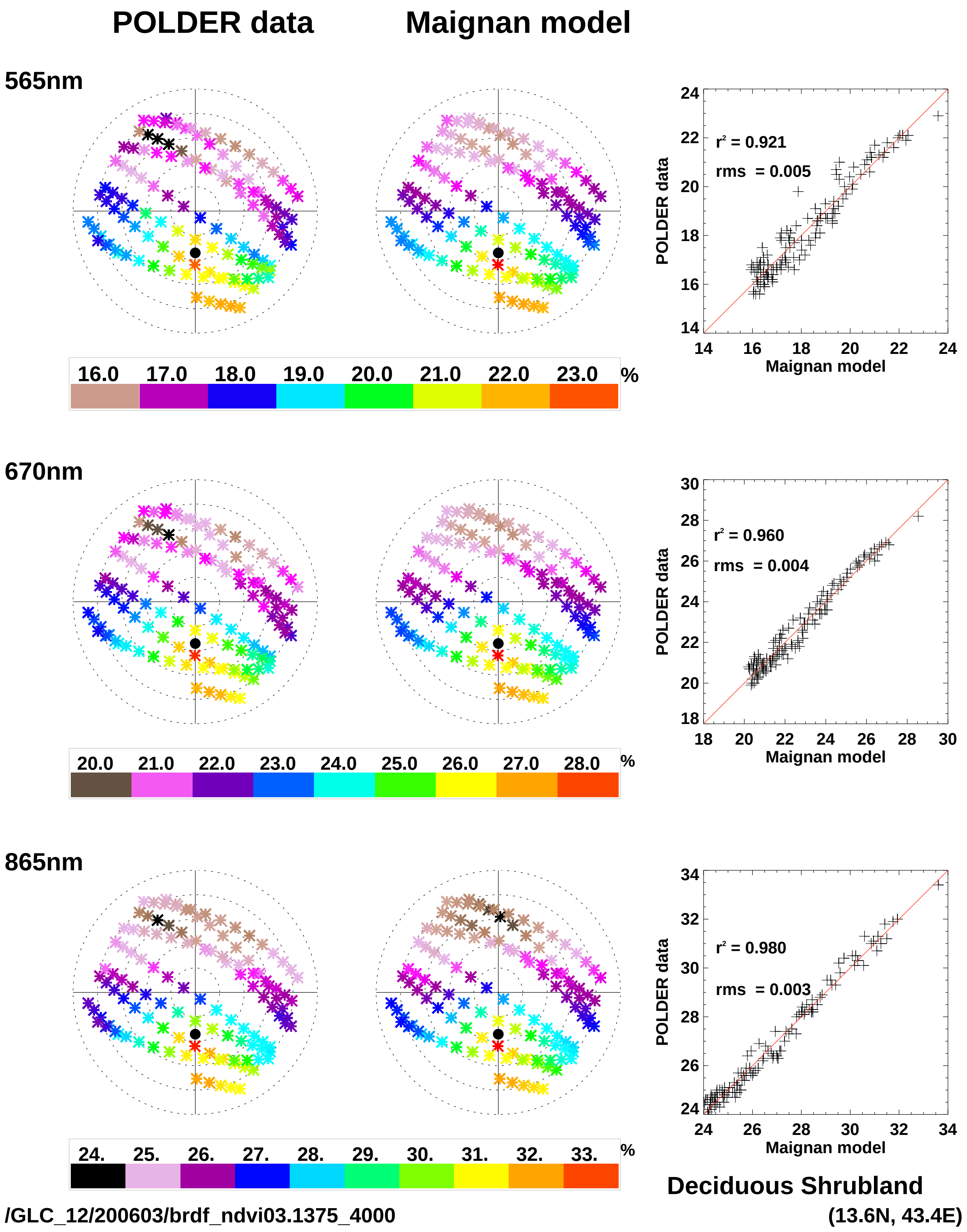

Annex5_ 8 : Measured BRDF (at left), simulated BRDF by the Maignan model (at center), and comparison of the both (at right) for a deciduous shrubland (as GLC2000) located in Yemen.

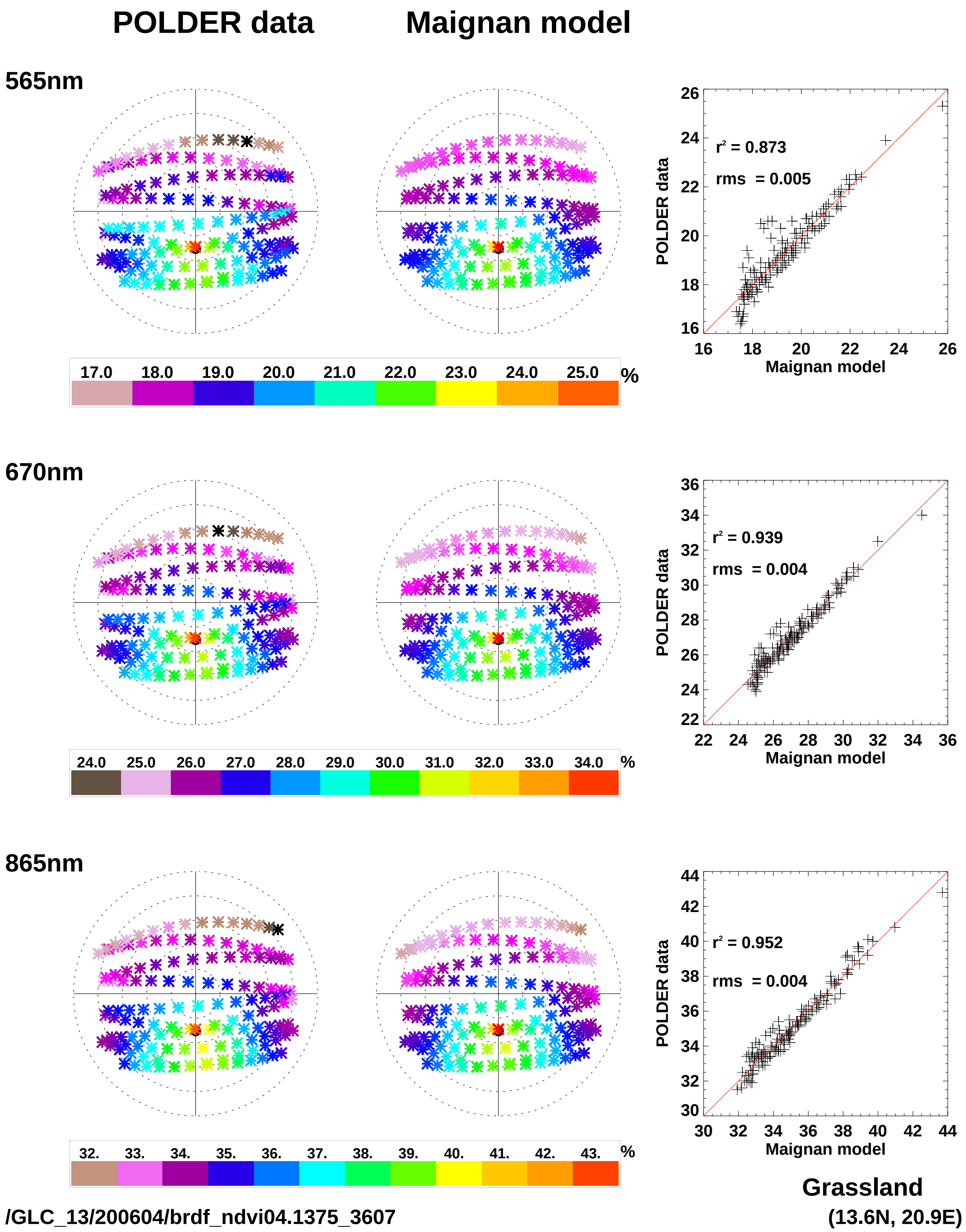

Annex5_ 9 : Measured BRDF (at left), simulated BRDF by the Maignan model (at center), and comparison of the both (at right) for a grassland located in Chad.

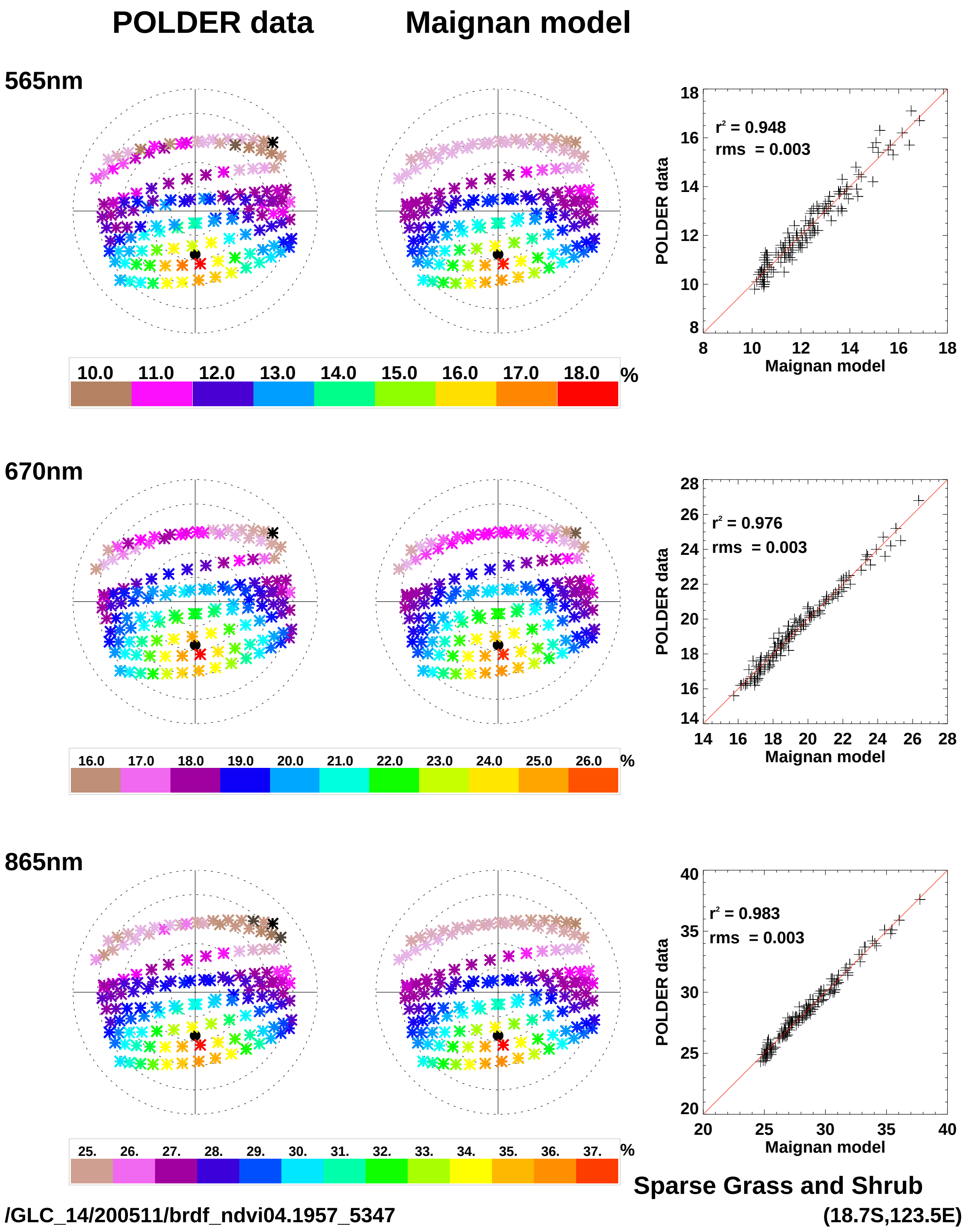

Annex5_ 10 : Measured BRDF (at left), simulated BRDF by the Maignan model (at center), and comparison of the both (at right) for a sparse grass and shrub area (as GLC2000) or an open shrubland (as IGBP) located in Northern Australia.

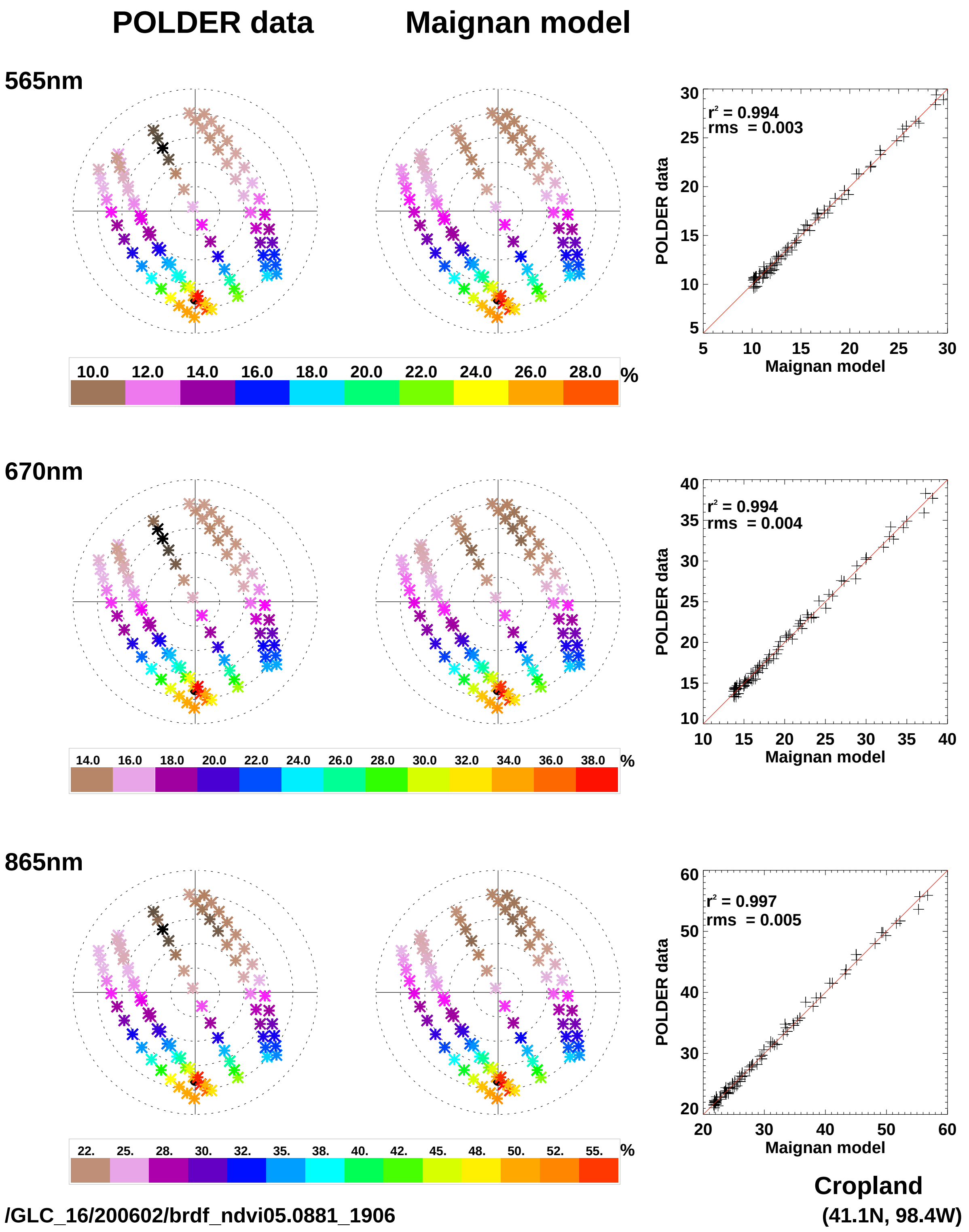

Annex5_ 11 : Measured BRDF (at left), simulated BRDF by the Maignan model (at center), and comparison of the both (at right) for a cropland area located in Middle West (USA).

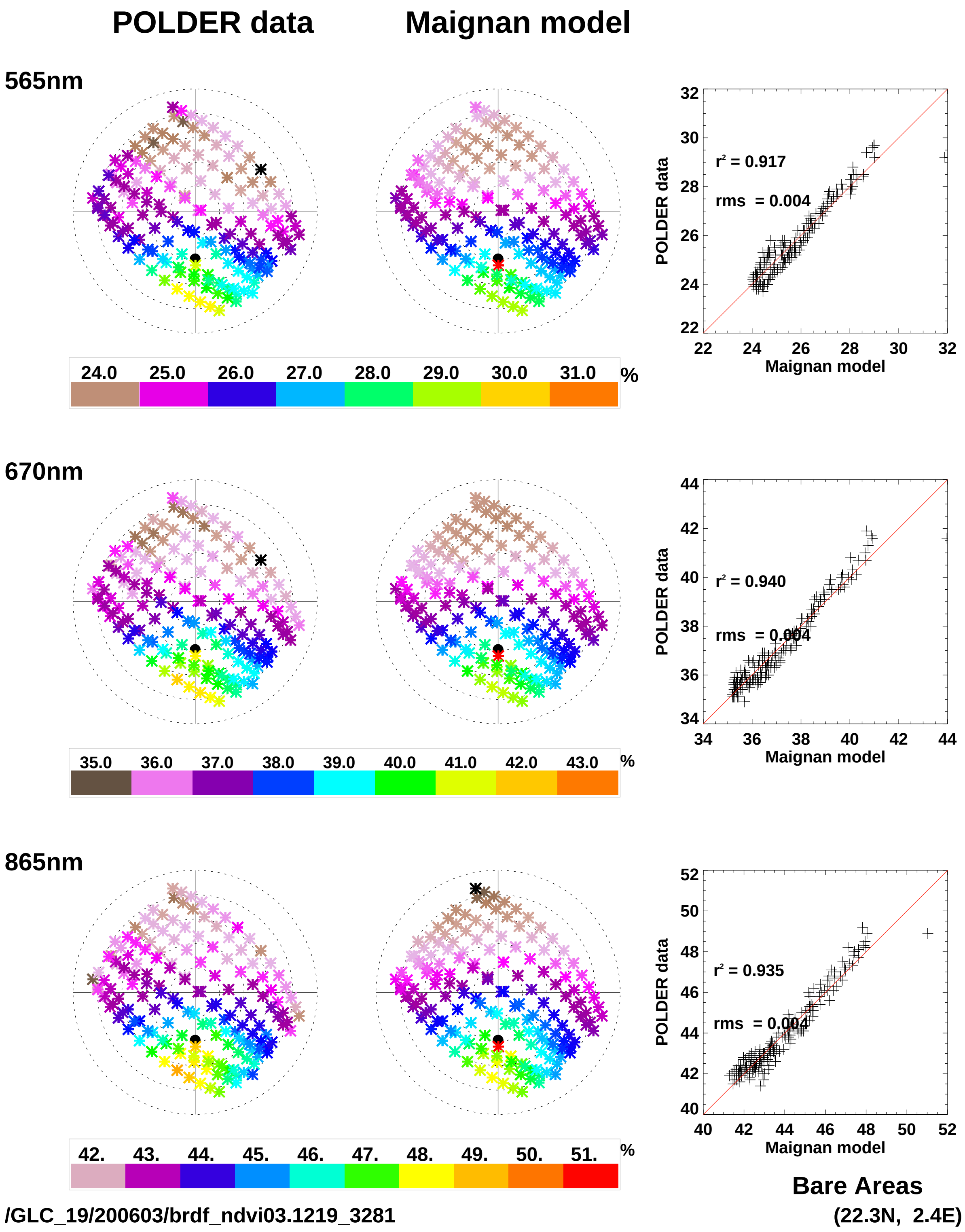

Annex5_ 12 : Measured BRDF (at left), simulated BRDF by the Maignan model (at center), and comparison of the both (at right) for a bare area located in Sahara.

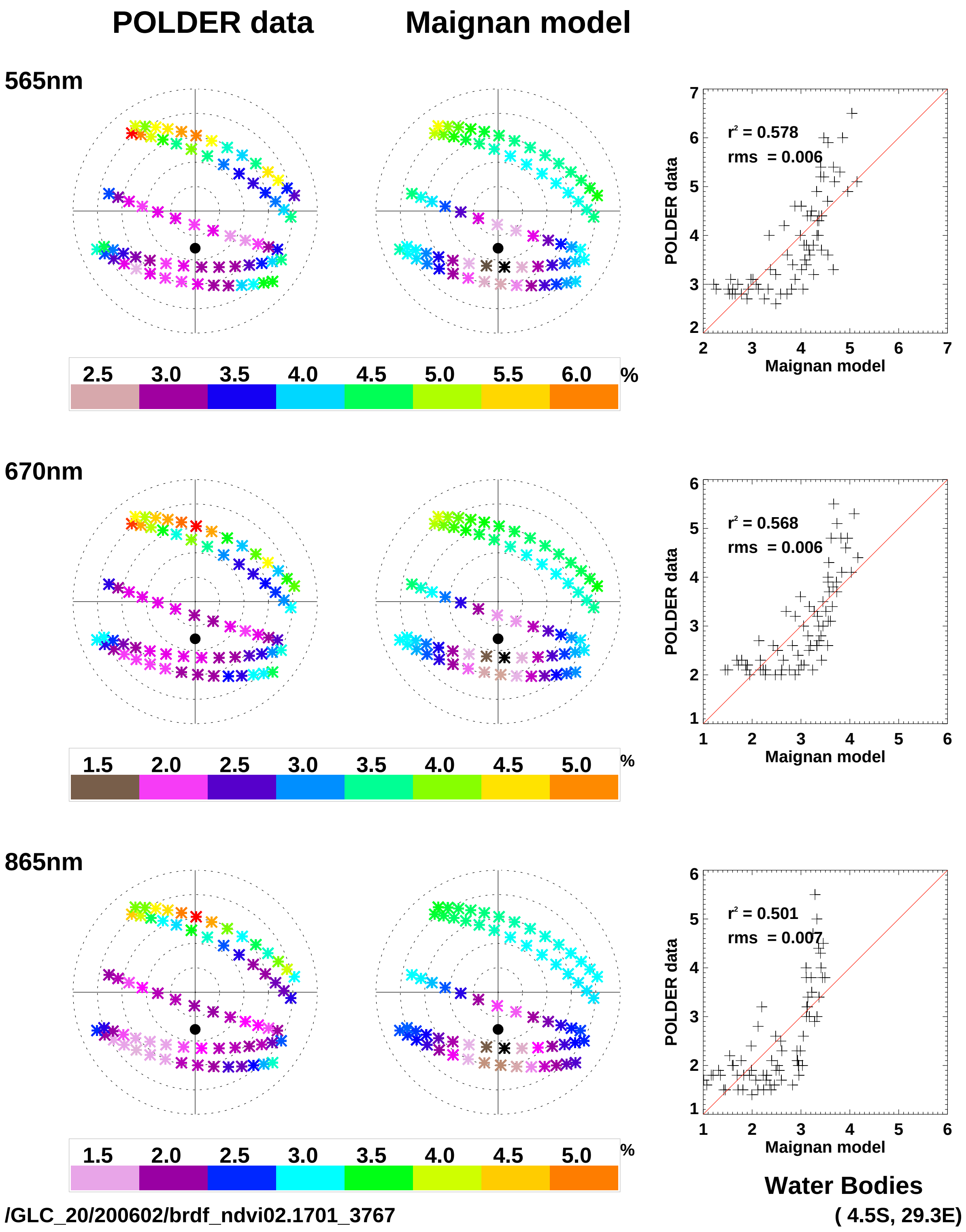

Annex5_ 13 : Measured BRDF (at left), simulated BRDF by the Maignan model (at center), and comparison of the both (at right) for a water pixel located in the Lake Tanganyika.

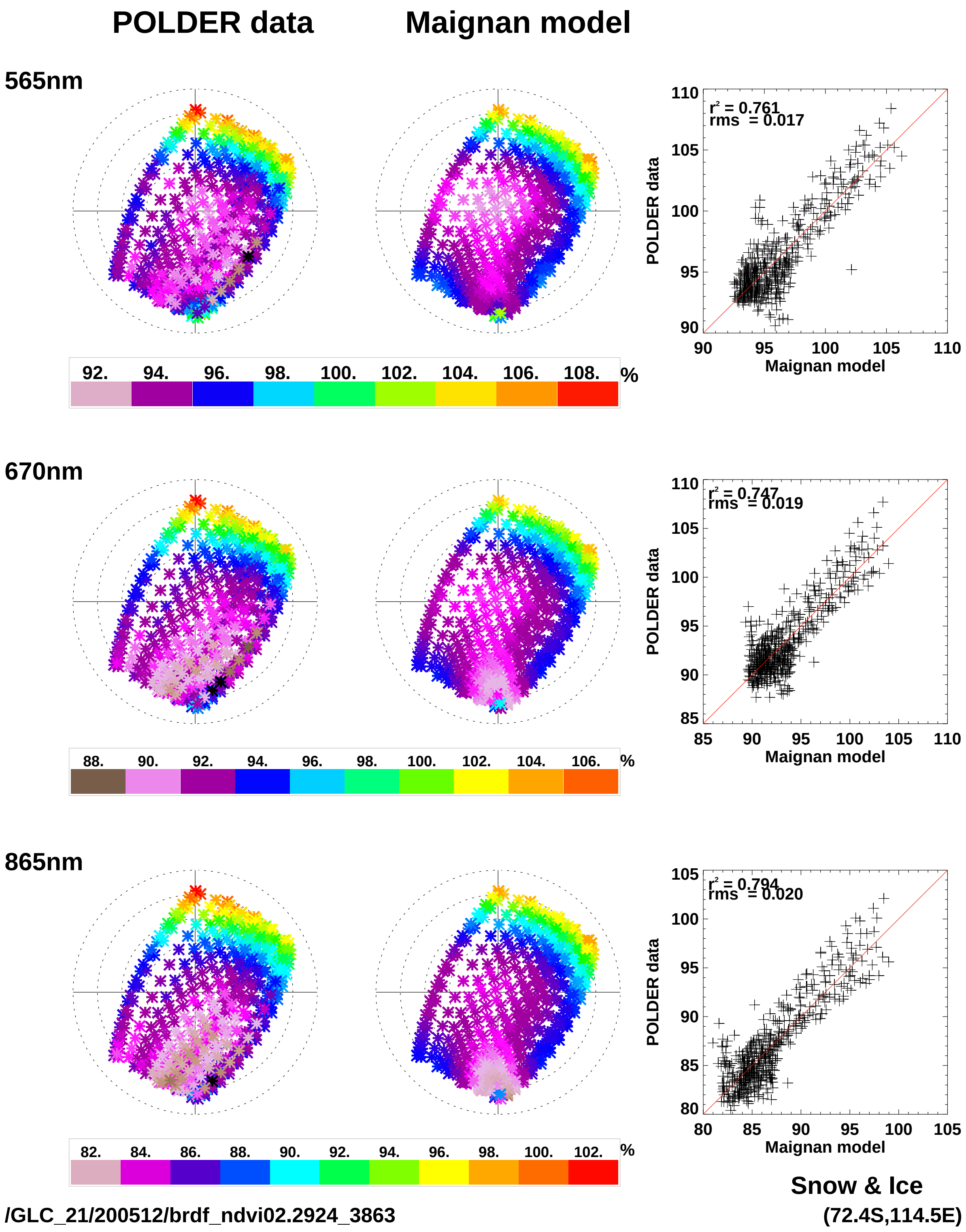

Annex5_ 14 : Measured BRDF (at left), simulated BRDF by the Maignan model (at center), and comparison of the both (at right) for a snowy area located in Antarctica.